Cerebellar control of eye movements: from cerebellar cortex to cerebellar nuclei

Dissertation

zur Erlangung des Grades eines
Doktors der Naturwissenschaften

der Mathematisch-Naturwissenschaftlichen Fakultät
und
der Medizinischen Fakultät
der Eberhard-Karls-Universität Tübingen

vorgelegt
von

Zong-Peng Sun
(孙宗鹏)
aus JiNan, China

August 2017

Tag der mündlichen Prüfung:	09.02.2018
Dekan der Math.-Nat. Fakultät:	Prof. Dr. W. Rosenstiel
Dekan der Medizinischen Fakultät:	Prof. Dr. I. B. Autenrieth
1. Berichterstatter:	Prof. Dr. Peter Thier
2. Berichterstatter:	Prof. Dr. Uwe Ilg
Prüfungskommission:	Prof. Dr. Peter Thier
	Prof. Dr. Uwe Ilg
	Prof. Dr. Martin Giese
	Prof. Dr. Andreas Nieder

Erklärung / Declaration:
Ich erkläre, dass ich die zur Promotion eingereichte Arbeit mit dem Titel:

"**Cerebellar control of eye movements: from cerebellar cortex to cerebellar nuclei**"

selbständig verfasst, nur die angegebenen Quellen und Hilfsmittel benutzt und wörtlich oder inhaltlich übernommene Stellen als solche gekennzeichnet habe. Ich versichere an Eides statt, dass diese Angaben wahr sind und dass ich nichts verschwiegen habe. Mir ist bekannt, dass die falsche Abgabe einer Versicherung an Eides statt mit Freiheitsstrafe bis zu drei Jahren oder mit Geldstrafe bestraft wird.

I hereby declare that I have produced the work entitled: "**Cerebellar control of eye movements: from cerebellar cortex to cerebellar nuclei**" submitted for the award of a doctorate, on my own (without external help), have used only the sources and aids indicated and have marked passages included from other works, whether verbatim or in content, as such. I swear upon oath that these statements are true and that I have not concealed anything. I am aware that making a false declaration under oath is punishable by a term of imprisonment of up to three years or by a fine.

Tübingen,

_____ _____

Datum/Date Unterschrift /Signature

Table of Contents

Summary

Arguably visual information is the most important source of sensory information for us human beings, allowing us to perceive the world. Almost a quarter of our brain is devoted to visual processing. To achieve a precise projection of objects of interest onto the retinal fovea, the region offering the highest spatial resolution and other advantages for the analysis of visual objects, two major types of eye movements, saccades and smooth pursuit are deployed. Saccades shift the image of an object of interest into the fovea. In case the object should be moving, smooth pursuit eye movements (SPEM) try to keep the image of the object within the confines of the fovea in order to ensure sufficient time for its analysis.

It has been known that the oculomotor vermis (OMV) of the cerebellar cortex is dedicated to the control of both saccades and SPEM. However, it has remained unclear if the same oculomotor vermal neurons contribute to controlling these two different types of movements, a scenario that does not look very likely considering their dramatically different kinematics. To address this question, we recorded the activity of OMV Purkinje cells (PCs), the only type of output neuron of cerebellar cortex, in monkeys, and the most suitable animal model for studies of the cerebellar control of eye movements made by humans. During recordings the monkeys were performing saccades and smooth pursuit eye movement (SPEM). Subjecting the recorded saccade and SPEM related PC simple spike responses to a multiple regression analysis, we found that, for saccades, the neural firing pattern is mainly determined by eye position. In contrast, in the case of SPEM, eye velocity plays the most important role in defining the firing pattern. These results indicate that the cerebellar computations for saccades and SPEM are different, even at the level of individual PCs.

Both saccades and SPEM can be adaptively changed by the experience of insufficiencies, compromising the precision of saccades or the minimization of object image slip in the case of SPEM. As both forms of adaptation rely on the cerebellar oculomotor vermis (OMV), most probably deploying a shared neuronal machinery, one might expect that the adaptation of one type of eye movement should affect the kinematics of the other. In order to test this expectation, we subjected 2 monkeys to a standard saccadic adaption paradigm with SPEM test trials at the end and, alternatively, the same 2 monkeys plus a 3rd one to a random saccadic adaptation paradigm with interleaved trials of SPEM. In contrast to our expectation we observed at best marginal transfer which, moreover was little consistent across experiments and subjects. The lack of consistent transfer of saccadic adaptation decisively constrains

models of the implementation of oculomotor learning in the OMV, suggesting an extensive separation of saccade and SPEM-related synapses on P-cell dendritic trees.

The OMV projects ipsilaterally to the caudal fastigial nuclei (cFN) (Yamada & Noda, 1987), which is also called the fastigial oculomotor region. Not surprisingly, in view of the established role of the OMV in the control of saccades and SPEM, also the cFN is known to contribute to both.

Microsaccades are small saccades produced during fixation, whose amplitudes are <1 degree. The concept of a microsaccade-saccade continuum is supported by the fact that studies on the underpinnings of microsaccades have shown that those oculomotor structures explored contribute to saccades of all sizes. The OMV is one of these structures for which a microsaccade-macrosaccade continuum has been established. As shown in this second work package, this continuum is maintained at the level of the cFN, the recipient of saccade-related signals from the OMV. Furthermore, we demonstrate that the pre-microsaccadic baseline firing rate of cFN neurons has properties suitable to ensure precise fixation.

In summary, our results demonstrate the participation of the cerebellum in the control of saccades and SPEM at the level of cerebellar cortex as well as at the level of the caudal fastigial nucleus. It establishes that, contrary to the still dominating view of a separation of the cerebellar machinery for saccades and SPEM, these two forms of goal-directed eye movements rely on largely overlapping, if not identical circuitry. Irrespective of this overlap, learning based adjustments maintain a stunning degree of independence. This is established by our behavioral work. It suggests that this specificity may be a consequence of delimiting distinct dendritic territories of OMV Purkinje cells for the two types of eye movements. Finally, this work supports the notion of a general micro- macrosaccade continuum by establishing that also cFN neurons care for both, micro- and macrosaccades.

Introduction

This dissertation addresses the role of cerebellum in the control of eye movements, using eye movements as a suitable model in our quest for the role of the cerebellum. The human brain involves roughly 86-100 billion neurons (Azevedo et al., 2009; Herculano-Houzel, 2009). The mammalian cerebellum takes up only 10% of the brain volume; however, it contains as many as 69 billion neurons, i.e. about two thirds of all brain neurons (Azevedo et al., 2009).

Vision is the dominant sense that we deploy to gather information about the surrounding world. In order to achieve clear vision, we have to orientate our line of sight towards the object of interest, ensuring that the retinal image is moved from the foveal periphery into its center, the rod-free foveola (Gass, 1999; Li, Tiruveedhula, & Roorda, 2010). This allows vision to exploit the superior visual acuity accommodated by this region (Poletti, Listorti, & Rucci, 2013; Putnam et al., 2005). Once shifted into the fovea by saccades, the object image is stabilized there by smooth pursuit eye movements, compensating movements of the object in the world.

The two types of goal directed eye movements are ideal models of visually guided behavior: eye movements are easy to measure, their biomechanics are comparatively simple with 6 muscles moving the eyes and the eye movement-control circuits do not need to compensate for variable loads. Saccades are brief ballistic movements that align the visual axis with a target. Saccades can reach velocities of many 100°/s. The velocity is positively correlated with the amplitude, a relationship that is called the saccadic main sequence (Bahill, Clark, & Stark, 1975). Although saccades shift the object image from one location on the retina to another one at high speed, we neither perceive a change of the position of the object nor object image motion during the saccade. The reason is that our brains suppress access of visual signals around the saccades (saccadic suppression, (Bridgeman, Hendry, & Stark, 1975; Thiele, Henning, Kubischik, & Hoffmann, 2002)) and use non-visual signals to maintain spatial stability of object location despite changes of the retinal position of the object image (McConkie & Currie, 1996; Poletti, Listorti, & Rucci, 2010). Given the fact that the duration of saccades, on the order of 20 to 100 ms, depending on amplitude, is less or equal the latencies of visual signals, there is no time for online visual feedback to correct saccades in progress. Although their latencies would in principle be short enough to serve feedback control, also proprioceptive signals from the eyes do not affect saccade trajectories (Guthrie, Porter, & Sparks, 1983; Keller & Robinson, 1971). The lack of benefit of sensory feedback notwithstanding, saccades are astonishingly precise. The

necessary precision of the control signals is warranted by a feedback circuit that does not rely on sensory feedback but on internal feedback, involving an efference copy of the saccade command (Enderle, Wolfe, & Yates, 1984; Moschovakis, 1994; D. A. Robinson, 1964; Scudder, 1988).

Smooth pursuit eye movements (SPEM) are used to track moving objects in order to keep their image on the fovea. They are confined to velocities below 10°/s or at most 30-50°/s (de Brouwer, Yuksel, Blohm, Missal, & Lefevre, 2002; Fuchs, 1967; D. A. Robinson, 1965; Westheimer, 1954). A feedback system that translates the motion of the target on the retina into an eye movement response is responsible for the generation of smooth pursuit (Rashbass, 1961; D. A. Robinson, Gordon, & Gordon, 1986). However, the first 100-150 ms of pursuit are still open loop, i.e. driven by uncompensated retinal target motion, due to the delay of the visual signals. In other words, the first 100-150 ms of SPEM are totally dependent on the retinal motion signal and a gain that transform the target movement into eye velocity. Hence, this early phase is called open-loop pursuit/ pursuit initiation.

The cerebellar control of saccade and pursuit has been well established, underlying the textbook view that the flocculus/paraflocculus is dedicated to SPEM (Lisberger & Fuchs, 1978) and the OMV to saccades (Kase, Miller, & Noda, 1980). Patients with cerebellar degeneration suffer from saccadic dysmetria (Buttner, Straube, & Spuler, 1994; Zee, Yee, Cogan, Robinson, & Engel, 1976) and they exhibit abnormal SPEM (Lekwuwa, Barnes, & Grealy, 1995; Moschner et al., 1999; Moschner, Zangemeister, & Demer, 1996). More specifically, with regard to saccades, clinical and experimental lesion studies showed that it is an impairment of vermal lobuli VIc and VIIa, the saccade-related region of cerebellar cortex that causes saccadic dysmetria (Barash et al., 1999; Golla et al., 2008; Ignashchenkova et al., 2009; Optican & Robinson, 1980; Ritchie, 1976; Takagi, Zee, & Tamargo, 1998). Furthermore, it has been shown recently that optical stimulation of PCs in this cerebellar region caused dysmetria as well (El-Shamayleh, Kojima, Soetedjo, & Horwitz, 2017). Therefore, lobules VIc and VII have been named the oculomotor vermis (OMV) (Noda & Fujikado, 1987).

With regard to SPEM, much of previous work has emphasized a major role of a different part of the cerebellum, namely the flocculus/paraflocculus complex (Blazquez & Yakusheva, 2015; Kahlon & Lisberger, 2000; Medina & Lisberger, 2008, 2009; Noda & Warabi, 1986; Rambold, Churchland, Selig, Jasmin, & Lisberger, 2002; Stone & Lisberger, 1990; Zee, Yamazaki, Butler, & Gucer, 1981). The assumption of an anatomical segregation is understandable in view of the profoundly different

kinematics of saccade and pursuit. Yet, it has more recently become clear that lesions of the OMV not only impair saccades but also the initiation of SPEM (Barash et al., 1999; Ohki et al., 2009; Takagi, Zee, & Tamargo, 2000; Vahedi, Rivaud, Amarenco, & Pierrot-Deseilligny, 1995), which suggests that the OMV may be involved in both types of eye movements. The lesion evidence for a role of the OMV in SPEM is supported by electrical stimulation experiments, which showed that stimulation here may not only evoke saccades (Fujikado & Noda, 1987; Ron & Robinson, 1973), but also pursuit-like slow eye movements (Krauzlis & Miles, 1998). Moreover, already early electrophysiological recording studies could establish that at least some individual PCs in the OMV respond to saccades as well as SPEM (Sato & Noda, 1992; Suzuki & Keller, 1988). Such 'dual' OMV PCs might be oddities with little if any functional relevance. On the other hand, they might be representatives of an important computational principle serving as common ground for saccades and SPEM, deployed by the OMV. In the first part of this dissertation (see study 1), I will attempt to address the properties of these neurons by recording PCs during saccades and SPEM (Sun, Smilgin, Junker, Dicke, & Thier, 2017).

The caudal fastigial oculomotor region (FOR), also known as cFN, is the major projecting target of the oculomotor vermis (Yamada & Noda, 1987), which in turn projects contralaterally to a number of brainstem nuclei implicated in saccades such as the paramedian reticular formation (PPRF), the dorsomedial medullary reticular formation, the omnipause neuron region and the more rostral parts of the superior colliculus (Batton, Jayaraman, Ruggiero, & Carpenter, 1977; Homma, Nonaka, Matsuyama, & Mori, 1995; May, Hartwich-Young, Nelson, Sparks, & Porter, 1990; Noda, Sugita, & Ikeda, 1990; Sato & Noda, 1991; Sugita & Noda, 1991), as well as the medial accessory nucleus of the inferior olive (MAO) (Dietrichs & Walberg, 1985; Ikeda, Noda, & Sugita, 1989; Ruigrok & Voogd, 1990). Not surprisingly, in view of its connectivity, previous work has been able to provide ample electrophysiological evidence for a role of the FOR in the control of saccades (Fuchs, Robinson, & Straube, 1993; Goffart, Chen, & Sparks, 2004; Helmchen, Straube, & Büttner, 1994; Hepp, Henn, & Jaeger, 1982; Inaba, Iwamoto, & Yoshida, 2003; Noda et al., 1988; Ohtsuka & Noda, 1991, 1992; Straube, Helmchen, Robinson, Fuchs, & Buttner, 1994; Vilis & Hore, 1981). In accordance with this evidence, lesions of the caudal fastigial nucleus (Fuchs et al., 1993; Goffart et al., 2004; Straube et al., 1994; Vilis & Hore, 1981) have shown to compromise the precise control of saccades, leading to "saccadic" dysmetria. Moreover, inactivation of cFN gave rise to the disruption of pursuit initiation due to abnormal initial eye acceleration by injecting muscimol (F. R. Robinson, Straube, &

Fuchs, 1997), a result which implied the participation of this nucleus in the control of SPEM. Indeed, also electrophysiological recordings have been able to support a role of the cFN in SPEM (Büttner, Fuchs, Markert-Schwab, & Buckmaster, 1991; Fuchs, Robinson, & Straube, 1994; F. R. Robinson, Straube, & Fuchs, 1993).

As mentioned before, rather than deploying distinct sets of PCs and fastigial neurons, some OMV PCs and fastigial neurons with oculomotor sensitivity are tuned to saccades as well as to SPEM. Given the fact that both control and adaptation of saccades and SPEM seem to rely on the OMV and as well on the FOR it seemed reasonable to hypothesize that adaptive changes of one of the two behaviors should have implications for the respective other. However, whether the adaptation of one type of eye movement can affect the other type of eye movement has never been tested. In other words, whether saccadic learning may spill over to SPEM should be studied. To examine this possibility was one of the aims of this dissertation (see study 2) (Sun et al., 2017).

We make big saccades when exploring objects in the world around us and they follow moving objects with SPEM. However, even during fixation of a static object, our eyes do not stay still. Actually, there are three types of small amplitude eye movements during fixation: microsaccades, drift and tremor. Microsaccades are small saccades with an amplitude of <1° down to a few minutes of arc seen during fixation (Martinez-Conde, Macknik, & Hubel, 2004), which had initially been deemed oculomotor noise (Kowler & Steinman, 1980). However, many studies have sustained the notion that microsaccades serve vision. A first line of evidence is that images tend to fade if image shifts due to microsaccades are prevented by technical means (Ditchburn & Ginsborg, 1952). However, a role in preventing fading would in principle not rule out that microsaccades are a manifestation of (uncontrolled) oculomotor noise. Nevertheless, recent findings have clearly suggested that microsaccades are indeed well controlled (Bridgeman & Palca, 1980; Cui, Wilke, Logothetis, Leopold, & Liang, 2009; Ko, Poletti, & Rucci, 2010; McCamy, Najafian Jazi, Otero-Millan, Macknik, & Martinez-Conde, 2013; Thaler, Schutz, Goodale, & Gegenfurtner, 2013; Winterson & Collewijn, 1976), ensuring the precise relocation of the retinal image towards the foveal center, the rod-free foveola (Gass, 1999; Li et al., 2010). Given the important role of the OMV in fine tuning the amplitude of macrosaccades, one might expect that also the programming of precise microsaccades might require the participation of cerebellum. In fact, a previous study has demonstrated that OMV P-cells are involved in the control of microsaccades (Arnstein, Junker, Smilgin, Dicke, & Thier, 2015). In a third project of

my dissertation (study 3), I explored if also the FOR, the major target of the oculomotor vermis, contributes to the control of microsaccades (Sun, Junker, Dicke, & Thier, 2016).

Aims of this dissertation

A first aim is to clarify the contribution of OMV PCs to the two types of goal directed eye movements. Do the same OMV PCs contribute to saccades and to SPEM or does the OMV offer distinct populations of saccade and SPEM PCs with some minor overlap? And in case of significant overlap, how do OMV PCs accommodate the very different kinematic requirements of saccades and SPEM? In order to find answers to these questions, we studied OMV PCs in experiments on saccades and SPEM in order to determine the influence of saccade and SPEM kinematics on the discharge (1st study, Appendix 1).

As the first study could establish that indeed practically every OMV PC contributes to both saccades and SPEM, our next aim was to test, if learning based adjustments of saccades, based on changes of information processing at the level of OMV PCs spill over to SPEM (2nd study, Appendix 2).

Finally, in a study of FOR neurons, we aimed at the cerebellar processing of information on microsaccades. More specifically, we tested the idea of a microsaccade-macrosaccade continuum, previously suggested by work on the OMV (3rd study, Appendix 3).

Summary of scientific findings

Study 1:

The same oculomotor vermal Purkinje cells encode the very different kinematics of saccades and of smooth pursuit eye movements.

Zong-Peng Sun, Aleksandra Smilgin, Marc Junker, Peter W. Dicke, Peter Thier.

Sci Rep, 7: 40613.

In this study we show that individual OMV PCs are involved in both saccades and SPEM, the very different kinematic requirements of the two types of eye movements notwithstanding. Based on a rigorous statistical analysis, we demonstrate that eye position and velocity are able to explain a substantial amount of the discharge variability independent of eye movement type. Yet, eye velocity sensitivity is substantially higher for SPEM, thereby compensating for the much lower eye velocities. This finding suggests that OMV PC SSs might deploy signals primarily to optimize eye movements in the face of viscous forces.

Study 2:

Short-term adaptation of saccades does not affect smooth pursuit eye movement initiation.

Zong-Peng Sun, Aleksandra Smilgin, Marc Junker, Peter W. Dicke, Peter Thier.

J Vis, 17 (9), 19-19

We tried to demonstrate transfer of saccadic adaptation using two different paradigms, a first one, in which saccadic adaptation blocks preceded tests of SPEM and a second one, in which saccadic adaptation trials and SPEM test trials were presented randomly interleaved. We observed at best marginal transfer which, moreover was little consistent across experiments and subjects. The lack of consistent transfer of saccadic adaptation decisively constrains models of the implementation of oculomotor learning in the OMV, suggesting an extensive separation of saccade and SPEM-related synapses on P-cell dendritic trees.

Study 3:

Individual neurons in the caudal fastigial oculomotor region (FOR) convey information on both macro- and microsaccades.

Zong-Peng Sun, Marc Junker, Peter W. Dicke, Peter Thier.

Eur J Neurosci, 44(8), 2531-2542.

We demonstrate that individual FOR neurons process both micro- and macrosaccade related signals. In accordance with previous studies, we found that FOR neurons exhibited saccade-related bursts earlier for contraversive saccades than for ipsiversive saccades, both for macro- and microsaccades. In general, the burst for macrosaccades started later compared to the one for microsaccades. These qualitative similarities suggest in principle similar contributions to the control of saccades independent of amplitude.

Conclusions and outlook

Taken together, our results indicate that the cerebellar system for goal-directed eye movements involving the OMV and its target in the deep cerebellar nuclei, the FOR, is identical for saccades and SPEM and, moreover, for macro- and microsaccades. This was completely unexpected as both the kinematic and the dynamic requirements of these various forms of eye movements are very different. Profound differences distinguish not only SPEM and saccades but also large and small amplitude saccades whose velocities may differ by a factor of 5 to 10. Although the cerebellar machinery serving micro- and macrosaccades and SPEM seems to be identical down to the level of single PCs, a certain degree of independence of different types of eye movements and their learning based adjustment could still be achieved if at least distinct dendritic territories with distinct sets of parallel fiber synapses were reserved for the various types of eye movements. Yet, as discussed in detail in (Sun, Smilgin, Junker, Dicke, & Thier, 2017), the price would be the need to invest into additional machinery separating saccade and SPEM related signals in cerebellum dependent target structures in the brain stem. Arguably such investments would not be too useful if the major role of the cerebellum were the compensation of influences that would affect distinct (oculo-) motor systems in a more or less selective and specific manner. On the other hand, they would help if the influence to deal with would be unspecific as to the specific (oculo-) motor system. Unveiling this common influence on (oculo-) motor behavior that is largely independent of the details of movement kinematics or dynamics will be the major task for future work on the cerebellum. It may in the end lead to a novel view of the scope of this most intriguing part of the brain.

References

Arnstein, D., Junker, M., Smilgin, A., Dicke, P. W., & Thier, P. (2015). Microsaccade control signals in the cerebellum. J Neurosci, 35(8), 3403-3411.

Azevedo, F. A., Carvalho, L. R., Grinberg, L. T., Farfel, J. M., Ferretti, R. E., Leite, R. E., et al. (2009). Equal numbers of neuronal and nonneuronal cells make the human brain an isometrically scaled-up primate brain. J Comp Neurol, 513(5), 532-541.

Bahill, A. T., Clark, M. R., & Stark, L. (1975). The main sequence, a tool for studying human eye movements. Math. Biosci, 24(3-4), 191-204.

Barash, S., Melikyan, A., Sivakov, A., Zhang, M., Glickstein, M., & Thier, P. (1999). Saccadic dysmetria and adaptation after lesions of the cerebellar cortex. J Neurosci, 19(24), 10931-10939.

Batton, R. R., Jayaraman, A., Ruggiero, D., & Carpenter, M. B. (1977). Fastigial efferent projections in the monkey: an autoradiographic study. J Comp Neurol, 174(2), 281-305.

Blazquez, P. M., & Yakusheva, T. A. (2015). GABA-A Inhibition Shapes the Spatial and Temporal Response Properties of Purkinje Cells in the Macaque Cerebellum. Cell Rep, 11(7), 1043-1053.

Bridgeman, B., Hendry, D., & Stark, L. (1975). Failure to detect displacement of the visual world during saccadic eye movements. Vision Res, 15(6), 719-722.

Bridgeman, B., & Palca, J. (1980). The role of microsaccades in high acuity observational tasks. Vision Res, 20(9), 813-817.

Büttner, U., Fuchs, A. F., Markert-Schwab, G., & Buckmaster, P. (1991). Fastigial nucleus activity in the alert monkey during slow eye and head movements. J Neurophysiol, 65(6), 1360-1371.

Buttner, U., Straube, A., & Spuler, A. (1994). Saccadic dysmetria and "intact" smooth pursuit eye movements after bilateral deep cerebellar nuclei lesions. J Neurol Neurosurg Psychiatry, 57(7), 832-834.

Cui, J., Wilke, M., Logothetis, N. K., Leopold, D. A., & Liang, H. (2009). Visibility states modulate microsaccade rate and direction. Vision Res, 49(2), 228-236.

de Brouwer, S., Yuksel, D., Blohm, G., Missal, M., & Lefevre, P. (2002). What triggers catch-up saccades during visual tracking? J Neurophysiol, 87(3), 1646-1650.

Dietrichs, E., & Walberg, F. (1985). The cerebellar nucleo-olivary and olivo-cerebellar nuclear projections in the cat as studied with anterograde and retrograde transport in the same animal after implantation of crystalline WGA-HRP. II. The fastigial nucleus. Anat Embryol (Berl), 173(2), 253-261.

Ditchburn, R. W., & Ginsborg, B. L. (1952). Vision with a stabilized retinal image. Nature, 170(4314), 36-37.

El-Shamayleh Y, Kojima Y, Soetedjo R, Horwitz G.D. (2017). Selective Optogenetic Control of Purkinje Cells in Monkey Cerebellum. Neuron, pii: S0896-6273(17)30500-7.

Enderle, J. D., Wolfe, J. W., & Yates, J. T. (1984). The linear homeomorphic saccadic eye movement model--a modification. IEEE Trans Biomed Eng, 31(11), 717-720.

Fuchs, A. F. (1967). Saccadic and smooth pursuit eye movements in the monkey. J Physiol, 191(3), 609-631.

Fuchs, A. F., Robinson, F. R., & Straube, A. (1993). Role of the caudal fastigial nucleus in saccade generation. I. Neuronal discharge pattern. J Neurophysiol, 70(5), 1723-1740.

Fuchs, A. F., Robinson, F. R., & Straube, A. (1994). Participation of the caudal fastigial nucleus in smooth-pursuit eye movements. I. Neuronal activity. J Neurophysiol, 72(6), 2714-2728.

Fujikado, T., & Noda, H. (1987). Saccadic eye movements evoked by microstimulation of lobule VII of the cerebellar vermis of macaque monkeys. J Physiol, 394, 573-594.

Gass, J. D. (1999). Muller cell cone, an overlooked part of the anatomy of the fovea centralis: hypotheses concerning its role in the pathogenesis of macular hole and foveomacualr retinoschisis. Arch Ophthalmol, 117(6), 821-823.

Goffart, L., Chen, L. L., & Sparks, D. L. (2004). Deficits in saccades and fixation during muscimol inactivation of the caudal fastigial nucleus in the rhesus monkey. J Neurophysiol, 92(6), 3351-3367.

Golla, H., Tziridis, K., Haarmeier, T., Catz, N., Barash, S., & Thier, P. (2008). Reduced saccadic resilience and impaired saccadic adaptation due to cerebellar disease. Eur J Neurosci, 27(1), 132-144.

Guthrie, B. L., Porter, J. D., & Sparks, D. L. (1983). Corollary discharge provides accurate eye position information to the oculomotor system. Science, 221(4616), 1193-1195.

Helmchen, C., Straube, A., & Büttner, U. (1994). Saccade-related activity in the fastigial oculomotor region of the macaque monkey during spontaneous eye movements in light and darkness. Exp Brain Res, 98(3), 474-482.

Hepp, K., Henn, V., & Jaeger, J. (1982). Eye movement related neurons in the cerebellar nuclei of the alert monkey. Exp Brain Res, 45(1-2), 253-264.

Herculano-Houzel, S. (2009). The human brain in numbers: a linearly scaled-up primate brain. Front Hum Neurosci, 3, 31.

Homma, Y., Nonaka, S., Matsuyama, K., & Mori, S. (1995). Fastigiofugal projection to the brainstem nuclei in the cat: an anterograde PHA-L tracing study. Neurosci Res, 23(1), 89-102.

Ignashchenkova, A., Dash, S., Dicke, P. W., Haarmeier, T., Glickstein, M., & Thier, P. (2009). Normal spatial attention but impaired saccades and visual motion perception after lesions of the monkey cerebellum. J Neurophysiol, 102(6), 3156-3168.

Ikeda, Y., Noda, H., & Sugita, S. (1989). Olivocerebellar and cerebelloolivary connections of the oculomotor region of the fastigial nucleus in the macaque monkey. J Comp Neurol, 284(3), 463-488.

Inaba, N., Iwamoto, Y., & Yoshida, K. (2003). Changes in cerebellar fastigial burst activity related to saccadic gain adaptation in the monkey. Neurosci Res, 46(3), 359-368.

Kahlon, M., & Lisberger, S. G. (2000). Changes in the responses of Purkinje cells in the floccular complex of monkeys after motor learning in smooth pursuit eye movements. J Neurophysiol, 84(6), 2945-2960.

Kase, M., Miller, D. C., & Noda, H. (1980). Discharges of Purkinje cells and mossy fibres in the cerebellar vermis of the monkey during saccadic eye movements and fixation. J Physiol, 300, 539-555.

Keller, E. L., & Robinson, D. A. (1971). Absence of a stretch reflex in extraocular muscles of the monkey. J Neurophysiol, 34(5), 908-919.

Ko, H. K., Poletti, M., & Rucci, M. (2010). Microsaccades precisely relocate gaze in a high visual acuity task. Nat Neurosci, 13(12), 1549-1553.

Kowler, E., & Steinman, R. M. (1980). Small saccades serve no useful purpose: reply to a letter by R. W. Ditchburn. Vision Res, 20(3), 273-276.

Krauzlis, R. J., & Miles, F. A. (1998). Role of the oculomotor vermis in generating pursuit and saccades: effects of microstimulation. J Neurophysiol, 80(4), 2046-2062.

Lekwuwa, G., Barnes, G., & Grealy, M. (1995). Effects of prediction on smooth pursuit velocity gain in cerebellar patients and controls. Studies in Visual Information Processing, 6, 119-129.

Li, K. Y., Tiruveedhula, P., & Roorda, A. (2010). Intersubject variability of foveal cone photoreceptor density in relation to eye length. Invest Ophthalmol Vis Sci, 51(12), 6858-6867.

Lisberger, S. G., & Fuchs, A. F. (1978). Role of primate flocculus during rapid behavioral modification of vestibuloocular reflex. I. Purkinje cell activity during visually guided horizontal smooth-pursuit eye movements and passive head rotation. J Neurophysiol, 41(3), 733-763.

Martinez-Conde, S., Macknik, S. L., & Hubel, D. H. (2004). The role of fixational eye movements in visual perception. Nat Rev Neurosci, 5(3), 229-240.

May, P. J., Hartwich-Young, R., Nelson, J., Sparks, D. L., & Porter, J. D. (1990). Cerebellotectal pathways in the macaque: implications for collicular generation of saccades. Neuroscience, 36(2), 305-324.

McCamy, M. B., Najafian Jazi, A., Otero-Millan, J., Macknik, S. L., & Martinez-Conde, S. (2013). The effects of fixation target size and luminance on microsaccades and square-wave jerks. PeerJ, 1, e9.

McConkie, G. W., & Currie, C. B. (1996). Visual stability across saccades while viewing complex pictures. J Exp Psychol Hum Percept Perform, 22(3), 563-581.

Medina, J. F., & Lisberger, S. G. (2008). Links from complex spikes to local plasticity and motor learning in the cerebellum of awake-behaving monkeys. Nat Neurosci, 11(10), 1185-1192.

Medina, J. F., & Lisberger, S. G. (2009). Encoding and decoding of learned smooth-pursuit eye movements in the floccular complex of the monkey cerebellum. J Neurophysiol, 102(4), 2039-2054.

Moschner, C., Crawford, T. J., Heide, W., Trillenberg, P., Kompf, D., & Kennard, C. (1999). Deficits of smooth pursuit initiation in patients with degenerative cerebellar lesions. Brain, 122 (Pt 11), 2147-2158.

Moschner, C., Zangemeister, W. H., & Demer, J. L. (1996). Anticipatory smooth eye movements of high velocity triggered by large target steps: normal performance and effect of cerebellar degeneration. Vision Res, 36(9), 1341-1348.

Moschovakis, A. K. (1994). Neural network simulations of the primate oculomotor system. I. The vertical saccadic burst generator. Biol Cybern, 70(3), 291-302.

Noda, H., & Fujikado, T. (1987). Topography of the oculomotor area of the cerebellar vermis in macaques as determined by microstimulation. J Neurophysiol, 58(2), 359-378.

Noda, H., Murakami, S., Yamada, J., Tamada, J., Tamaki, Y., & Aso, T. (1988). Saccadic eye movements evoked by microstimulation of the fastigial nucleus of macaque monkeys. J Neurophysiol, 60(3), 1036-1052.

Noda, H., Sugita, S., & Ikeda, Y. (1990). Afferent and efferent connections of the oculomotor region of the fastigial nucleus in the macaque monkey. J Comp Neurol, 302(2), 330-348.

Noda, H., & Warabi, T. (1986). Discharges of Purkinje cells in monkey's flocculus during smooth-pursuit eye movements and visual stimulus movements. Exp Neurol, 93(2), 390-403.

Ohki, M., Kitazawa, H., Hiramatsu, T., Kaga, K., Kitamura, T., Yamada, J., et al. (2009). Role of primate cerebellar hemisphere in voluntary eye movement control revealed by lesion effects. J Neurophysiol, 101(2), 934-947.

Ohtsuka, K., & Noda, H. (1991). Saccadic burst neurons in the oculomotor region of the fastigial nucleus of macaque monkeys. J Neurophysiol, 65(6), 1422-1434.

Ohtsuka, K., & Noda, H. (1992). Burst discharges of fastigial neurons in macaque monkeys are driven by vision- and memory-guided saccades but not by spontaneous saccades. Neurosci Res, 15(3), 224-228.

Optican, L. M., & Robinson, D. A. (1980). Cerebellar-dependent adaptive control of primate saccadic system. J Neurophysiol, 44(6), 1058-1076.

Poletti, M., Listorti, C., & Rucci, M. (2010). Stability of the visual world during eye drift. J Neurosci, 30(33), 11143-11150.

Poletti, M., Listorti, C., & Rucci, M. (2013). Microscopic eye movements compensate for nonhomogeneous vision within the fovea. Curr Biol, 23(17), 1691-1695.

Putnam, N. M., Hofer, H. J., Doble, N., Chen, L., Carroll, J., & Williams, D. R. (2005). The locus of fixation and the foveal cone mosaic. J Vis, 5(7), 632-639.

Rambold, H., Churchland, A., Selig, Y., Jasmin, L., & Lisberger, S. G. (2002). Partial ablations of the flocculus and ventral paraflocculus in monkeys cause linked deficits in smooth pursuit eye movements and adaptive modification of the VOR. J Neurophysiol, 87(2), 912-924.

Rashbass, C. (1961). The relationship between saccadic and smooth tracking eye movements. J Physiol, 159, 326-338.

Ritchie, L. (1976). Effects of cerebellar lesions on saccadic eye movements. J Neurophysiol, 39(6), 1246-1256.

Robinson, D. A. (1964). THE MECHANICS OF HUMAN SACCADIC EYE MOVEMENT. J Physiol, 174, 245-264.

Robinson, D. A. (1965). The mechanics of human smooth pursuit eye movement. J Physiol, 180(3), 569-591.

Robinson, D. A., Gordon, J. L., & Gordon, S. E. (1986). A model of the smooth pursuit eye movement system. Biol Cybern, 55(1), 43-57.

Robinson, F. R., Straube, A., & Fuchs, A. F. (1993). Role of the caudal fastigial nucleus in saccade generation. II. Effects of muscimol inactivation. J Neurophysiol, 70(5), 1741-1758.

Robinson, F. R., Straube, A., & Fuchs, A. F. (1997). Participation of caudal fastigial nucleus in smooth pursuit eye movements. II. Effects of muscimol inactivation. J Neurophysiol, 78(2), 848-859.

Ron, S., & Robinson, D. A. (1973). Eye movements evoked by cerebellar stimulation in the alert monkey. J Neurophysiol, 36(6), 1004-1022.

Ruigrok, T. J., & Voogd, J. (1990). Cerebellar nucleo-olivary projections in the rat: an anterograde tracing study with Phaseolus vulgaris-leucoagglutinin (PHA-L). J Comp Neurol, 298(3), 315-333.

Sato, H., & Noda, H. (1991). Divergent axon collaterals from fastigial oculomotor region to mesodiencephalic junction and paramedian pontine reticular formation in macaques. Neurosci Res, 11(1), 41-54.

Sato, H., & Noda, H. (1992). Posterior vermal Purkinje cells in macaques responding during saccades, smooth pursuit, chair rotation and/or optokinetic stimulation. Neurosci Res, 12(5), 583-595.

Scudder, C. A. (1988). A new local feedback model of the saccadic burst generator. J Neurophysiol, 59(5), 1455-1475.

Stone, L. S., & Lisberger, S. G. (1990). Visual responses of Purkinje cells in the cerebellar flocculus during smooth-pursuit eye movements in monkeys. I. Simple spikes. J Neurophysiol, 63(5), 1241-1261.

Straube, A., Helmchen, C., Robinson, F., Fuchs, A., & Buttner, U. (1994). Saccadic dysmetria is similar in patients with a lateral medullary lesion and in monkeys with a lesion of the deep cerebellar nucleus. J Vestib Res, 4(5), 327-333.

Sugita, S., & Noda, H. (1991). Pathways and terminations of axons arising in the fastigial oculomotor region of macaque monkeys. Neurosci Res, 10(2), 118-136.

Sun, Z., Junker, M., Dicke, P. W., & Thier, P. (2016). Individual neurons in the caudal fastigial oculomotor region convey information on both macro- and microsaccades. Eur J Neurosci, 44(8), 2531-2542.

Sun, Z., Smilgin, A., Junker, M., Dicke, P. W., & Thier, P. (2017). Short-term adaptation of saccades does not affect smooth pursuit eye movement initiation. J Vis, 17 (9), 19.

Sun, Z., Smilgin, A., Junker, M., Dicke, P. W., & Thier, P. (2017). The same oculomotor vermal Purkinje cells encode the different kinematics of saccades and of smooth pursuit eye movements. Sci Rep, 7, 40613.

Suzuki, D. A., & Keller, E. L. (1988). The role of the posterior vermis of monkey cerebellum in smooth-pursuit eye movement control. II. Target velocity-related Purkinje cell activity. J Neurophysiol, 59(1), 19-40.

Takagi, M., Zee, D. S., & Tamargo, R. J. (1998). Effects of lesions of the oculomotor vermis on eye movements in primate: saccades. J Neurophysiol, 80(4), 1911-1931.

Takagi, M., Zee, D. S., & Tamargo, R. J. (2000). Effects of lesions of the oculomotor cerebellar vermis on eye movements in primate: smooth pursuit. J Neurophysiol, 83(4), 2047-2062.

Thaler, L., Schutz, A. C., Goodale, M. A., & Gegenfurtner, K. R. (2013). What is the best fixation target? The effect of target shape on stability of fixational eye movements. Vision Res, 76, 31-42.

Thiele, A., Henning, P., Kubischik, M., & Hoffmann, K. P. (2002). Neural mechanisms of saccadic suppression. Science, 295(5564), 2460-2462.

Vahedi, K., Rivaud, S., Amarenco, P., & Pierrot-Deseilligny, C. (1995). Horizontal eye movement disorders after posterior vermis infarctions. J Neurol Neurosurg Psychiatry, 58(1), 91-94.

Vilis, T., & Hore, J. (1981). Characteristics of saccadic dysmetria in monkeys during reversible lesions of medial cerebellar nuclei. J Neurophysiol, 46(4), 828-838.

Westheimer, G. (1954). Eye movement responses to a horizontally moving visual stimulus. AMA Arch Ophthalmol, 52(6), 932-941.

Winterson, B. J., & Collewijn, H. (1976). Microsaccades during finely guided visuomotor tasks. Vision Res, 16(12), 1387-1390.

Yamada, J., & Noda, H. (1987). Afferent and efferent connections of the oculomotor cerebellar vermis in the macaque monkey. J Comp Neurol, 265(2), 224-241.

Zee, D. S., Yamazaki, A., Butler, P. H., & Gucer, G. (1981). Effects of ablation of flocculus and paraflocculus of eye movements in primate. J Neurophysiol, 46(4), 878-899.

Zee, D. S., Yee, R. D., Cogan, D. G., Robinson, D. A., & Engel, W. K. (1976). Ocular motor abnormalities in hereditary cerebellar ataxia. Brain, 99(2), 207-234.

Appended papers/manuscripts

Appendix 1: Sun, Z., Smilgin, A., Junker M., Dicke, PW., their, P. (2017) The same oculomotor vermal Purkinje cells encode the different kinematics of saccades and of smooth pursuit eye movements. Sci Rep, 7, 40613.

Appendix 2: Sun, Z. *, Smilgin, A. *, Junker M., Dicke, PW., their, P. (2017) Short-term adaptation of saccades does not affect smooth pursuit eye movement initiation. J Vis, 17 (9), 19-19. (*co-first author).

Appendix 3: Sun, Z., Junker, M., Dicke, P.W., Thier, P. (2016) Individual neurons in the caudal fastigial oculomotor region convey information on both macro- and microsaccades. Eur J Neurosci, 44(8), 2531-2542.

Personal contribution statement

Study 1: Sun, Z., Smilgin, A., Junker M., Dicke, PW., Thier, P. (2017) The same oculomotor vermal Purkinje cells encode the different kinematics of saccades and of smooth pursuit eye movements. Sci Rep, 7, 40613.

Z.S., A.S., M.J., P.W.D. and P.T. designed research, A.S., M.J. and **Z.S.** performed research, **Z.S.** analyzed the data; **Z.S.** wrote the manuscript and revised it based on **P.T.**'s comments and suggestions. All authors read and approved the final manuscript.

Study 2: Sun, Z.*, Smilgin, A.*, Junker, M., Dicke, P.W., Thier, P. (2017) Short-term adaptation of saccades does not affect smooth pursuit eye movement initiation. J Vis, 17 (9), 19-19. (*co-first author).

Z.S., A.S., M.J and P.W.D. acquired the data. **Z.S.** and A.S. analyzed the data. **Z.S.**, A.S. and P.T. designed the paradigms. **Z.S.** wrote the manuscript and revised it based on **P.T.**'s comments and suggestions. All authors reviewed the manuscript.

Study 3: Sun, Z., Junker, M., Dicke, P.W., Thier, P. (2016) Individual neurons in the caudal fastigial oculomotor region convey information on both macro- and microsaccades. Eur J Neurosci, 44(8), 2531-2542.

Z.S. and P.T. conceived and designed the experiments. **Z.S.** collected the data. **Z.S.** and M.J. analyzed the data. **Z.S.** wrote the manuscript and revised it based on **P.T.**'s comments and suggestions. All authors reviewed the manuscript.

Acknowledgments

First of all, I would like to thank my supervisor Prof. Peter Thier for offering such opportunity to work at Department of Cognitive Neurology of the Hertie Institute for Clinical Brain Research. I am really grateful to him for his support, supervision and guidance throughout my PhD thesis. I would like to thank my advisory board members Prof. Uwe Ilg and Prof. Fahad Sultan for their valuable feedback. I would also like to thank Dr. Peter W. Dicke for his technical support and many scientific discussions.

I thank all my colleagues in the Department of Cognitive Neurology for their help and useful feedback during my talks. Especially, I express my gratitude to my co-workers Aleksandra Smilgin and Marc Junker for nice collaboration and stimulating discussions. I really enjoyed working together with them and I had great time during my study. Many thanks to Ute Großhennig for her experimental assistance.

I want to express my special gratitude to my family. Without their endless love and constant support over the years, I could not have accomplished this much. I am beyond grateful for what my parents have done for me.

Appendix 1:

Sun, Z., Smilgin, A., Junker M., Dicke, PW., Thier, P. (2017) The same oculomotor vermal Purkinje cells encode the different kinematics of saccades and of smooth pursuit eye movements. Sci Rep, 7, 40613.

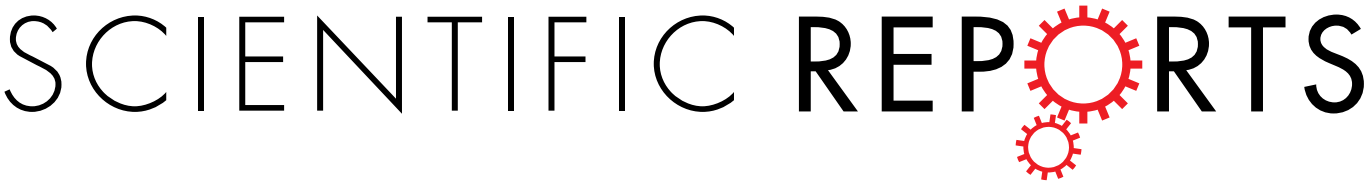

OPEN

The same oculomotor vermal Purkinje cells encode the different kinematics of saccades and of smooth pursuit eye movements

Received: 14 September 2016
Accepted: 07 December 2016
Published: 16 January 2017

Zongpeng Sun[1,2], Aleksandra Smilgin[1,2], Marc Junker[1,2], Peter W. Dicke[1] & Peter Thier[1]

Saccades and smooth pursuit eye movements (SPEM) are two types of goal-directed eye movements whose kinematics differ profoundly, a fact that may have contributed to the notion that the underlying cerebellar substrates are separated. However, it is suggested that some Purkinje cells (PCs) in the oculomotor vermis (OMV) of monkey cerebellum may be involved in both saccades and SPEM, a puzzling finding in view of the different kinematic demands of the two types of eye movements. Such 'dual' OMV PCs might be oddities with little if any functional relevance. On the other hand, they might be representatives of a generic mechanism serving as common ground for saccades and SPEM. In our present study, we found that both saccade- and SPEM-related responses of individual PCs could be predicted well by linear combinations of eye acceleration, velocity and position. The relative weights of the contributions that these three kinematic parameters made depended on the type of eye movement. Whereas in the case of saccades eye position was the most important independent variable, it was velocity in the case of SPEM. This dissociation is in accordance with standard models of saccades and SPEM control which emphasize eye position and velocity respectively as the relevant controlled state variables.

Saccades and smooth pursuit eye movements (SPEM) are two synergistic types of eye movements which allow the visual system to exploit the advantages of foveal vision for the analysis of objects of interest ('targets'). Whereas saccades shift the target image onto the fovea, SPEM are deployed to stabilize it there despite movements of the target relative to the observer. The kinematics of these two types of goal-directed eye movements differ profoundly. Saccades are fast, short-duration eye movements, reaching peak velocities of many 100°/s. These features ensure that the time during which vision is compromised because of retinal image slip is kept to a minimum. On the other hand, SPEM are continuous eye movements confined to velocities below 10°/s or at most 30–50°/s[1–4]. To accommodate the very different kinematics of saccades and SPEM, different control strategies are needed. This is why the discussion of their implementation has been dominated by the assumption of specialization and segregation[5] (for another view see refs 6 and 7). Early work on the oculomotor role of the cerebellum seemed to be in line with the concept of segregation, namely the flocculus/paraflocculus as cerebellar substrate of SPEM[8] and the oculomotor vermis (OMV) subserving saccades[9]. Yet, it later became clear that lesions of the OMV not only impair saccades[10–12] but also the initiation of SPEM[13–15], indicating a role of OMV in both types of eye movements. Correspondingly, electrical stimulation of the OMV not only evoke saccades[16,17] but also pursuit-like slow eye movements[4]. Finally, single-unit recording studies have shown that some Purkinje cells (PC) in the OMV respond to both saccades and SPEM[18,19]. Are these 'dual' PCs representative of OMV PCs at large or are they oddities with little if any functional relevance? However, if these PC units are representative of the whole population rather than oddities, this would probably suggest that such PCs offer a hitherto unknown functional contribution to an aspect of eye movements shared by saccades and SPEM.

Studies on the role of the OMV in SPEM have suggested that it may play a major role in controlling eye velocity in specific directions. The earliest evidence came from a study of smooth-pursuit of targets moving sinusoidally along the horizontal[20]. The authors of this study reasoned that responses reflected primarily eye velocity

[1]Department of Cognitive Neurology, Hertie Institute for Clinical Brain Research, University of Tübingen, 72076 Tübingen, Germany. [2]Graduate School of Neural and Behavioural Sciences, International Max Planck Research School for Cognitive and Systems Neuroscience, University of Tübingen, 72074 Tübingen, Germany. Correspondence and requests for materials should be addressed to P.T. (email: thier@uni-tuebingen.de)

because OMV PC simple spike (SS) units increased their modulation with increasing target speed. Later work, employing pursuit targets that moved according to a sinusoidal profile, showed that at least some neurons in the OMV seemed to prefer gaze velocities in directions other than the horizontal[21]. In our previous work on smooth-pursuit- related OMV PC SS units, we explored the kinematic preferences in more detail by modeling the relationship between discharge and the early, open-loop SPEM based on a linear combination of eye acceleration, velocity and position. This analysis clearly indicated that indeed eye velocity is the most relevant kinematic parameter[22].

Given that velocities of saccadic eye movements are much higher than those of SPEM, a simple linear encoding of eye velocity for both types of eye movements would not work and a coding scheme reflecting the different kinematics of saccades and SPEM should be expected. Moreover, how representative are the 'dual' PC SS units? To answer these questions we set out to compare the discharge characteristics of eye movement-related PC SS units recorded from the OMV during saccades and SPEM in the same direction or to saccades and SPEM in 8 directions. We report that many PC SS units are sensitive to saccades and SPEM and, moreover, that different kinematic parameters are emphasized during SPEM and saccades.

Materials and Methods

Animals and surgical procedures. Two male rhesus monkeys E and I (Macaca mulatta, males, 10 and 6 years old; purchased from the German Primate Centre, Göttingen, Germany) were subjects in this study. In both monkeys, the recording chamber (diameter 30 mm) was implanted in the sagittal midline, tilted posterior by 20° (monkey E) and 40° (monkey I), respectively, allowing us to explore larger parts of their brainstem. For monkey E, in order to optimally reach the OMV, the chamber was fitted with an adapter reducing the tilt angle by 20°, while in monkey I, an adapter reducing it by 35° was chosen (see Supplementary Fig. S1). The experiments on these animals including the surgical and behavioural protocols were approved by the Regierungspräsidium Baden-Württemberg (Ref. 35; permit-number N6/13), conducted in accordance with the guidelines of the National Institutes of Health for Care and Use of Laboratory Animals and supervised by the veterinary administration (Landratsamt Tübingen (Abt. 32)).

Behavioural tasks. The monkeys were seated head-fixed 40 cm in front of a CRT monitor in darkness. The eye position measured by eye coil was calibrated using a 9-point calibration that considered linear, quadratic and mixed term dependencies (typical grid size: 30×30°, target diameter: 0.4°). Next they were trained to keep stable eye fixation on the visual target (dot diameter 0.2–0.4°, depending on animal), displayed on a CRT monitor in front of them at a distance of 40 cm. Proper fixation was assumed if the eyes stayed within an invisible rectangular window of 1.5–4° around every displayed target and a trial was aborted if eye position exceeded the limits of this window.

Visually guided saccades. The monkeys were required to make precise saccades starting from the straight ahead fixation dot to a peripheral target having the same size and appearance. The peripheral target was presented in 8 possible positions in the frontoparallel plane (rightward: 0°, right-up: 45°, upward: 90°, left-up: 135°, leftward: 180°, left-down: 225°, downward: 270°, right-down: 315°) at constant eccentricities of 10°. The peripheral target appeared after a variable (500–1000 ms) time of fixation at which time the central target was turned off. The transition from the central to the peripheral target was the go signal for the monkey to make a saccade to the peripheral target and to maintain fixation there for at least 300 ms before being allowed to return to straight ahead. A trial was aborted if the monkey did not initiate a saccade within 400 ms after the go signal. The eyes had to stay within an invisible eye position window (1.5–4°) centered on the target independent of its location. This window was transiently turned off during the transition of the target to the periphery. Target directions were randomly chosen from trial to trial.

In many experiments, we kept the saccade target direction constant in order to be able to vary target eccentricity randomly between 10°, 7° and 4°. Here, in the interest of time, the experimenter tested a few trials of up, down, left and right saccades in order to choose a "best" direction from this set by listening to the audiomonitor and inspecting the online records of the spike trains. In these experiments the direction of smooth pursuit eye movements tested (see the following) was the same and likewise constant.

Smooth pursuit eye movements (SPEM). To evoke SPEM with no catch-up saccades in at least the first 200–250 ms after eye movement onset we deployed a step-ramp paradigm[23]. Each SPEM trial started with a variable period of fixation on the target displayed in the central position for 500–1500 ms. Then the target stepped by 1.4–2.4° in a particular direction, a step that was immediately followed by a ramp-like movement of the target at a velocity of 12°/s in the opposite direction. The pursuit directions were chosen from the same set of directions also used for saccades. The step amplitude was adjusted individually for each monkey such that the target ramp would have moved the image of the target back into the fovea at the time of the onset of the smooth-pursuit eye movement, thereby eliminating the need for catch up saccades. The trial duration was always 2400 ms. The eye position control window had a size of 2–4° throughout a trial.

In experiments, in which saccade- and SPEM-related responses were collected in 8 directions, the two types of eye movements were studied in separate blocks whose order changed from neuron to neuron. Within individual blocks, the 8 eye movement directions were presented randomly interleaved. In experiments, in which 10°, 7° and 4° saccades and SPEM were studied in an identical direction, trials were presented randomly interleaved.

Electrophysiological procedures. Action potentials of PCs were recorded extracellularly using glass-coated tungsten microelectrodes (1–2 MΩ impedance at 1 kHz; Alpha Omega Engineering, Nazareth, Israel) advanced with an 8-probe electrode system (Alpha Omega Engineering, Nazareth, Israel). In most cases

we used maximally 4 electrodes, arranged linearly either along the rostrocaudal or the medio-lateral axis and separated by 2 mm each. We approached the OMV by using the stereotaxic coordinates provided by the anatomical MRI scans and identified the OMV by resorting to well established criteria, namely the dense saccade-related granule cell background and the appearance of saccade-related single units in the neighbouring layers. The electrode signal was band-pass filtered for frequencies from 300 to 3000 Hz to enable the isolation of spikes. SS and CS were detected online by using a Multi Spike Detector (Alpha Omega Engineering, Nazareth, Israel) which detects and sorts spikes according to the features of template waveforms.

Data analysis. All analyses were performed with in-house Matlab programs (The MathWorks Inc., Natick, MA). Saccades were automatically detected by applying an eye velocity threshold of 20°/s. The detection of the onset of SPEM required several computational steps. A first approximation of movement onset was obtained by identifying the time point at which the eye velocity exceeded the mean eye velocity in the first 80 ms after the onset of the target ramp by three standard deviations for 40 consecutive milliseconds. Then two linear regressions were fitted to the eye velocity records - the first one on the eye velocity in the 200 ms before this time point and the second one on the 150 ms to follow. The interception point of the two regression lines was used as final estimate of SPEM onset. SPEM trials were discarded if they contained saccades in the first 200 ms after SPEM onset.

To detect if the recorded PCs demonstrated saccade-related SS responses, we compared the mean SS firing rate during the baseline period (100–300 ms before saccade onset) with the mean SS firing rate during 100 ms before until 200 ms after saccade onset for each of the 8 saccade directions using a Wilcoxon signed-rank test ($p < 0.05$). A PC SS unit was considered to be saccade-related if it showed a significant SS firing rate modulation in at least one saccade direction. In order to pinpoint the preferred direction of neurons, we fitted the plot of discharge rate as function of direction with a sine function. Neurons for which this fit was significant (χ^2 test, $p < 0.05$) were considered in a subsequent analysis of direction preferences in the sample. PC SS units with saccade-related activity beyond or below baseline firing rate by 3 times standard deviation were classified as bursting or pausing units, respectively. If both significant bursting and pausing components were found in a PC unit, this unit was considered as biphasic and both components were considered independently in the later analysis of direction selectivity. For the bursting component the direction with the largest discharge as predicted by the sine fit was taken as the preferred one and correspondingly in the case of a pausing component the direction with the lowest predicted discharge. For units with only one component in the firing patterns, the angular distance between the preferred directions was calculated by comparing the preferred directions for saccades and SPEM based on that component. For units with two components during at least one type of eye movement, the angular distance was calculated by comparing the preferred directions based on the component(s) present in the responses to both types of eye movements.

To assess if PC SS units exhibited SPEM-related modulation we compared the SS firing rate during the baseline period with the SS firing rate in the period of 100 ms before and 200 ms after SPEM onset for each of the SPEM directions tested (Wilcoxon sign rank, $p < 0.05$)[24]. The preferred direction of those neurons, for which the fit was significant (χ^2 test, $p < 0.05$), was computed separately for bursting and pausing components, which is similar to what we did for saccade-related neurons.

To analyse the relationship between the SS discharge rate (FR) and eye movement kinematics within a time period of −100 to +200 ms relative to movement onset, we fitted the average spike density function of individual PC SS units with a linear model with eye position (pos(t)), velocity (vel(t)) and acceleration (acc(t)) as independent variables.

$$\mathrm{FR}(t - \mathrm{delta}) = a * \mathrm{pos}(t) + b * \mathrm{vel}(t) + c * \mathrm{acc}(t) + d$$

The coefficients a, b, c, d and the time shift delta coefficient in the above equation were chosen such as to maximize the coefficient of determination (CD), which indicates the goodness of the fit capturing the proportion of the variance in the dependent variable predicted from the independent variables. The time shift delta coefficient was restricted to values between −100 and +100 ms. To reveal the relative contributions of each kinematic variable, we omitted one or two variables in the equation and compared the resulting CD with the one for the complete fit. Cohen's D[25] was used to compare the quality of the fits between various models. It was obtained by dividing the difference between mean CDs of the two by the pooled standard deviation of their CDs. Cohen's D values bigger than 0.8 indicate 'large' effects, whereas those smaller than 0.3 reflect 'small' effects. The remainder is considered as 'medium' effect.

Results

Sample of OMV PCs. We recorded a total of 165 PCs with eye movement-related SS discharge from the OMV (n = 92 in subject E and n = 73 in subject I) (Fig. 1A). In 72 out of the 165 units, the comparison was confined to one direction chosen by the experimenter as best direction based on subjective criteria (see Methods). The other 93 units could be tested for responses to saccades and/or SPEM for the full set of 8 directions in the frontoparallel plane. For a subgroup of 60 out of the 93 units complete direction tuning functions could be obtained for both types of eye movements. In the remainder it was restricted to either saccades (15 units) or SPEM (18 units) and supplemented by a single direction test of the respective other type of eye movement. 133 out of all 165 eye movement-related units (=81%) exhibited significant discharge modulation for saccades and SPEM in the same direction. As summarized in Fig. 1B the numbers of neurons with eye movement-related discharge increases, decreases and, occasionally, more complex profiles (i.e. increase–decrease or decrease–increase) was comparable in the 7 groups of units distinguished in the pie chart shown in Fig. 1A. As discussed in more detail further below, response types for saccades and SPEM were mostly, but not always, congruent (97 out of

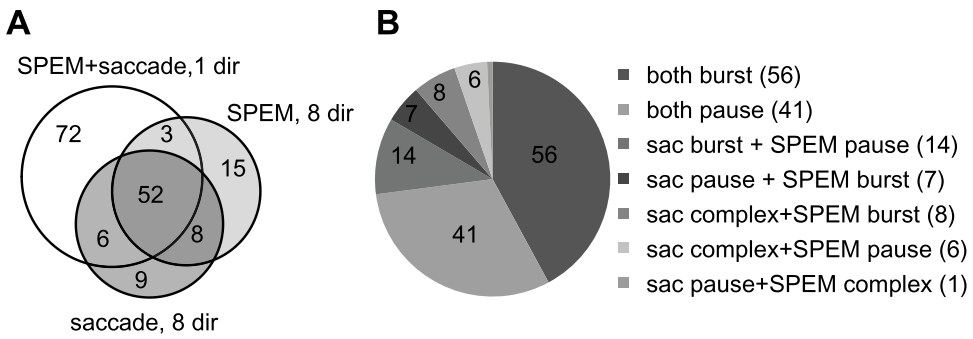

Figure 1. Breakdown of eye movement-related OMV PC SS units studied. (**A**) Venn diagram of units summarizing how many units subjected to various paradigms were considered. (**B**) The pie chart shows the numbers of units exhibiting specific firing pattern for saccades and SPEM. The number of units for each category is shown in brackets.

133 units), meaning that PCs that for instance fired a burst in conjunction with saccades usually also exhibited a discharge increase during pursuit initiation (Fig. 2A).

Individual PCs SS could exhibit their highest (in the case of bursting units) or lowest (in the case of pausing units) firing rate for any of the three saccade amplitudes tested (Fig. 2A–C). However, more units preferred 10° saccades (see Fig. 2D). This population bias for larger amplitude saccades explains that also the population firing rates calculated separately for the subgroups of bursting and pausing units exhibited the strongest modulation for the largest saccade amplitude (Fig. 2E).

PC SS encode eye movement kinematics. To study the relationship of eye movement kinematics and saccade- and SPEM-related responses respectively, we investigated how well the discharge of individual PCs could be predicted by a linear combination of eye acceleration, velocity and position independently for saccades and SPEM. To this end, the responses to saccades of 10°, 7° and 4° saccades and to SPEM were fitted separately, but for the same reference direction. This reference direction was the best direction for saccades as determined by a quantitative analysis of responses to saccades in 8 directions (58 units) or the preferred saccade direction as estimated subjectively by the experimenter, listening to the audiomonitor (75 units). Figure 3 summarizes the results obtained for the 133 units subjected to this analysis. As shown in the first three panels in column 1 of Fig. 3A–D, the mean coefficients of determination (CDs) were about 0.8 for both saccades, independent of amplitude, and for SPEM. In other words, the linear kinematic model was able to predict most of the variance in the PC simple-spike discharge rate based on the eye movement data. We next tried to estimate the contribution of each kinematic parameter by removing one out of the 3 kinematic parameters from the model or, alternatively, by keeping just 1 particular parameter. The distribution of CDs obtained after removal of eye acceleration, velocity or position respectively from the model is shown in columns 2–4 of Fig. 3A–D, whereas columns 5–7 present the CDs obtained when restricting the model to a single kinematic parameter. In the case of saccades, removal of any one or two kinematic parameters resulted in significant decreases of CDs (Friedman's 2-way rank ANOVA comparisons of the CD distribution for the 3-parameter model with the CD distributions for any of the reduced models with the factors 'model type' and 'saccade amplitude', factor model type: $p < 0.001$ and factor saccade amplitude: $p = 0.0074$). However, the extent of these decreases was different as indicated by the plot of Cohen's D for the various paired model comparisons shown in Fig. 3F: removal of eye acceleration or velocity reduced the CDs only slightly (Cohen's $D < 0.8$) to a median of 0.76 in the case of acceleration and of 0.76 in the case of velocity. On the other hand, removing eye position from the model resulted in a substantially higher decrease of the CDs to a median CD of 0.54 (Cohen's $D > 0.8$). These results indicate that eye position is the most important kinematic parameter encoded by PC SS during saccades. This conclusion is supported by constraining the linear model to one kinematic parameter only (see columns 5–7 in Fig. 3A–C). Restricting the model to eye position yielded a median CD of 0.71, only marginally smaller than the median CD obtained when applying the full-fledged model (Cohen's $D < 0.8$). On the other hand, fits based on either acceleration or velocity yielded substantially smaller median CDs (Cohen´s $D > 0.8$, eye acceleration: median CD = 0.48, eye velocity: CD= 0.43). As shown in Fig. 3F, the pattern of effect sizes of the various model modifications was similar, which indicates that the pattern was independent of saccade amplitude.

Also fitting the PC SS responses to SPEM in the same direction as the one for saccades by the linear combination of all 3 kinematic parameters yielded a substantial explanation of the variance as indicated by a median CD of 0.89 (Fig. 3D). In the case of SPEM, removal of any parameter, except acceleration, resulted in a significant CD decrease (U-test, $p < 0.05$). The analysis of Cohen's D (Fig. 3F, panel 4) demonstrated that removal of eye velocity and eye position had a medium effect ($0.3 <$ Cohen's $D < 0.8$), causing a decrease of CD to 0.79 and 0.83, respectively. On the other hand, removal of eye acceleration had weaker effects as indicated by small Cohen's D (Cohen's $D < 0.3$) (acceleration removal: median CD = 0.87, U test, $p = 0.29$). Correspondingly, restricting the model to velocity caused only a weak drop of CDs to a median CD of 0.81; $0.3 <$ Cohen's $D < 0.8$). Restricting the model to eye position caused a modest decrease to a median CD of 0.74 ($0.3 <$ Cohen's $D < 0.8$) and finally, restricting the model to eye acceleration resulted in a substantial decrease to a median CD = 0.32; Cohen's $D > 0.8$). Figure 3E provides a visual summary of the modeling results discussed before. Figure 3G depicts the distributions of the

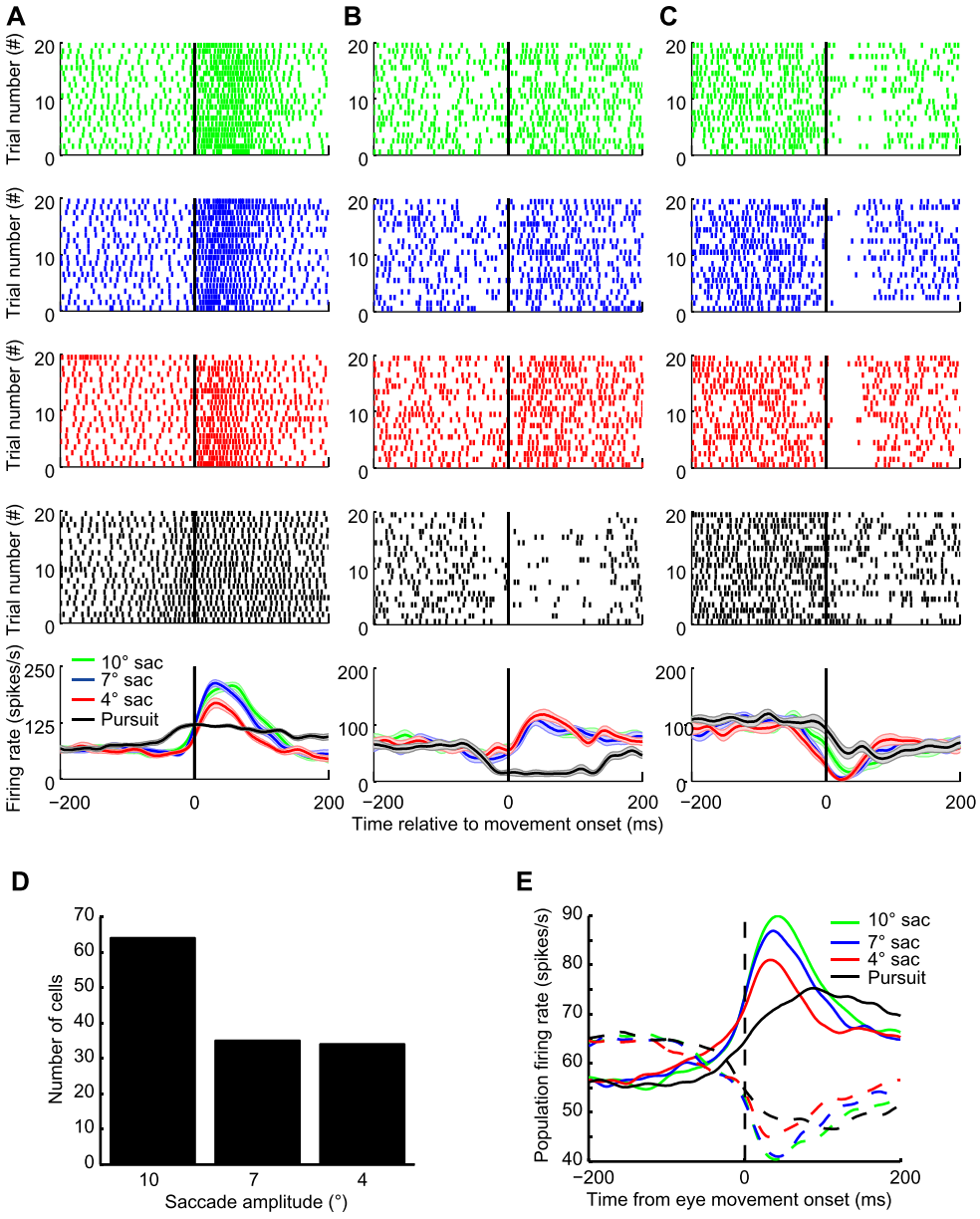

Figure 2. (**A–C**) Responses of three exemplary OMV PC SS units to saccades of different amplitudes and to SPEM in the same direction (A. 180° (left), B. 135° (upper-left), C. 0° (right)). The neuronal activity is characterized by raster plots (4 upper rows) and by mean spike density functions (last row) aligned to movement onset are plotted below the raster plot. 10°, 7°, 4° saccades and SPEM are represented in green, blue, red and black respectively. The partially transparent bands surrounding the mean spike density functions reflect the SEM. (**D**) Histogram of preferred saccades amplitudes based on n = 133 units. (**E**) Plots of population activity of all bursting units (n = 69, closed lines) and all pausing units (n = 64, dash line) for 10° (green), 7° (blue) and 4° (red) saccades. Population activity for SPEM is plotted in black.

position, velocity and acceleration coefficients for the two types of eye movements. Figure 3H shows the distribution of the time shifts (delta) between the eye movements and the discharge giving the best fits for both saccades and SPEM. The fact that the delta for saccades peaked around 10 ms indicates that the discharge usually lagged the saccade. In contrast to the distribution for saccades the one for SPEM was rather flat, reflecting a mixture of leading and lagging responses. Note that occasionally the best fits were found for latencies at the boundaries of the range of ±100 ms, both for saccades as well as for SPEM. However, the pattern of CDs obtained did not change significantly when excluding these odd cases (see Supplementary Fig. S2). Consistent with a previous study of abducens neurons, a negative correlation was found between position and velocity coefficients and eye velocity[26]. The aforementioned analysis was based on regressing discharge as a function of movement kinematics within a window of −100 to 200 ms relative to eye movement onset. One may wonder if the results depended on the choice of the window. All in all, this is not the case. As summarized in Supplementary Figs S3 and S4, the basic pattern of the relative weights of acceleration, velocity and position was the same when choosing a narrower window.

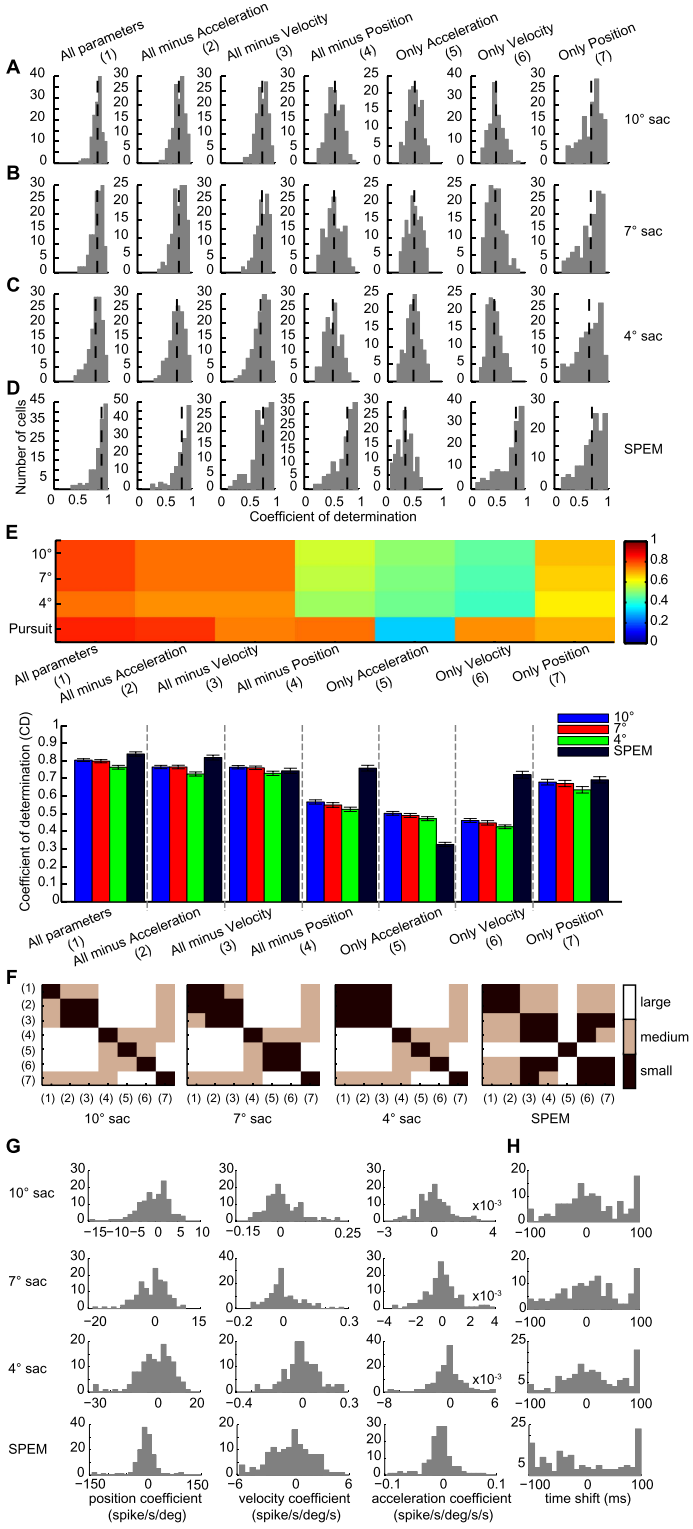

Figure 3. (**A–D**) Distribution of coefficients of determination (CDs) obtained by fitting discharge rates of individual OMV PC SS as function of the kinematic variables eye position, velocity and acceleration and different versions of slimmed down models for different amplitude saccades (**A–C**) and SPEM (**D**). The vertical dashed lines indicate the median CD for each model and paradigm. (**E**) The upper panel depicts a plot of mean CDs represented by different colors for the various models and paradigms also shown in A-D. The lower panel is a bar chart of the mean CDs. Error bars indicate SEM. Model types are identified by numbers shown in parentheses. (**F**) Plot of the size of the effect of moving from one particular type of model to another one indicated by the number as measured by Cohen´s D for 10°, 7°, 4° saccades (first three plots) and SPEM (plot on the most right). The three effect size categories (small, medium, large; see Methods) are color coded. (**G**) Distribution of position, velocity and acceleration coefficients. (**H**) Distribution of time shifts.

However, the choice of the window affected the delta, i.e. the latency between discharge and the eye movement as the clear peak in the distribution indicating that on average discharge lagging saccades was no longer visible when choosing shift ranging from −50 to 50 ms and data from 50 ms before and 100 ms after movement onset (see Supplementary Fig. S3).

Taken together, the results clearly show that the PC SS firing patterns can be well explained by the linear model. Although all three kinematic parameters make contributions to an explanation of the discharge variance, their relative weights are not the same for the two types of eye movements compared. Rather the weight profiles depend on the type of goal directed eye movement considered. Whereas saccade-related responses are dominated by eye position, those to SPEM are mostly dependent on eye velocity and eye position.

Comparison of directional preferences of eye movement-related PC SS units for saccades and SPEM. Figure 4A and B depict the responses of an exemplary PC SS unit to saccades and SPEM in 8 directions, respectively. This neuron exhibited higher firing rate for rightward saccades and lower left SPEM. To compare the directional preferences of PC SS units for saccades and SPEM, we plotted the mean saccade- and SPEM-related discharge rates as function of the 8 directions and fitted sine wave functions to the plots (see Methods for details). Figure 5 depicts the distribution of preferred directions for saccades (Fig. 5A) and SPEM (Fig. 5B). For the subset of 21 units for which preferred directions could be determined for both saccades and SPEM, we calculated the angular differences between the preferred directions for the two types of eye movements for each individual unit. Figure 5C shows the distribution of these differences. It clearly indicates a lack of relationship between preferred directions for the two types of eye movements: no unit exhibited identical preferred directions for saccades and SPEM and overall angular differences were distributed uniformly over all 4 quadrants (Rayleigh test, $p = 0.61$).

The kinematic analysis discussed above was confined to saccades and SPEM made in one and the same direction. We wondered if the kinematic preferences of PC SS units suggested by the 1-direction approach would remain valid for other directions as well. To obtain an answer we subjected the units for which datasets for all 8 directions were available for saccades (75 units) or for SPEM (78 units; intersection between the two 60 units) to a multi-linear regression analysis of discharge as function of eye movement kinematics. The analysis was carried out separately for saccades and SPEM and for each direction.

Figure 6 plots the mean CDs as function of direction for the 3 parameter model and the various 2 and 1 parameter models as described earlier for saccades (A) and for SPEM (B). The results are in line with the ones obtained for the units that were tested for one direction only. Based on a linear combination of the three kinematic parameters, the PC SS discharge could be reliably predicted as indicated by median CDs > 0.75 with eye position being the dominant parameter in case of saccades and eye velocity plus a weaker contribution of eye position in the case of SPEM. Removal of any one or two kinematic parameters resulted in a significant decrease of CDs (U test, $p < 0.001$), except the removal of acceleration in case of SPEM (U test, $p = 0.13$). Importantly, the CD patterns for different directions were quite similar (correlation $r > 0.9$, $p < 0.001$), indicating that the kinematic profiles of individual units were independent of eye movement direction. The effect sizes as gauged by Cohen's D, calculated for a 'reference' direction of 0° for saccades and SPEM are summarized in Fig. 6C and D, respectively. The pattern shown is very similar to the one yielded by the analysis of the sample of units tested for various saccade amplitudes but for only one direction of eye movements summarized in Fig. 3F.

Finally, we calculated the collective instantaneous discharge rate, separately for each direction and separately for saccades and SPEM for the same units considered before. Figure 6E,G plot the resulting collective discharge rate as function of time relative to the onset of the movement (E: smooth pursuit, G: saccades) separately for units with burst and pause responses. The panels on the right plot the CDs as function of direction for bursting units and pausing units respectively. In Fig. 6F,H we summarized the results obtained when subjecting the population discharge to the same multiple linear regression as used for the modelling of individual units. The modelling results for the population discharge were fully consistent with the results for individual units, the only difference being that the CDs (median CD > 0.87) were significantly higher than those obtained based on individual units (median CD about 0.75; t-test, $p < 0.001$). This is not surprising given the fact that averaging neuronal responses and eye movement data will lower the variance.

Discussion

The aim of this study was to compare the sensitivity of PC SS to saccades and to SPEM. The reason for this interest was the increasing evidence - discussed in the introduction - for a role of the OMV in both types of goal directed eye movements, including anecdotal descriptions of some PCs SS responding to both saccades and SPEM[18,19]. Actually, we now found that the overwhelming majority of PC SS units in the OMV are 'dual' PCs responding to both types of goal-directed eye movements. The discharge associated with saccades as well as with SPEM depended on the kinematics of the eye movements made. However, the kinematic variables of particular significance for the prediction of spike trains differed for the two. Whereas both saccade- and SPEM-related responses were influenced by all three kinematic variables considered in a multiple linear regression of discharge rate as function of eye movement kinematics, the relative weights of the kinematic variables depended on the type of goal directed eye movement performed. In the case of saccades, eye position was the most important kinematic variable, whereas it was eye velocity in the case of SPEM. These distinct kinematic profiles were independent of eye movement direction in the frontoparallel plane. Individual PC SS units not only exhibited different kinematic preferences for saccades and SPEM but, surprisingly, also unrelated directional preferences for eye movements in the frontoparallel plane.

The dependence of SPEM responses of dual OMV PC SSs on eye velocity is in line with previous reports on the kinematic preferences of OMV PCs, tested for SPEM only[22,24]. However, one might think that the strong influence of eye position in the case of saccades is at odds with a previous report[27] emphasizing a reflection of eye speed and direction in the population discharge of OMV PCs. However, closer consideration indicates that there is actually

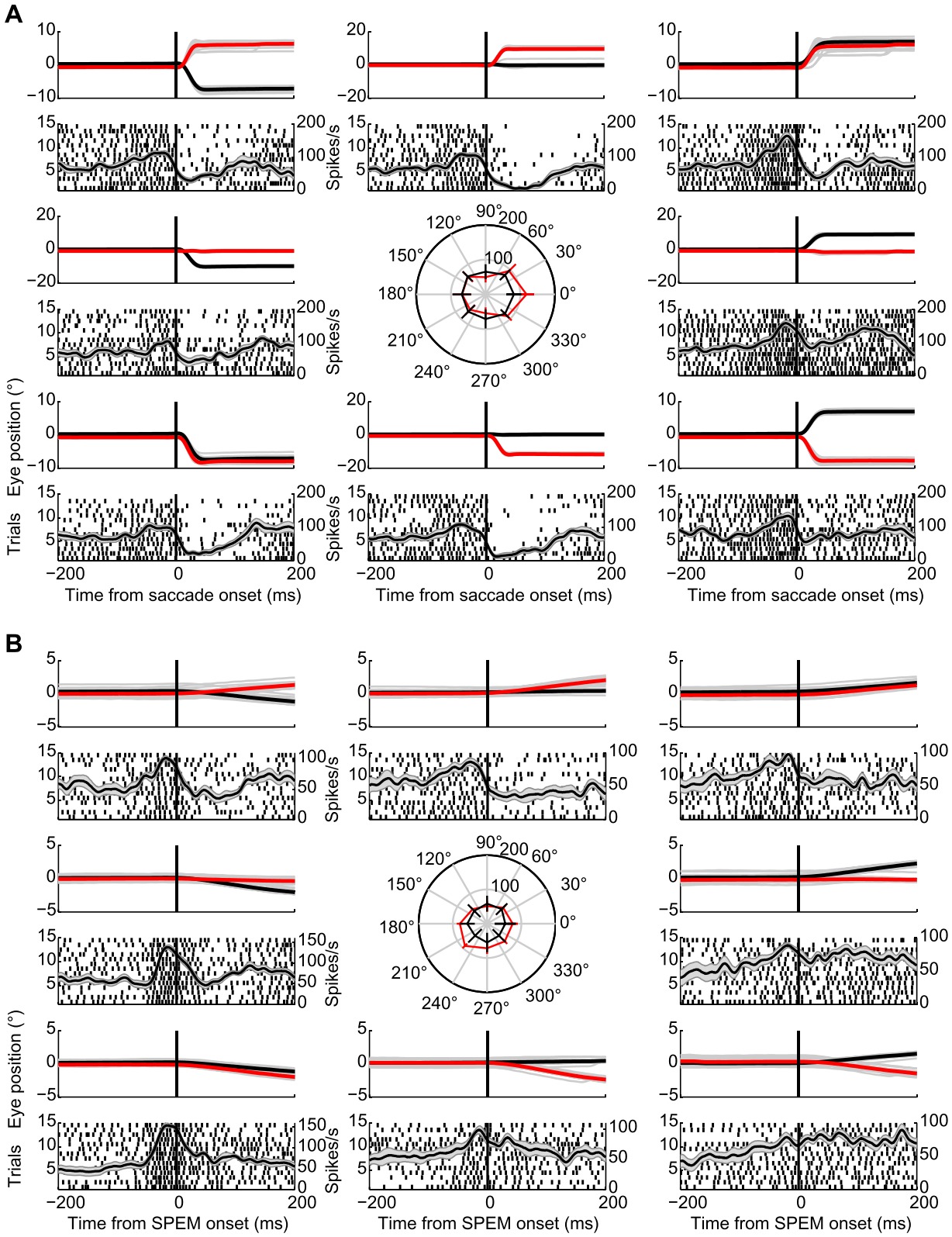

Figure 4. Responses of exemplary OMV PC SS to saccades (**A**) and SPEM (**B**) made in 8 directions in the frontoparallel plane. The top traces in each panel depict the mean horizontal (black) and vertical (red) eye positions with gray lines indicating the eye position for each trial. Neural activity is represented underneath the eye movements records by raster plots aligned to saccade onset and spike density functions plotted on top of the raster plots. The grey bands underneath the spike density functions characterize the SEM. The central panels in A and B present polar plots of mean firing rates plus standard deviation as function of direction.

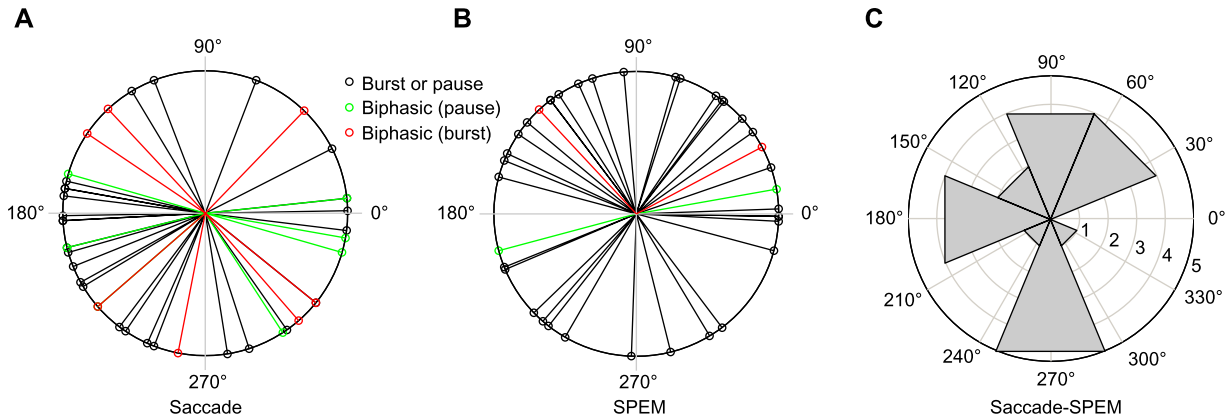

Figure 5. Polar distribution of the eye movement directions exhibiting the most vigorous firing for each neuron. (**A**) Polar distribution of preferred saccade directions (see Methods, Results for details) based on n = 41 units. Units with only one firing component are shown in black and preferred directions of the pausing and bursting components of units with two firing components are displayed in green and red, respectively. (**B**) Polar distribution of preferred SPEM directions of n = 38 units tested for SPEM-related responses. (**C**) Polar distribution of angular distance between preferred saccade and SPEM directions for the n = 21 units for which complete direction tuning data were available for both saccades and SPEM.

no contradiction whatsoever. On the one hand, our kinematic analysis also showed that eye velocity mattered, albeit to a less extent than eye position. On the other hand, we have previously demonstrated that the OMV PC SS population discharge predicts saccade duration, which in turn is tightly correlated with saccade amplitude[28,29]. In other words, a strong influence of eye position had to be expected. The notion that the OMV controls eye position in the case of saccades and eye velocity in the case of SPEM is in good accordance with key assumptions of well-established models of saccade and SPEM generation respectively, reflecting the need to integrate latency-free estimates of relevant state variables. In the case of saccades, the state variable emphasized is current eye position that is compared with desired target location, the difference of the two telling the system how much further to move the eyes[30,31]. In the case of SPEM, models usually build on a prediction of eye velocity, avoiding the detrimental delay of visual feedback on the pursuit eye movement[32,33].

Optimal saccade and SPEM performance requires short-term calibration of these state variables, an adjustment that is known to depend on the integrity of the cerebellum[10,11,14,34] and the adjustment of the OMV SS output[24,35]. The evidence available suggests that the learning-based adjustments of saccade amplitude are a consequence of error-based changes of the synaptic weights of parallel fiber (PF) synapses[36,37]. Most probably, the same holds for learning-based changes of SPEM velocity. We have recently obtained preliminary behavioral evidence suggesting that learning-based adjustments of one type of goal-directed eye movement do not spill over to the other one. Such a high degree of specificity is surprising if – as shown by the study at hand – OMV PCs are a common node shared by the two pathways for saccades and SPEM. How can specificity of learning be maintained although information on the two types of eye movements converges on individual OMV PCs? If we assume that both saccadic and SPEM learning are the result of changes of the strength of parallel fiber synapses due to an interaction between PF signals and error information conveyed by the climbing fiber system, one likely answer is that the OMV PCs must reserve individual synapses for the one or the other type of goal-directed eye movement. The duality of OMV PCs might pose a second problem, though, namely the ambiguity of their output signals which is not resolved at the level of the caudal fastigial nucleus (cFN). The latter conclusion is based on our recent observation that also cFN eye movement-related neurons are predominantly dual, i.e. driven by both saccades and SPEM[38]. In other words, the premotor and motor brainstem machinery for saccades and smooth pursuit will have to deal with cerebellar information not unambiguously associated with the one or the other type of eye movement. Hence, if the brainstem machinery were organized in an eye movement type-specific way, PC activity related to eye movement type A should exert a spurious influence on the brainstem center for eye movement type B. In order to avoid the activation of the inexpedient eye movement B, the type A-related PC signal would have to be thwarted at the center for B by the absence of direct, extracerebellar input related to eye movement B. This complication would only be avoided if SPEM and saccades shared a common brainstem pathway. If this is the case is unclear. It is usually assumed that the same motoneurons support saccades and SPEM and in general different types of eye movements[6,7]. However, anecdotal physiological observations[39] and anatomical studies[40,41] have suggested that the eye muscle fibers and the motoneurons that support them show heterogeneity related to different types of oculomotor behaviors. On the other hand, the immediate premotor targets of cFN axons, like the paramedian pontine reticular formation (PPRF), the rostral interstitial nucleus of the medial longitudinal fasciculus (riMLF), the central mesencephalic reticular formation (cMRF), the perihypoglossal nucleus (PHN) and the pontine raphe (PR)[42], are commonly discussed as saccade-specific. However, at least in the case of the omnipause neurons, located in the PR, there is evidence that the discharge is not only suppressed by saccades but also inhibited to some extent during SPEM[43]. Also neurons in the PPRF, the riMLF and the cMRF have been shown to contain neurons that are both saccade- and pursuit-related[44–47]. Hence, although much of the evidence

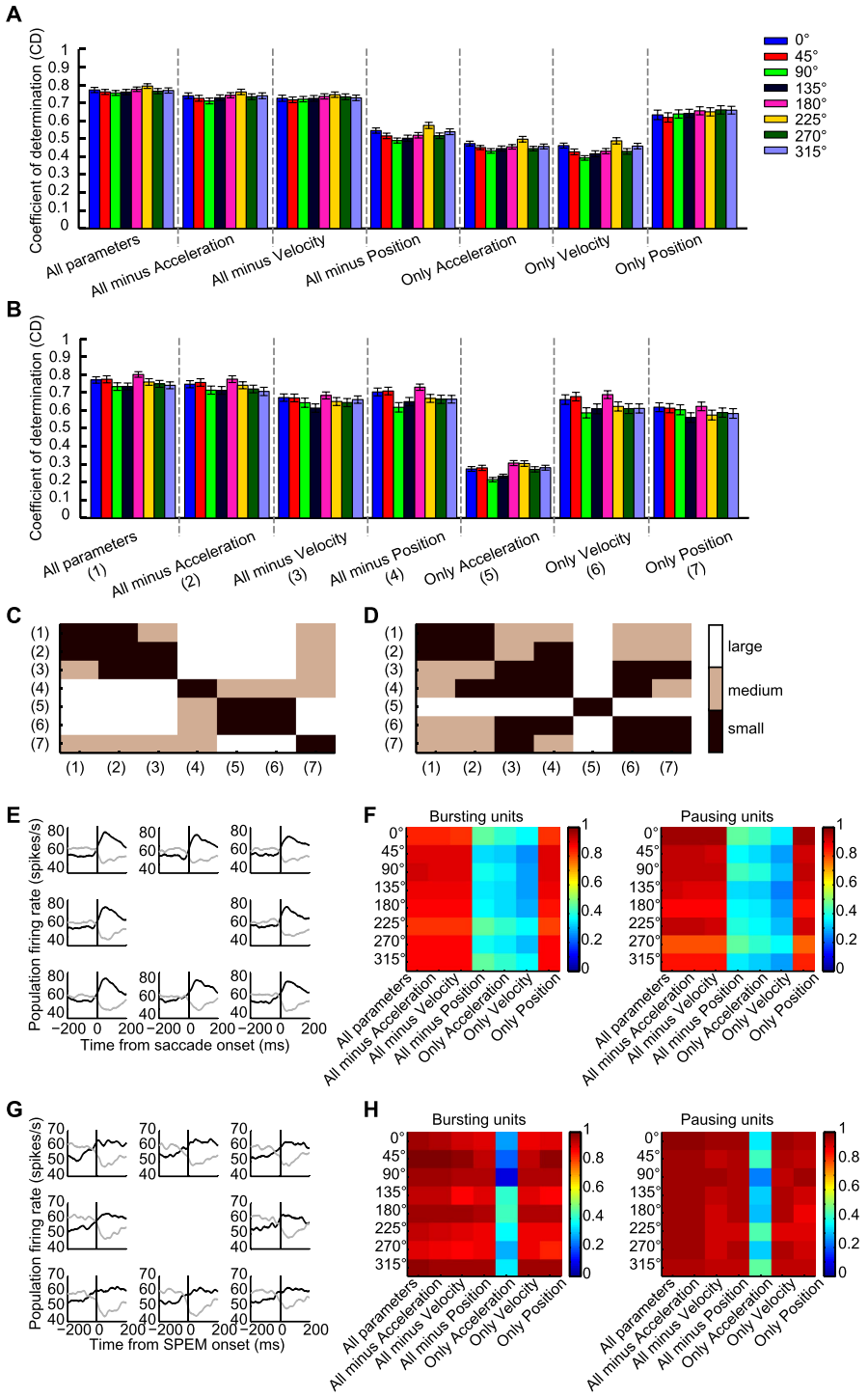

Figure 6. Distribution of coefficients of determination (CDs) obtained by fitting the population discharge as a function of the kinematic variables eye position, velocity and acceleration and different versions of slimmed down models for the 8 directions in the frontoparallel plane. (**A**) presents the CDs for the various variable constellations and the 8 directions for all PC SS tested for saccades. (**B**) all PC units tested for SPEM. Error bars in (**A**) and (**B**) indicate SEM. (**C** and **D**) Plots (**C**), saccades; (**D**) SPEM) of the size of the effect (measured by Cohen's (**D**) of moving from one particular type of model to another one. The model types compared are indicated by the numbers on the two axes. The plots are based on eye movements to 0° serving as reference direction. The three effect size categories (small, medium, large; see Methods) are color coded. (**E**) The left panel depicts the population spike density functions aligned with saccade onset separately for bursting units (n = 40) and for pausing units (n = 35) for the 8 directions tested. (**F**) Plots of CDs represented by different colors for the various models and directions. The panel on the left represents all bursting units; the one on the right represents all pausing units. (**G** and **H**) Population activity for SPEM in 8 directions and corresponding CDs (35 bursting units, 43 pausing units). Format of presentation is the same as for saccades in (**C** and **D**).

available seems to be in line with the notion that the pathway downstream of the OMV shares the duality of the OMV output, this question cannot be conclusively answered. Therefore it remains open if the organization of the downstream pathway is such as to make additional circuitry for the identification of the type of eye movement at stake dispensable. Irrespective of the question if these thoughts on the wiring of input and output of dual OMV PC are close to reality or not, the convergence of saccade- and SPEM-related signals at the level of single OMV PCs probably comes with costs. Hence, what could the gain be that outweighs these costs? An obvious answer is that convergence allows the cerebellum to accommodate two types of eye movements with one set rather than two sets of PC. Yet, this answer can only satisfy if the additional investments needed in order to disentangle the saccade and SPEM signals downstream of the OMV PCs will indeed be dispensable.

References

1. Robinson, D. A. The mechanics of human smooth pursuit eye movement. *J Physiol* **180,** 569–591 (1965).
2. Westheimer, G. Eye movement responses to a horizontally moving visual stimulus. *AMA Arch Ophthalmol* **52,** 932–941 (1954).
3. Fuchs, A. F. Saccadic and smooth pursuit eye movements in the monkey. *J Physiol* **191,** 609–631 (1967).
4. Krauzlis, R. J. & Miles, F. A. Role of the oculomotor vermis in generating pursuit and saccades: effects of microstimulation. *J Neurophysiol* **80,** 2046–2062 (1998).
5. Petit, L. & Haxby, J. V. Functional anatomy of pursuit eye movements in humans as revealed by fMRI. *J Neurophysiol* **82,** 463–471 (1999).
6. Krauzlis, R. J. Recasting the smooth pursuit eye movement system. *J Neurophysiol* **91,** 591–603, doi:10.1152/jn.00801.2003 (2004).
7. Keller, E. L. & Missal, M. Shared brainstem pathways for saccades and smooth-pursuit eye movements. *Ann N Y Acad Sci* **1004,** 29–39 (2003).
8. Lisberger, S. G. & Fuchs, A. F. Role of primate flocculus during rapid behavioral modification of vestibuloocular reflex. I. Purkinje cell activity during visually guided horizontal smooth-pursuit eye movements and passive head rotation. *J Neurophysiol* **41,** 733–763 (1978).
9. Kase, M., Miller, D. C. & Noda, H. Discharges of Purkinje cells and mossy fibres in the cerebellar vermis of the monkey during saccadic eye movements and fixation. *J Physiol* **300,** 539–555 (1980).
10. Takagi, M., Zee, D. S. & Tamargo, R. J. Effects of lesions of the oculomotor vermis on eye movements in primate: saccades. *J Neurophysiol* **80,** 1911–1931 (1998).
11. Barash, S. *et al.* Saccadic dysmetria and adaptation after lesions of the cerebellar cortex. *The Journal of neuroscience: the official journal of the Society for Neuroscience* **19,** 10931–10939 (1999).
12. Ignashchenkova, A. *et al.* Normal spatial attention but impaired saccades and visual motion perception after lesions of the monkey cerebellum. *J Neurophysiol* **102,** 3156–3168, doi: 10.1152/jn.00659.2009 (2009).
13. Ohki, M. *et al.* Role of primate cerebellar hemisphere in voluntary eye movement control revealed by lesion effects. *J Neurophysiol* **101,** 934–947, doi: 10.1152/jn.90440.2009 (2009).
14. Takagi, M., Zee, D. S. & Tamargo, R. J. Effects of lesions of the oculomotor cerebellar vermis on eye movements in primate: smooth pursuit. *J Neurophysiol* **83,** 2047–2062 (2000).
15. Vahedi, K., Rivaud, S., Amarenco, P. & Pierrot-Deseilligny, C. Horizontal eye movement disorders after posterior vermis infarctions. *J Neurol Neurosurg Psychiatry* **58,** 91–94 (1995).
16. Ron, S. & Robinson, D. A. Eye movements evoked by cerebellar stimulation in the alert monkey. *J Neurophysiol* **36,** 1004–1022 (1973).
17. Fujikado, T. & Noda, H. Saccadic eye movements evoked by microstimulation of lobule VII of the cerebellar vermis of macaque monkeys. *J Physiol* **394,** 573–594 (1987).
18. Suzuki, D. A. & Keller, E. L. The role of the posterior vermis of monkey cerebellum in smooth-pursuit eye movement control. II. Target velocity-related Purkinje cell activity. *J Neurophysiol* **59,** 19–40 (1988).
19. Sato, H. & Noda, H. Posterior vermal Purkinje cells in macaques responding during saccades, smooth pursuit, chair rotation and/or optokinetic stimulation. *Neuroscience research* **12,** 583–595 (1992).
20. Kase, M., Noda, H., Suzuki, D. A. & Miller, D. C. Target velocity signals of visual tracking in vermal Purkinje cells of the monkey. *Science* **205,** 717–720 (1979).
21. Shinmei, Y., Yamanobe, T., Fukushima, J. & Fukushima, K. Purkinje cells of the cerebellar dorsal vermis: simple-spike activity during pursuit and passive whole-body rotation. *J Neurophysiol* **87,** 1836–1849, doi: 10.1152/jn.00150.2001 (2002).
22. Dash, S., Catz, N., Dicke, P. W. & Thier, P. Encoding of smooth-pursuit eye movement initiation by a population of vermal Purkinje cells. *Cereb Cortex* **22,** 877–891, doi: 10.1093/cercor/bhr153 (2012).
23. Rashbass, C. The relationship between saccadic and smooth tracking eye movements. *J Physiol* **159,** 326–338 (1961).
24. Dash, S., Dicke, P. W. & Thier, P. A vermal Purkinje cell simple spike population response encodes the changes in eye movement kinematics due to smooth pursuit adaptation. *Frontiers in systems neuroscience* **7,** 3, doi: 10.3389/fnsys.2013.00003 (2013).
25. Cohen, J. *Statistical Power Analysis for the Behavioral Sciences*. Ch. 3, 79–81 (Lawrence Erlbaum Associates, 1988).
26. Sylvestre, P. A. & Cullen, K. E. Quantitative analysis of abducens neuron discharge dynamics during saccadic and slow eye movements. *J Neurophysiol* **82,** 2612–2632 (1999).
27. Herzfeld, D. J., Kojima, Y., Soetedjo, R. & Shadmehr, R. Encoding of action by the Purkinje cells of the cerebellum. *Nature* **526,** 439–442, doi: 10.1038/nature15693 (2015).
28. Thier, P., Dicke, P. W., Haas, R. & Barash, S. Encoding of movement time by populations of cerebellar Purkinje cells. *Nature* **405,** 72–76, doi: 10.1038/35011062 (2000).
29. Bahill, B. L. & Clark, S. A. & Stark, R. j. The main sequence, a tool for studying human eye movements. *Math. Biosci* **24,** 191–204 (1975).
30. Robinson, D. A. Models of the saccadic eye movement control system. *Kybernetik* **14,** 71–83 (1973).
31. Scudder, C. A. A new local feedback model of the saccadic burst generator. *J Neurophysiol* **59,** 1455–1475 (1988).
32. Robinson, D. A., Gordon, J. L. & Gordon, S. E. A model of the smooth pursuit eye movement system. *Biological cybernetics* **55,** 43–57 (1986).
33. Krauzlis, R. J. & Lisberger, S. G. A model of visually-guided smooth pursuit eye movements based on behavioral observations. *J Comput Neurosci* **1,** 265–283 (1994).
34. Zee, D. S. Brain stem and cerebellar deficits in eye movement control. *Trans Ophthalmol Soc U K* **105** (Pt 5), 599–605 (1986).
35. Catz, N., Dicke, P. W. & Thier, P. Cerebellar-dependent motor learning is based on pruning a Purkinje cell population response. *Proc Natl Acad Sci USA* **105,** 7309–7314, doi: 10.1073/pnas.0706032105 (2008).
36. Prsa, M. & Thier, P. The role of the cerebellum in saccadic adaptation as a window into neural mechanisms of motor learning. *Eur J Neurosci* **33,** 2114–2128, doi: 10.1111/j.1460-9568.2011.07693.x (2011).
37. Kojima, Y., Soetedjo, R. & Fuchs, A. F. Changes in simple spike activity of some Purkinje cells in the oculomotor vermis during saccade adaptation are appropriate to participate in motor learning. *J Neurosci* **30,** 3715–3727, doi:10.1523/jneurosci.4953-09.2010 (2010).

38. Sun, Z. P., Dicke, P. W. & Thier, P. Most caudal fastigial neurons of the monkey respond to saccades as well as smooth-pursuit eye movements. *Soc Neurosci Abstr* **518,** 16 (2015).
39. Henn, V. & Cohen, B. Eye muscle motor neurons with different functional characteristics. *Brain Res* **45,** 561–568 (1972).
40. Ugolini, G. *et al.* Horizontal eye movement networks in primates as revealed by retrograde transneuronal transfer of rabies virus: differences in monosynaptic input to "slow" and "fast" abducens motoneurons. *J Comp Neurol* **498,** 762–785, doi: 10.1002/cne.21092 (2006).
41. Buttner-Ennever, J. A., Buttner, U., Cohen, B. & Baumgartner, G. Vertical glaze paralysis and the rostral interstitial nucleus of the medial longitudinal fasciculus. *Brain* **105,** 125–149 (1982).
42. Noda, H., Sugita, S. & Ikeda, Y. Afferent and efferent connections of the oculomotor region of the fastigial nucleus in the macaque monkey. *J Comp Neurol* **302,** 330–348, doi: 10.1002/cne.903020211 (1990).
43. Missal, M. & Keller, E. L. Common inhibitory mechanism for saccades and smooth-pursuit eye movements. *J Neurophysiol* **88,** 1880–1892 (2002).
44. Missal, M. & Keller, E. L. Neurons active during both saccades and smooth pursuit suggest a convergence of oculomotor systems in the pontine reticular formation. *Soc Neurosci Abstr* **27,** 208 (2001).
45. Missal, M., de Brouwer, S., Lefevre, P. & Olivier, E. Activity of mesencephalic vertical burst neurons during saccades and smooth pursuit. *J Neurophysiol* **83,** 2080–2092 (2000).
46. Waitzman, D. M., Silakov, V. L. & Cohen, B. Central mesencephalic reticular formation (cMRF) neurons discharging before and during eye movements. *J Neurophysiol* **75,** 1546–1572 (1996).
47. Aravamuthan, B. R. & Angelaki, D. E. Vestibular responses in the macaque pedunculopontine nucleus and central mesencephalic reticular formation. *Neuroscience* **223,** 183–199, doi: 10.1016/j.neuroscience.2012.07.054 (2012).

Acknowledgements

The work was supported by a grant from the Deutsche Forschungsgemeinschaft (FOR 1847-A3 TH425/13-1), grants from the Marie Curie Initial Training Network (PITN-GA-2009-238214) and the German Ministry of Education, Science, Research, and Technology (Bernstein Center for Computational Neuroscience (FKZ 01GQ1002)).

Author Contributions

Z.S., A.S., M.J., P.W.D. and P.T. designed research, A.S., M.J. and Z.S. performed research, Z.S. analyzed data; Z.S. and P.T. wrote the paper.

Additional Information

Supplementary information accompanies this paper at http://www.nature.com/srep

Competing financial interests: The authors declare no competing financial interests.

How to cite this article: Sun, Z. *et al.* The same oculomotor vermal Purkinje cells encode the different kinematics of saccades and of smooth pursuit eye movements. *Sci. Rep.* **7**, 40613; doi: 10.1038/srep40613 (2017).

Publisher's note: Springer Nature remains neutral with regard to jurisdictional claims in published maps and institutional affiliations.

Appendix 2:

Sun, Z. *, Smilgin, A. *, Junker M., Dicke, PW., Thier, P. (2017) Short-term adaptation of saccades does not affect smooth pursuit eye movement initiation. J Vis, 17 (9), 19-19. (co-first author)

Short-term adaptation of saccades does not affect smooth pursuit eye movement initiation

Zongpeng Sun[12ǂ], Aleksandra Smilgin[12ǂ], Marc Junker[12], Peter W. Dicke[1], Peter Thier[1]

[1]Department of Cognitive Neurology, Hertie Institute for Clinical Brain Research, Tübingen 72076, Germany

[2]Graduate School of Neural and Behavioural Sciences, International Max Planck Research School for Cognitive and Systems Neuroscience, University of Tübingen, Tübingen 72074, Germany

ǂ These authors contributed equally to this work.

Correspondence should be addressed to Peter Thier, Department of Cognitive Neurology, Hertie Institute for Clinical Brain Research, Hoppe-Seyler-Str. 3, 72076 Tübingen, Germany. Email: thier@uni-tuebingen.de

Keywords: Saccadic adaptation, Smooth pursuit eye movement, Purkinje cell, Cerebellum, Rhesus monkey

Abstract

Scrutiny of the visual environment requires saccades that shift gaze to objects of interest. In case the object should be moving, smooth pursuit eye movements (SPEM) try to keep the image of the object within the confines of the fovea in order to ensure sufficient time for its analysis. Both saccades and SPEM can be adaptively changed by the experience of insufficiencies, compromising the precision of saccades or the minimization of object image slip in the case of SPEM. As both forms of adaptation rely on the cerebellar oculomotor vermis (OMV), most probably deploying a shared neuronal machinery, one might expect that the adaptation of one type of eye movement should affect the kinematics of the other. In order to test this expectation, we subjected 2 monkeys to a standard saccadic adaption paradigm with SPEM test trials at the end and, alternatively, the same 2 monkeys plus a 3rd one to a random saccadic adaptation paradigm with interleaved trials of SPEM. In contrast to our expectation we observed at best marginal transfer which, moreover was little consistent across experiments and subjects. The lack of consistent transfer of saccadic adaptation decisively constrains models of the implementation of oculomotor learning in the OMV, suggesting an extensive separation of saccade and SPEM-related synapses on P-cell dendritic trees.

Introduction

Human as well as nonhuman primates use saccades to shift their gaze to objects of interest and deploy smooth-pursuit eye movements (SPEM) to keep the object image within the confines of the fovea, should it be moving not too fast relative to the beholder. Accurate saccades require the conversion of the retinal vector pinpointing the target into an appropriate motor vector. The relationship between the two is not fixed. Rather matching the two requires the choice of appropriate parameters that will need updating in case the saccades generated may have failed to hit the target, for instance because the glasses worn by the beholder may change the metric of the retinal image. By the same token, the initial velocity of smooth-pursuit in its early, still open-loop phase requires the choice and eventually updating of the parameters mapping target velocity onto eye velocity (Rashbass, 1961). Both forms of parametric adjustment are short-term as already the experience of only a few and at least in the case of saccades even only one exemplar of an inappropriate saccade or smooth-pursuit eye movement may induce changes visible in following manifestations of the same oculomotor behavior (Collins, 2014; Havermann & Lappe, 2010; Srimal, Diedrichsen, Ryklin, & Curtis, 2008). And both saccadic learning (Barash et al., 1999; Golla et al., 2008; Optican & Robinson, 1980; Straube, Deubel, Ditterich, & Eggert, 2001) and SPEM learning (Dash & Thier, 2013; Ohki et al., 2009; Takagi, Zee, & Tamargo, 2000) depend on the integrity of lobules VI and VII of the vermis (the "oculomotor vermis"=OMV) as lesions of these lobules leads to a severe - and most probably - irreversible loss of the ability to adjust the relevant parameters short term. The kinematics of saccades and smooth-pursuit eye movements are grossly different. Whereas saccades are high velocity, short duration movements in which the eyes reach peak velocities of up to 1000°/s, smooth pursuit eye movements are confined to a range of small velocities not exceeding a few 10°/s (de Brouwer, Yuksel, Blohm, Missal, & Lefevre, 2002; Fuchs, 1967; D. A. Robinson, 1965; Westheimer, 1954), a range that is spared by even the slowest (=small amplitude) saccades (Martinez-Conde, Macknik, Troncoso, & Hubel, 2009). In view of the very different kinematic requirements of the two, one might expect that the cerebellar circuits for the control of saccade and SPEM kinematics are separate. Yet, contrary to this expectation, recordings from OMV output neurons, i.e. Purkinje cells (P-cells), in monkeys carrying out SPEM or saccades indicate that the OMV encodes the kinematics of both saccades and SPEM (Dash, Catz, Dicke, & Thier, 2012; Sun, Smilgin, Junker, Dicke, & Thier, 2017). As a matter of fact rather than deploying distinct sets of P-cells, one tuned to the parameter space of saccades, a second one to that of SPEM, practically all OMV P-cells with oculomotor sensitivity are tuned

to saccades as well as to SPEM (Sun et al., 2017). The OMV P-cell is the substrate of the short-term learning based adjustment or adaptation of saccades (Catz, Dicke, & Thier, 2008) and of SPEM (Dash et al., 2013). Hence, one might expect that changes of a P-cell underlying short term saccadic adaptation should affect SPEM, supported by the same P-cell. In other words, saccadic learning should spill over to SPEM. We tested this prediction in behavioral experiments on 3 monkeys in which we explored if short-term saccadic adaptation induced by two different regimes was transferred to catch trials of linear smooth pursuit. We observed at best marginal transfer, not very consistent over experiments and subjects. As both the adjustment of saccades and of SPEM depend on synaptic adjustments at the level of cerebellar P-cells, the low degree of transfer suggests an extensive separation of saccade- and SPEM-related synapses on P-cell dendritic trees.

Materials and methods

Animals and surgical procedures

Three rhesus monkeys (Macaca mulatta, males; M1-3) purchased from the German Primate Centre, Göttingen, Germany) participated in this study which tested for a transfer of short-term saccadic adaptation to SPEM-initiation. The experiments on these animals including the surgical and behavioural protocols were approved by the local animal care committee, conducted in accordance with the guidelines of the National Institutes of Health for Care and Use of Laboratory Animals and supervised by the veterinary administration (Regierungspräsidium Baden-Württemberg und Landratsamt Tübingen). M1 and M2 participated in an experiment in which saccadic adaptation was induced by exposing the monkey observers to the same visual error over a longer series of trials ("consistent error" adaptation experiment). In a second experiment, which involved M1, M2 and M3, we deployed a random error paradigm in which adaptation of saccades in trial n was induced by presenting a visual error in the preceding trial n-1, whose direction flipped randomly.

All monkeys underwent a surgical procedure needed to implant a titanium head post and scleral search coils. The head post was required to painlessly restrict the head movements during experiments. The search coil allowed the high-resolution measurement of instantaneous eye position by picking up a small, eye position dependent voltage induced by an alternating magnetic field around the monkey's head (Fuchs & Robinson, 1966; D. A. Robinson, 1963). The surgical procedures used were identical as in previous studies (Sun et al., 2017) and described in more detail there. Briefly, monkeys were anaesthetized using a combination of isoflurane and remifentanyl while carefully monitoring all vital parameters (body temperature, carbon dioxide, oxygen, blood pressure, electrocardiography (ECG). Animals were supplied with analgesics until any signs of pain disappeared and allowed to fully recover before conducting the experiments. Each monkey was trained to voluntarily come to his customized primate chair. During experiments they were seated in the chair at a distance of 40 cm in front of the CRT monitor in complete darkness. Each monkey was extensively trained to execute precise saccades and SPEM. The motivation to participate in the experiments was achieved by asking the monkeys to cover their daily fluid intake needs by complying with the behavioral demands. Specifically, each successful eye movement trial was rewarded with water. If needed, additional fluid and/or juicy fruits were provided after experiments to satisfy the daily fluid requirements. However, the monkeys did not get water in their home cages during periods of

work. Usually every fortnight, they were granted a 2 days' vacation with free access to water and juicy fruits in their home cages. Each animal was regularly inspected by the university´s veterinarians to ensure that they were in good health.

Behavioural tasks

The visual stimuli were presented on a 22 inch diameter Cathode Ray Tube monitor (Ilyama MA203DT) operating at 88 Hz and at a resolution of 1600 × 1200 pixels. For the control of the experiments as well as data acquisition we deployed software developed in house freely available (nrec, http://nrec.neurologie.uni-tuebingen.de), running under Linux on a standard PC.

Eye position calibration

The eye movement signal delivered by the scleral search coil was sampled at 1 kHz. Prior to each experimental session it was calibrated using the know position of a white fixation target dots diameter: 0.4°) that appeared at random on the monitor in one out of nine positions defining a 30×30° grid centered on straight ahead. Monkeys were asked to maintain fixation at each target for approximately 1 s in order to get a liquid reward and then to proceed to the next cued location. The data acquired was subjected to a regression analysis that considered linear, quadratic and mixed term dependencies in order to predict eye position based on the search coil voltage.

Visually guided saccades and saccadic adaptation

A visually guided saccade trial consisted of a fixation period of 500-1000 ms, after which the fixation target (white dot, diameter: 0.4°) was replaced by a target of the same appearance presented at 10° horizontal eccentricity, eliciting a visually guided saccade (Figure 1A top row). The monkey was rewarded if he was able to keep his eyes within the confines of an invisible squared fixation window of 1.5-3° side length. In order to prompt saccadic adaptation, the peripheral target originally presented at an eccentricity of 10°, jumped to a new position (an eccentricity of 7° or 13° depending on the direction of adaptation) during the execution of the visually guided saccade. In order to trigger the target jump we used an analogue saccade detector that determined the point in time, the eye velocity signal exceeded a preset velocity threshold, triggering a target shift of either 3° outwards (saccade outward adaptation experiments) or 3° inwards (saccade inward adaptation experiments) at this point. These

intrasaccadic target shifts induced a secondary corrective saccade bringing the eyes closer to the final target location (Figure 1A middle row).

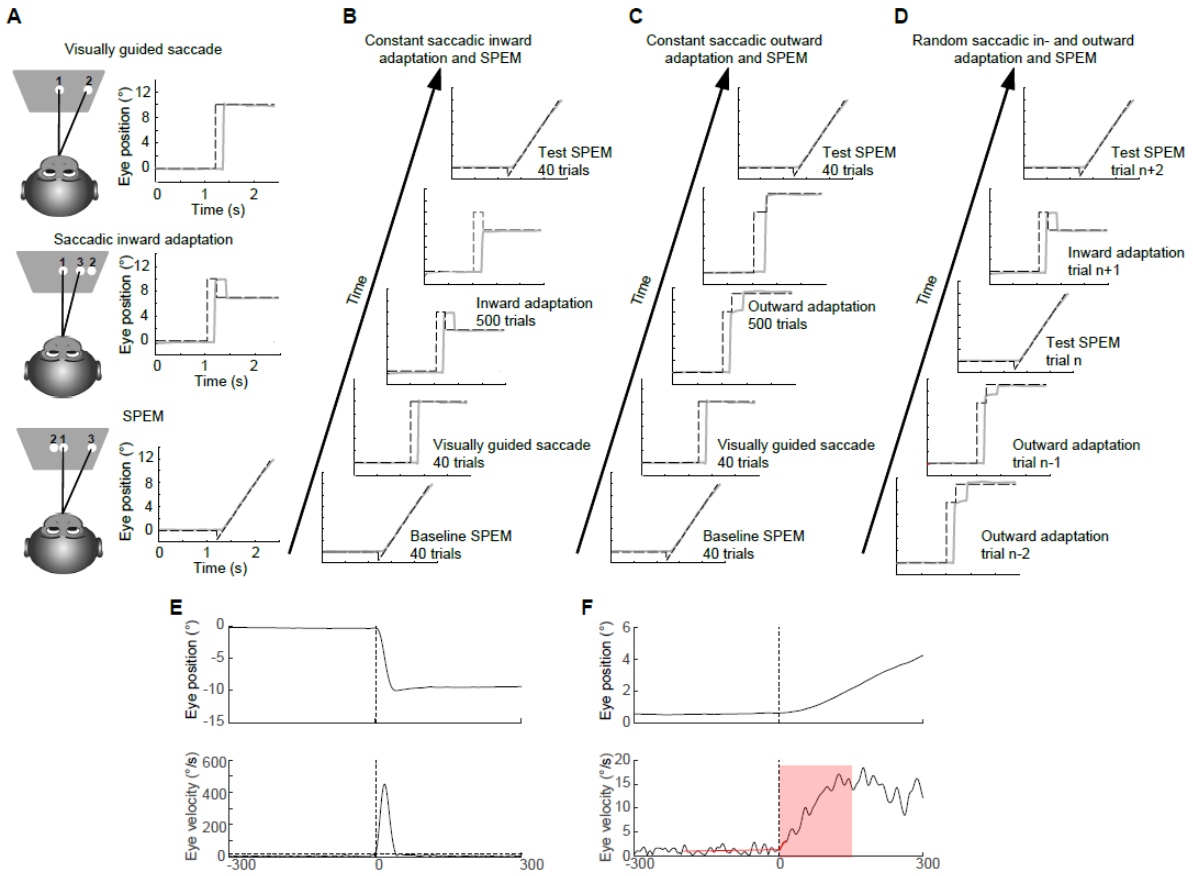

Figure 1. Experimental paradigms. (A) Exemplary saccade trial, followed by a saccadic adaptation trial prompting gain decrease adaptation and a SPEM trial. **(B)** Sequence of events in the consistent error experiment with errors causing saccadic inward adaptation. **(C)** Sequence of events in the consistent saccadic error experiment causing outward adaptation. **(D)** Sequence of events in the experiment on the transfer of random saccadic errors to SPEM showing. Five exemplary consecutive trials are shown. Note that the amplitude of the primary saccade in the second trial increased due to the preceding outward adapting saccade trial. **(E,F)** Detection of saccades (left) and SPEM (right). The top panels show plots of eye position as function of time (bottom) for exemplary saccade and SPEM trials, the lower panels eye velocity. The vertical dashed lines indicate eye movement onset determined as described in Methods. The horizontal dashed lines in the velocity plots give the velocity thresholds used and the red lines in the SPEM velocity plot represent the two intersection regression lines pinpointing SPEM onset. The shaded area indicates the period of open-loop SPEM.

Smooth pursuit eye movements

In SPEM trials, a white 0.4° target was presented in the center of the screen for 500-1000 ms and the monkey was required to maintain fixation. Then this central fixation target jumped to a new location 1.4-2.4° (chosen depending on the properties of a subject´s initial SPEM, see below) from the original straight ahead position on the horizontal and started to move in the opposite direction with a constant velocity of 12 °/s (Figure 1A bottom row). The purpose of the initial target step was to ensure that the subsequent target ramp would have moved the target back to straight ahead at the time of SPEM onset, thus reducing the need to generate an early catch-up saccade (Rashbass, 1961).

Transfer of saccadic adaptation with consistent target shifts to SPEM

The experimental session started with 40 baseline SPEM trials as described before and ended with 40 test SPEM trials. The initial block of SPEM trials was followed by a block of trials in which the monkey was asked to carry out saccades towards an eccentric target, followed by a block of 500-1000 saccadic adaptation trials in which the target was shifted either consistently out- or inward by 3° thereby inducing outward or inward saccadic adaptation (McLaughlin, 1967) (Figure 1B and C). The direction of the SPEM and saccades was consistent for a particular session either to the left or the right.

Transfer of random saccadic adaptation to SPEM

Visually guided saccades, saccadic out- and inward adaptation trials and SPEM were presented in random order in blocks of about 200 trials. In individual sessions the direction of SPEM and of primary saccades was consistent either to the left or to the right. In saccadic adaptation trials the target jumped from its initial location at 10° during the primary saccade to a new one at 7, 8, 9, 11, 12 or 13°, each possible location chosen at random with equal probabilities. The probability of SPEM and saccade trials was 50% each (Figure 1D).

Data analysis

Data processing and statistical analysis was based on custom written routines in MATLAB (The MathsWorks Inc., Natick, MA).

The onset and offset of a saccade were detected using an eye velocity threshold of 20°/s (see Fig. 1E). In the saccadic adaptation experiment with consistent error, the gain was calculated by dividing the mean saccade amplitude of the last 40 saccade trials by the mean amplitude of the first 40 saccade trials of the session. The saccadic adaptation gain in the random saccadic

adaptation experiment was calculated for each session by dividing the mean saccade amplitude for a particular class of target shifts (i.e. from 10 to 11, from 10 to 9 etc.) by the mean saccade amplitude of all trials without target shifts that preceded them**.**

The saccadic visual error (SVE) in the random saccadic adaptation experiment was defined as the difference between the final target location and the saccadic end position of the first saccade after the first target shift.

Each SPEM trial was visually inspected. The detection of the onset of SPEM required several steps. First, we determined the point in time at which the velocity exceeded the mean eye velocity in the first 80 ms after the target backshift by three standard deviations for 40 consecutive ms. Then two regression lines were computed: one on the eye velocity during the 200 ms before this time point and a second one on the following 15 ms (as shown in Fig. 1F). The interception of these two regression lines was then taken as the time of SPEM onset. Trials including saccades in the first 200 ms of the SPEM as well as trials in which the careful visual inspection suggested that the automatic onset detection had obviously failed to identify SPEM onset were excluded. In the saccadic adaptation experiment with consistent error, SPEM gain was taken as the ratio of the mean peak velocity in a period of 0-150 ms (open-loop SPEM, highlighted in Fig. 1F) after SPEM onset of the last 40 SPEM trials divided by the mean peak velocity of the first 40 SPEM trials. The SPEM gain in the random saccadic adaptation experiment was calculated in the following way: the peak velocity of SPEM in trials following saccadic adaptation trials with target shifts from one of the 6 classes was divided by the mean peak velocity of all SPEM trials, which were preceded by saccade trials without target shift.

Results

Effects of consistent visual errors on saccades

We collected a total of 40 experimental sessions (20 with inward errors, 20 with outward errors, 10 from each subject). Each session started with 40 baseline SPEM trials, followed by 40 visually guided saccades and then either by consistent saccadic out- or inward trials. The session then ended with 40 test SPEM trials. Figure 2 depicts exemplary sessions, one with an outward error (Fig. 2A) and one with an inward error (Fig. 2B), documenting the expected amplitude increase and decrease respectively with trial number. Over all sessions, saccadic gain increased on average by 14 % in the case of outward adaptation and decreased by 19 % in the case of inward adaptation (Fig. 2D). As documented by the exemplary velocity traces in Fig. 2C and the group data in Fig. 2E, F, the gain changes were the result of a decline in peak velocity not compensated by changes in saccade duration in the case of inward adaptation ($p=0.0004$, Wilcoxon signed rank test) and by an increase of saccade duration associated with constant saccade peak velocity in the case of outward adaptation ($p<0.01$). The differential effects of inward and outward adaptation on saccade velocity and duration are in accordance with previous findings (Prsa, Dicke, & Thier, 2010).

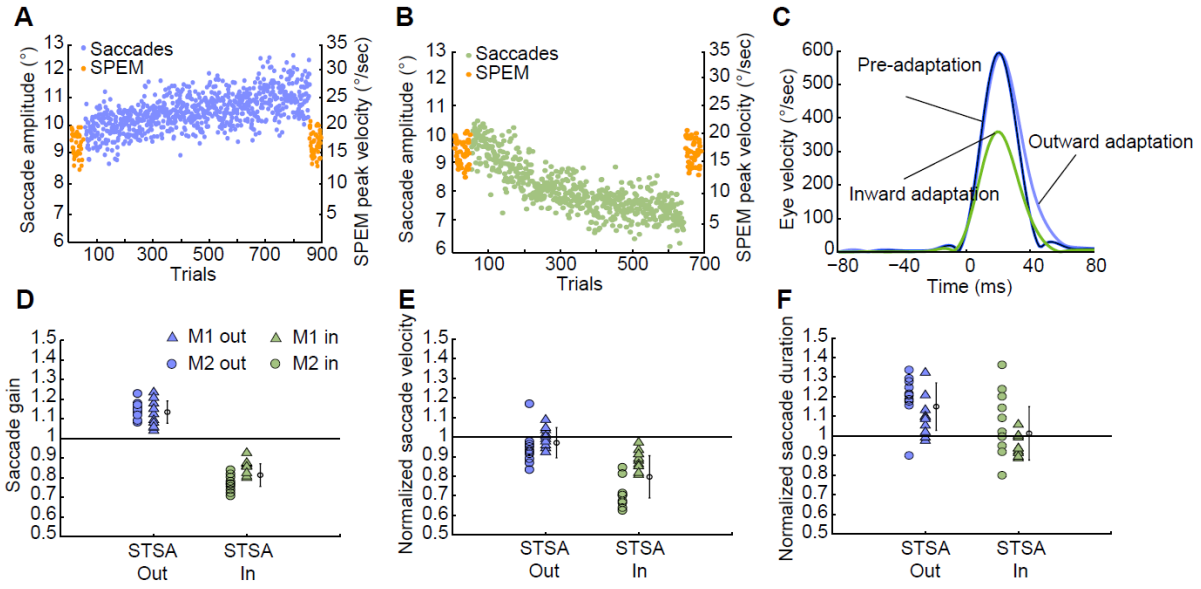

Figure 2. Short-term saccadic adaptation prompted by consistent errors**.** Exemplary adaptation sessions based on a consistent saccadic outward error **(A)** and inward error **(B)** embedded in two blocks of SPEM. The performance of SPEM is qualified by their peak velocity (orange) and saccades are characterized by their amplitudes (800 trials of outward saccades, violet and 600 trials of inward saccades, green). **(C)** Exemplary saccade velocity profiles

aligned to the onset of a visually guided saccade collected before adaptation onset (black) and at the end of an out- (blue) and inward (green) adaptation experiment. **(D)** Saccade gain, **(E)** normalized saccade velocity and **(F)** normalized saccade duration based on all 20 outward (left panel) and 20 inward (right panel) adaptation sessions of two subjects. Black open circles with error bars beside color symbols represent mean ± SD for each condition.

We next asked whether the changes of saccade metrics due to inward or outward shifts of the target had any effect on the following SPEM tested in a block of trials (SPEM test block) following the adaptation block. To this end, we compared the mean peak velocity of SPEM in the block of trials before a saccadic adaptation block (SEPM baseline block) with the peak velocity of SPEM test trials (Figure 3). The comparison was based on a consideration of the first SPEM test trial, probably the one most affected by the preceding saccadic adaptation trials and a consideration of the mean performance in the test block, arguably better able to reveal subtle changes persisting longer than a few trials. The peak velocity of the first SPEM trial after a saccadic adaptation block did not change significantly, neither in the case of outward nor in the case of inward adaptation (Wilcoxon signed rank test outward: M1: p=0.32, median=0.92; M2: p=0.38, median=1.02, inward: M1: p=0.7, median=1.04; M2: p=0.92, median=1.02). In the case of saccadic outward adaptation the comparison of the mean peak velocity of all SPEM trials in one subject (M1) failed to reveal any transfer. The other subject (M2) exhibited a tiny, yet significant decrease in its mean SPEM peak velocity, i.e. a change that is opposite to a true learning transfer effect (M1: p=0.11, median=1.03; M2: p=0.04, median=0.97, Wilcoxon signed rank test). In the case of saccadic inward adaptation, both subjects showed significant changes. Whereas subject M2 exhibited a decrease, consistent with a transfer of learning transfer, M1 showed an increase in average peak velocity SPEM, i.e. a change that is opposite to a transfer effect (M1: p= 0.02, median=1.04; M2: p=0.004, median=0.94, Wilcoxon signed rank test) (Fig. 3A). Hence, overall significant changes obtained were few and inconsistent and hardly supporting the notion that substantial saccadic learning would transfer to SPEM. We wondered if the significant changes observed might not actually have been artifacts of longer term behavioral trends. For instance a general decline in performance over time, due to cognitive fatigue might feign as transfer of gain-decrease adaptation. If performance had indeed changed continuously over time, one might expect to see changes in SPEM velocity also along the sequence of the 40 SPEM test trials. However, no significant differences in SPEM velocity were obtained when we compared the first half of SPEM test trials after saccadic adaptation

with the second half in any of the monkeys, neither for inward nor for outward adaptation experiments ($p>0.05$, Wilcoxon signed rank test). While this negative result does not support an influence of longer-term performance changes, it does not necessarily rule it out as changes within a block of only two times 20 trials may have been too subtle to stand out. Independent of the question as to the relevance of long-term behavioral trends, the suspicion that the small and somewhat inconsistent changes observed at the transition from saccadic adaptation to the SPEM test block may not necessarily reflect true learning transfer is also nourished by the fact that a direct comparison of test block SPEM velocity between outward and inward experiments revealed few differences. We considered both the first test block trials and the averages across the test blocks. The only significant difference was obtained for M2 who exhibited larger peak eye velocities in the test block after gain increase adaptation when considering the average across the test block trials ($p=0.014$, Wilcoxon signed rank test).

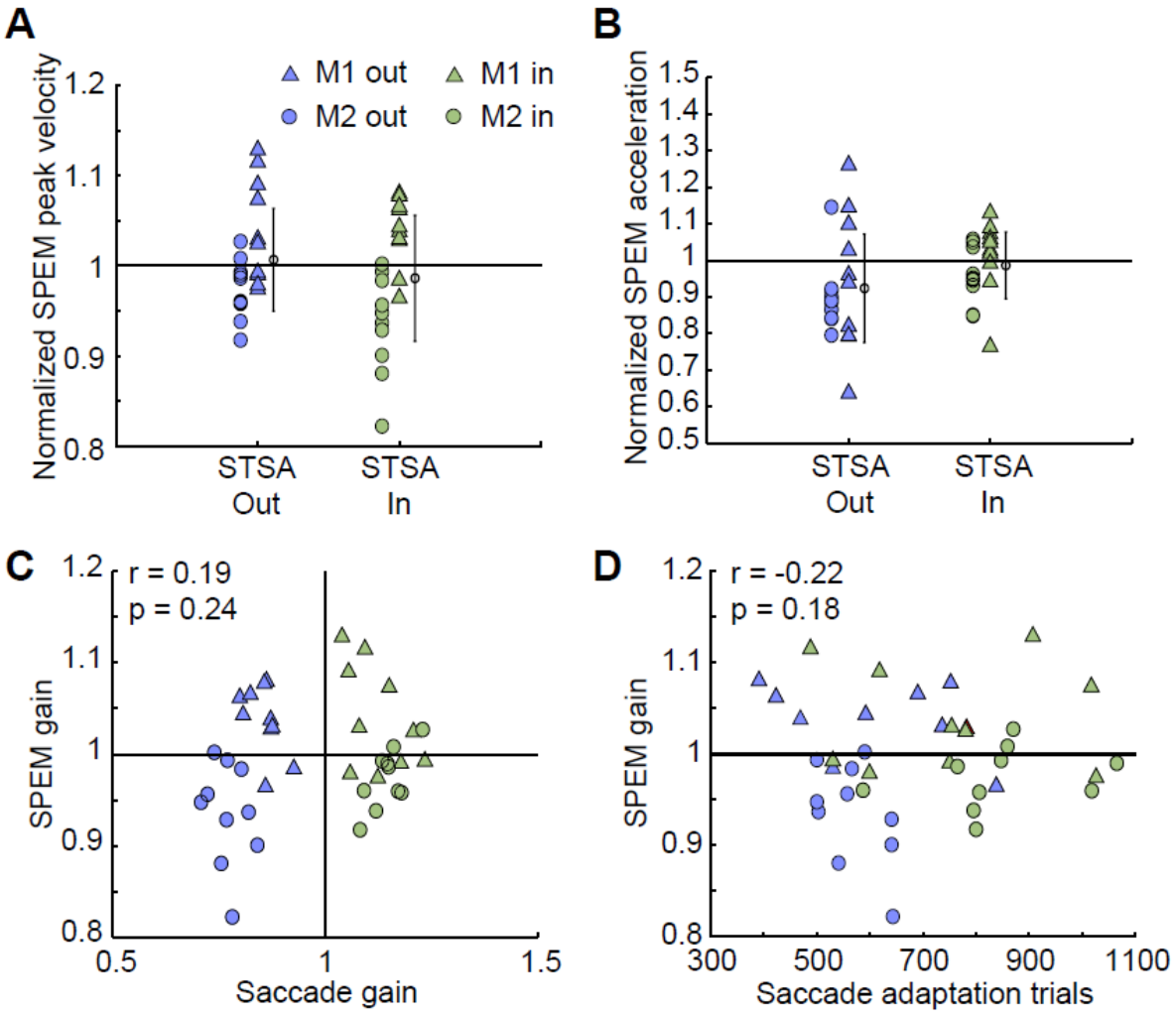

Figure 3. Effects of consistent error saccadic adaptation on SPEM initiation. (A) Mean normalized SPEM peak velocity of the all SPEM test block trials following saccadic adaptation for all 40 saccadic out- (left panel) and inward (right panel) adaptation sessions. Black open circles with error bars beside color symbols represent mean ± SD for each condition. **(B)** Normalized SPEM peak acceleration of all SPEM test block trials following saccadic adaptation for all 40 saccadic out- (left panel) and inward (right panel) adaptation sessions. **(C)** Correlation of saccade gain and SPEM gain in all test block trials for all 40 sessions. **(D)** Plot of the number of saccadic adaptation trials as function of SPEM gain based on all test block trials.

We also analyzed the influence of saccadic adaptation on the peak acceleration in the first 150 ms of SPEM. Similar to our approach to peak velocity, we compared this kinematic measure in the first trial of SPEM after saccadic adaptation and its mean over all test block trials with mean peak SPEM acceleration in the baseline block. As summarized in Fig. 3B (First SPEM trial: Outward: M1: p= 0.92, median=0.97; M2: p= 0.19, median=0.85; Inward: M1: p= 0.19, median=0.82; M2: p= 0.38, median=1.11) (All SPEM trials: Outward: M1: p= 0.43, median=0.95; M2: p= 0.04, median=0.89; Inward, M1: p=0.32, median=1.04; M2: p= 0.13, median=0.95), neither saccadic gain decrease nor gain increase adaptation had a significant impact. Last but not least, we asked if the saccadic gain resulting from saccadic adaptation had an influence on SPEM gain. Saccadic gain was taken as the ratio of the mean saccade amplitude of the last 40 trials at the end of the adaptation period and the mean saccade amplitude in the block of saccades before the onset of the target shifts. SPEM gain was given by dividing the peak velocity in the first trial of the test or, alternatively, the mean over all trials in this block by the mean peak velocity in the baseline period. We then pooled the data from saccadic gain decrease and increase experiments and subjected the plots of the two measures of SPEM gain as function of saccadic adaptation gain to a linear regression analysis (Fig. 3C shows the plot for all SPEM trials). Both failed to reveal a significant correlation (First SPEM trial: p=0.95, r=0.001; All SPEM trials: p=0.24, r=0.19).

As individual sessions differed regarding the number of saccadic adaption trials, we checked if the number of saccadic adaption trials mattered for SPEM gain based on the average of all test block trials. As shown in Fig. 3 D the plot of SPEM gain as a function of the number of saccadic trials did not reveal a significant relationship between the two (First SPEM trial: p=0.2, r=0.21; All SPEM trials: p=0.18, r=-0.22).

Effects of random visual error on ensuing saccade

Just one or a few SPEM trials might suffice to largely reset the saccadic adaptation achieved. In this case measures of SPEM based on the mean performance in the first trial of the test blocks would hardly be able to reveal any transfer. The reason is that the number of experimental sessions and therefore the number of first trials is comparatively small which is why subtle remaining transfer effects may simply be hidden by noise. This consideration was the reason to embark on a second series of experiments, resorting to a random error design, allowing us to substantially increase the number of potential transfer trials. The approach chosen was guided by previous demonstrations of clear saccadic adaptation prompted by a visual error in the immediately preceding saccade trial (Collins, 2014; Havermann & Lappe, 2010; Srimal et al., 2008). In order to verify the trial-by-trial effects of saccadic adaptation on the open-loop SPEM initiation, we collected a total of 25573 trials from three subjects.

In order to assess the effect of a visual error in a saccade trial on the saccade amplitude in a subsequent saccade trial, we separated the saccade trials according to the target shift in the preceding trial into 3 groups: an adaptive outward target shift independent of its size, an adaptive inward target shift independent of its size and saccade trials preceded by SPEM. Saccades made in trials following trials without preceding target shifts were hypometric in all three subjects. The median visual errors of all sessions were -1.39°, -0.83° and -1.07° for M1, M2 and M3 respectively. In each session these saccades served as reference for the others, setting their amplitudes to 1 (**Fig. 4A**). All three subjects showed normalized saccade amplitudes significantly smaller than 1 for saccade trials preceded by trials with inward shifts of the saccade target ($p<0.01$, Mann-Whitney *U*-test). Accordingly, the normalized amplitude of saccades with preceding outward shifts of the saccade target was significantly larger than 1 ($p<0.01$, Mann-Whitney *U*-test). Unexpectedly, also the saccade trials preceded by SPEM trials, exhibited a tiny, yet significant gain increase ($p<0.01$, Mann-Whitney *U*-test).

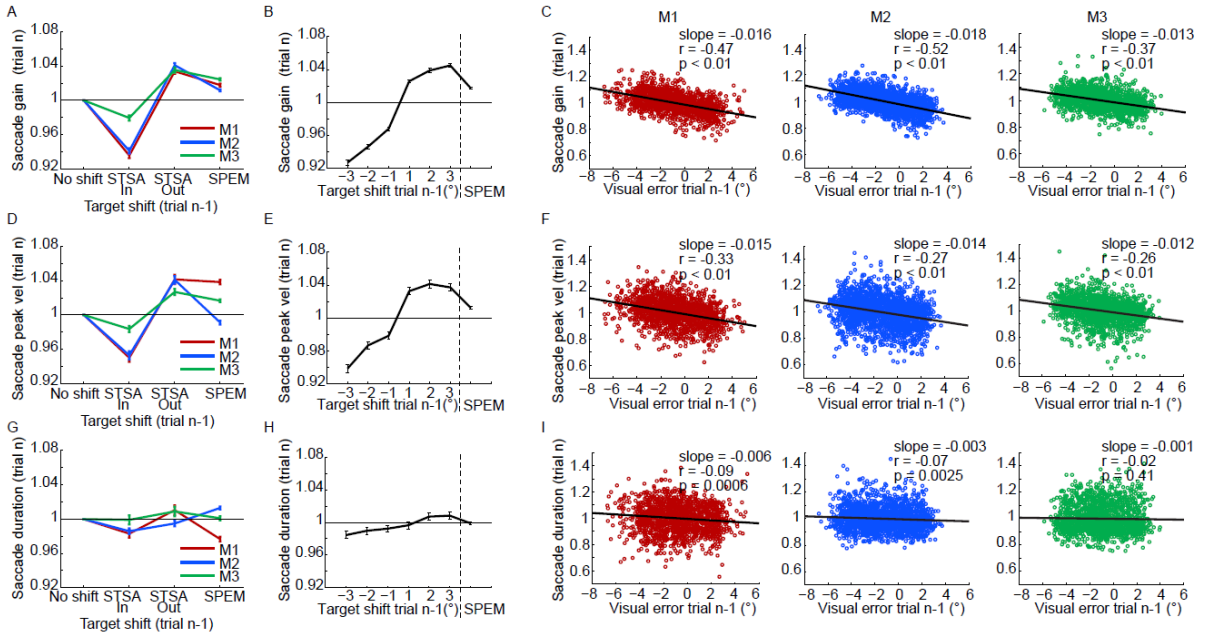

Figure 4. Effect of the random errors on saccadic adaptation. (A) Mean saccade gain in trial n as a function of trial n-1 (either a no target shift trial, an in- or outward saccadic adaptation (short-term saccadic adaptation, STSA) or a SPEM trial) for the three subjects M1-3. **(B)** Plot of saccade gain in trial n as a function of the size of target shift in trial n-1 for the three monkeys. **(C)** Correlation of saccade gain in trial n with saccadic visual error in trial n-1 for the three monkeys. **(D)** Saccade peak velocity in trial n as a function of the type of trial n-1 (no target shift trial, in- or outward saccade adaptation or SPEM trial) for monkeys M1-3. **(E)** Plot of saccade peak velocity in trial n as a function of size of target shift in trial n-1 for all monkeys. **(F)** Correlation of saccade peak velocity in trial n with saccadic visual error in trial n-1 for the three monkeys. **(G)** Saccade duration in trial n as a function of type of trial n-1 (no target shift trial, in- or outward saccade adaptation trial or SPEM trial) for the three subjects. **(H)** Plot of saccade duration in trial n as a function of size of target shift in trial n-1 for all monkeys. **(I)** Correlation of saccade duration in trial n with saccadic visual error in trial n-1 for each monkey. Error bars indicate SEM.

We next addressed the question if not only the direction of the target shift in a saccade trial but also its size mattered for the saccade made in a subsequent trial. As shown by Fig. 4B, which plots normalized saccade amplitude as a function of the size and direction of the target shift in the preceding trial, the modification of saccade amplitudes clearly scaled with target shift size in the preceding trial (p=0.0014, r=0.9689, slope=0.026). As a consequence of the variability of saccadic responses also the saccadic visual errors (SVEs) associated with trials in which the

target exhibited a particular shift behavior varied. It is the actual size of the SVE in a given saccade trial that determines the size and direction of adaptation in the ensuing saccade trial, which is indicated by the significant correlation between SVE in trial n-1 and saccade gain in trial n ($p<0.01$) (**Fig. 4C**). Not only the amplitude but also the peak velocity of saccades depended on the size and direction of the target shift ($p=0.0043$, $r=0.9458$, slope=0.022) (Fig. 4D, E) and the size and direction of the SVE in preceding saccade trials (Fig. 4F). Finally, unlike saccade amplitude and peak velocity, saccade duration in a given trial was only marginally affected by the features of the preceding saccade trials (Fig. 4G) as indicated by the almost flat regression line fitted to the plot of saccade duration as function of target shift size and direction ($p<0.01$, $r=0.978$, slope=0.005) (Fig. 4 H) and SVE (Fig. 4I) respectively in trials n-1 and saccade duration in trials n.

Effects of random saccade errors on ensuing SPEM

To evaluate the trial-by-trial effects of saccade errors and saccadic adaptation on the gain of the open-loop SPEM response in interleaved trials of SPEM, we grouped SPEM trials based on the features of the one back and two back saccade trials. We distinguished four cases: a given SPEM trial could have been preceded by either one saccadic out- or inward adaptation trial (trial n-1) or preceded by two sequential in- or two sequential out- or inward adaptation trials (n-1 and n-2). Fig. 5A compares the mean open-loop SPEM peak velocity for these four groups, separately for the three monkeys. Whereas monkeys M1 and M3 did not exhibit a significant effect of preceding saccadic adaptation trials on the velocity of the open-loop SPEM for any of the four cases distinguished ($p>0.01$, Mann-Whitney *U*-test), monkey M2 showed a small (3 %), yet significant decrease of his open-loop SPEM peak velocity if the SPEM trial was preceded by two prior inward adaptation trials ($p=0.0003$, Mann-Whitney *U*-test).

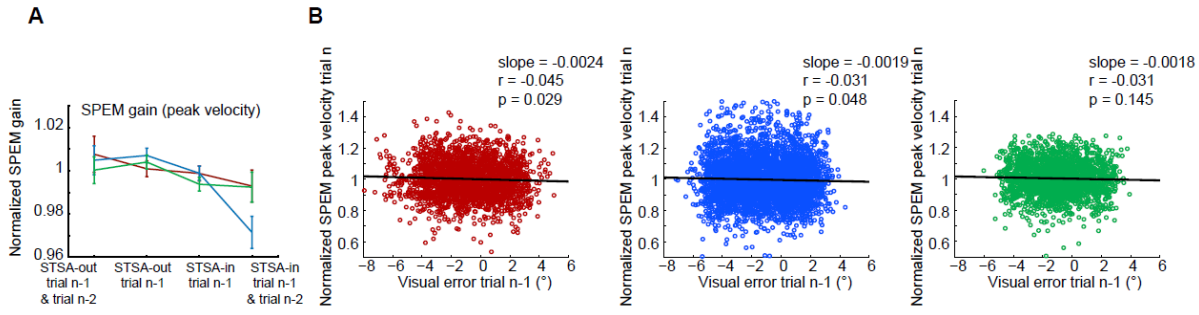

Figure 5. Effects of random saccadic adaptation on the open-loop SPEM gain. (A) SPEM gain change after different types of preceding types of trials. **(B)** Correlation between

normalized SPEM peak velocity and the size of the saccadic visual error in the preceding trial n-1 for the three individual monkeys (red=M1, blue=M2, green=M3).

In order to capture potential changes in open-loop SPEM peak velocity due to the size of the SVE in the immediately preceding saccade trial, we plotted SPEM velocity as a function of preceding SVE for each individual subject (Figure 5 B). We obtained significant linear regressions for 2 of the 3 monkeys (M1, M2). Yet, the slopes of the resulting linear regressions were without exception very close to 0, indicating that the effect of SVE on SPEM peak was in any case subliminal.

Discussion

In this study we addressed the question if saccadic adaptation prompted by a history of prior saccadic errors transfers to the open-loop segment of ensuing SPEM. Saccadic adaptation was either induced by a sequence of consistent target shifts during saccades or, alternatively, by target shifts whose size and direction was chosen randomly from 6 classes. Both paradigms elicited clear saccadic adaptation with features in accordance with previous work (Noto & Robinson, 2001; F. R. Robinson, Noto, & Bevans, 2003; Srimal et al., 2008; Wallman & Fuchs, 1998), such as the velocity decrease but no change of duration caused by inward adaptation, and prolongation of duration but no change of velocity in the case of outward adaptation. Yet, independent of the paradigm chosen, significant influences on test SPEM following saccadic adaptation were absent in most of the cases, if present often in a direction opposite to the direction of learning transfer and in any case tiny, reflecting only a very small fraction of the adaptation based changes of saccades. Most of the few cases of minimal change were obtained when running the consistent target shift paradigm. As any consistency in trial structure has the potential to cause long-term behavioral changes, e.g. due to cognitive fatigue and thereby changes in performance over time, we were concerned that the transition effects might have been confounded by such trends. While our control analysis could not support this concern, more subtle changes of performance over time in the first experiment, building on consistent shifts of the saccade target cannot be excluded. One of the virtues of the second experiment, characterized by a completely randomized trial structure, was that it was optimally suited to prevent the confounding influence of time dependent performance changes on potential learning transfer. Using this paradigm, we observed a significant decrease in open-loop SPEM peak velocity in one (M2) of the three monkeys in individual SPEM trials following saccadic adaptation trials if the SPEM trial was preceded by two trials of saccades with target shifts in

an inward direction. Yet, this transfer effect was tiny, amounting to a drop in peak velocity of 3% only. This percentage must be compared to the 6 % decrease of the amplitude of saccades, preceded by only one trial of saccade with inward shift in the random saccadic adaptation experiment. That transfer effects – if detected at all - are indeed very small is also supported by the minimal slopes of regressions of the size of the visual error in saccade trial preceding SPEM trials in the random saccadic adaptation paradigm.

Our finding that short-term saccadic adaptation has small, albeit quite inconsistent effects on the kinematics of the ensuing SPEM may support a role of small savings from learning. However, even if such small savings from saccadic learning existed, the need to perform SPEM as precisely as possible seems to easily overcome the savings, thereby concealing their influence. Crosstalk between saccades and SPEM is not confined to saccadic learning. Also catch-up saccades may affect the velocity of post-saccadic pursuit (Schutz & Souto, 2011). Actually, in this case the impact seems to be much stronger and more consistent than the small and somewhat inconsistent learning transfer seen in our experiments. This difference may be a consequence of the distinct requirements of catch-up saccades which have to take the velocity of moving target into account, which is different from normal visually guided saccades (de Brouwer, Missal, & Lefevre, 2001).

Our study demonstrates some evidence for transfer of learning in short-term adaptation tasks, a form of adaptation that is based on adjustments at the level of individual Purkinje cells (Catz et al., 2008). Although minimal and not very consistent over experiments and subjects and therefore probably not to relevant in functional terms, the demonstration of occasional transfer is in line with the notion that the same OMV P-cells convey saccade- and SPEM information. It is commonly held that saccadic learning and other forms of cerebellum-dependent learning are based on changes of the strength of parallel fiber synapses (Albus, 1971; Marr, 1969). If OMV P-cells deployed largely congruent sets of parallel fiber synapses for the control of saccades and SPEM, we might have expected stronger and more consistent transfer effects. In other words the minor crosstalk observed argues for synaptic territories for saccade- and SPEM-related parallel fiber input on P-cell dendritic trees that are largely separate. However, reserving distinct pools of synapses for saccades and for SPEM would only help if also the mossy fiber (MF)-PF signals for saccades and SPEM offered to OMV P-cells formed functionally distinct and anatomically segregated pools. The finding of unrelated preferred directions of P-cell simple spikes for saccades and SPEM would be compatible with this assumption (Sun et al., 2017). However, it is questionable if and to what extent the requirement of segregation is really

met. Although for instance MF-PF input from the paramedian reticular formation (PPRF) (Gerrits & Voogd, 1986; Thielert & Thier, 1993) devoted to saccades (Hepp & Henn, 1983) complies with this requirement, a substantial fraction of eye movement-related neurons in the dorsal pontine nuclei (DPN), another source of MF-PF input to the OMV, are responding to saccades as well as to SPEM (Dicke, Barash, Ilg, & Thier, 2004). The latter might actually suggest that the duality of OMV P-cells is an inevitable consequence of the tight integration of information on saccades and SPEM on the input side as witnessed by the DPN but also other structures such as the reticular nucleus of the pontine tegmentum (NRTP) (Giolli et al., 2001) and superior colliculus (Krauzlis, 2003). We cannot say if the overlap between saccade and SPEM input to OMV P-cells is strong enough to override the impact of afferent fibers specifically devoted to the one or the other type of eye movement. In the case of dominating dual eye movement input, probably the only way to explain the observed small and inconsistent transfer would be to assume that the sensitivity of the behavioral tasks deployed may have been too poor to unravel larger savings of learning. Although this reservation has to be made, we think our demonstration of little transfer of saccadic adaptation SPEM, undoubtedly involving cerebellar P-cells, rather argues for distinct synaptic pools on P-cell dendritic trees, one reserved for saccades, the other for SPEM.

Acknowledgements:

The work was supported by a Marie Curie Initial Training Network (PITN-GA-2009-238214; to P.T.), the German Ministry of Education, Science, Research, and Technology through the Bernstein Center for Computational Neuroscience (FKZ 01GQ1002), and a grant from the Deutsche Forschungsgemeinschaft (FOR 1847-A3 TH425/13-1; to P.T).

The authors declare no competing financial interests.

Author contributions statement

A.S., Z.S., M.J and P.W.D. performed the experiments. Z.S. and A.S. analyzed the data. P.W.D. edited the manuscript. Z.S., A.S. and P.T. designed the paradigms and wrote the paper. All authors reviewed the manuscript.

References

Albus, J. S. (1971). A theory of cerebellar function. Math. Biosci., 10, 25-26.

Barash, S., Melikyan, A., Sivakov, A., Zhang, M., Glickstein, M., & Thier, P. (1999). Saccadic dysmetria and adaptation after lesions of the cerebellar cortex. J Neurosci, 19(24), 10931-10939.

Catz, N., Dicke, P. W., & Thier, P. (2008). Cerebellar-dependent motor learning is based on pruning a Purkinje cell population response. Proc Natl Acad Sci U S A, 105(20), 7309-7314.

Collins, T. (2014). Trade-off between spatiotopy and saccadic plasticity. J Vis, 14(12).

Dash, S., Catz, N., Dicke, P. W., & Thier, P. (2012). Encoding of smooth-pursuit eye movement initiation by a population of vermal Purkinje cells. Cereb Cortex, 22(4), 877-891.

Dash, S., & Thier, P. (2013). Smooth pursuit adaptation (SPA) exhibits features useful to compensate changes in the properties of the smooth pursuit eye movement system due to usage. Front Syst Neurosci, 7, 67.

de Brouwer, S., Missal, M., & Lefevre, P. (2001). Role of retinal slip in the prediction of target motion during smooth and saccadic pursuit. J Neurophysiol, 86(2), 550-558.

de Brouwer, S., Yuksel, D., Blohm, G., Missal, M., & Lefevre, P. (2002). What triggers catch-up saccades during visual tracking? J Neurophysiol, 87(3), 1646-1650.

Dicke, P. W., Barash, S., Ilg, U. J., & Thier, P. (2004). Single-neuron evidence for a contribution of the dorsal pontine nuclei to both types of target-directed eye movements, saccades and smooth-pursuit. Eur J Neurosci, 19(3), 609-624.

Fuchs, A. F. (1967). Saccadic and smooth pursuit eye movements in the monkey. J Physiol, 191(3), 609-631.

Fuchs, A. F., & Robinson, D. A. (1966). A method for measuring horizontal and vertical eye movement chronically in the monkey. J Appl Physiol, 21(3), 1068-1070.

Gerrits, N. M., & Voogd, J. (1986). The nucleus reticularis tegmenti pontis and the adjacent rostral paramedian reticular formation: differential projections to the cerebellum and the caudal brain stem. Exp Brain Res, 62(1), 29-45.

Giolli, R. A., Gregory, K. M., Suzuki, D. A., Blanks, R. H., Lui, F., & Betelak, K. F. (2001). Cortical and subcortical afferents to the nucleus reticularis tegmenti pontis and basal pontine nuclei in the macaque monkey. Vis Neurosci, 18(5), 725-740.

Golla, H., Tziridis, K., Haarmeier, T., Catz, N., Barash, S., & Thier, P. (2008). Reduced saccadic resilience and impaired saccadic adaptation due to cerebellar disease. Eur J Neurosci, 27(1), 132-144.

Havermann, K., & Lappe, M. (2010). The influence of the consistency of postsaccadic visual errors on saccadic adaptation. J Neurophysiol, 103(6), 3302-3310.

Hepp, K., & Henn, V. (1983). Spatio-temporal recoding of rapid eye movement signals in the monkey paramedian pontine reticular formation (PPRF). Exp Brain Res, 52(1), 105-120.

Krauzlis, R. J. (2003). Neuronal activity in the rostral superior colliculus related to the initiation of pursuit and saccadic eye movements. J Neurosci, 23(10), 4333-4344.

Marr, D. (1969). A theory of cerebellar cortex. J Physiol, 202(2), 437-470.

Martinez-Conde, S., Macknik, S. L., Troncoso, X. G., & Hubel, D. H. (2009). Microsaccades: a neurophysiological analysis. Trends Neurosci, 32(9), 463-475.

McLaughlin, S. (1967). Parametric adjustment in saccadic eye movements. Percept Psychophys, 2, 359–362.

Noto, C. T., & Robinson, F. R. (2001). Visual error is the stimulus for saccade gain adaptation. Brain Res Cogn Brain Res, 12(2), 301-305.

Ohki, M., Kitazawa, H., Hiramatsu, T., Kaga, K., Kitamura, T., Yamada, J., et al. (2009). Role of primate cerebellar hemisphere in voluntary eye movement control revealed by lesion effects. J Neurophysiol, 101(2), 934-947.

Optican, L. M., & Robinson, D. A. (1980). Cerebellar-dependent adaptive control of primate saccadic system. J Neurophysiol, 44(6), 1058-1076.

Prsa, M., Dicke, P. W., & Thier, P. (2010). The absence of eye muscle fatigue indicates that the nervous system compensates for non-motor disturbances of oculomotor function. J Neurosci, 30(47), 15834-15842.

Rashbass, C. (1961). The relationship between saccadic and smooth tracking eye movements. J Physiol, 159, 326-338.

Robinson, D. A. (1963). A method of measuring eye movement using a scleral search coil in a magnetic field. IEEE Trans Biomed Eng, 10, 137-145.

Robinson, D. A. (1965). The mechanics of human smooth pursuit eye movement. J Physiol, 180(3), 569-591.

Robinson, F. R., Noto, C. T., & Bevans, S. E. (2003). Effect of visual error size on saccade adaptation in monkey. J Neurophysiol, 90(2), 1235-1244.

Schutz, A. C., & Souto, D. (2011). Adaptation of catch-up saccades during the initiation of smooth pursuit eye movements. Exp Brain Res, 209(4), 537-549.

Srimal, R., Diedrichsen, J., Ryklin, E. B., & Curtis, C. E. (2008). Obligatory adaptation of saccade gains. J Neurophysiol, 99(3), 1554-1558.

Straube, A., Deubel, H., Ditterich, J., & Eggert, T. (2001). Cerebellar lesions impair rapid saccade amplitude adaptation. Neurology, 57(11), 2105-2108.

Sun, Z., Smilgin, A., Junker, M., Dicke, P. W., & Thier, P. (2017). The same oculomotor vermal Purkinje cells encode the different kinematics of saccades and of smooth pursuit eye movements. Sci Rep, 7, 40613.

Takagi, M., Zee, D. S., & Tamargo, R. J. (2000). Effects of lesions of the oculomotor cerebellar vermis on eye movements in primate: smooth pursuit. J Neurophysiol, 83(4), 2047-2062.

Thielert, C. D., & Thier, P. (1993). Patterns of projections from the pontine nuclei and the nucleus reticularis tegmenti pontis to the posterior vermis in the rhesus monkey: a study using retrograde tracers. J Comp Neurol, 337(1), 113-126.

Wallman, J., & Fuchs, A. F. (1998). Saccadic gain modification: visual error drives motor adaptation. J Neurophysiol, 80(5), 2405-2416.

Westheimer, G. (1954). Eye movement responses to a horizontally moving visual stimulus. AMA Arch Ophthalmol, 52(6), 932-941.

Appendix 3:

Sun, Z., Junker, M., Dicke, P.W., Thier, P. (2016) Individual neurons in the caudal fastigial oculomotor region convey information on both macro- and microsaccades. Eur J Neurosci, 44(8), 2531-2542.

EJN European Journal of Neuroscience

FENS Federation of European Neuroscience Societies

European Journal of Neuroscience, Vol. 44, pp. 2531–2542, 2016 doi:10.1111/ejn.13289

NEUROSYSTEMS

Individual neurons in the caudal fastigial oculomotor region convey information on both macro- and microsaccades

Zongpeng Sun,[1,2,3] Marc Junker,[1,2,3] Peter W. Dicke[1] and Peter Thier[1]

[1]Department of Cognitive Neurology, Hertie Institute for Clinical Brain Research, Hoppe-Seyler-Str. 3, Tübingen 72076, Germany

[2]Graduate School of Neural and Behavioural Sciences, University of Tübingen, Tübingen, Germany

[3]International Max Planck Research School for Cognitive and Systems Neuroscience, University of Tübingen, Tübingen, Germany

Keywords: cerebellum, fastigial nucleus, microsaccades, monkey, saccades

Edited by John Foxe

Received 25 January 2016, revised 24 May 2016, accepted 24 May 2016

Abstract

Recent studies have suggested that microsaccades, the small amplitude saccades made during fixation, are precisely controlled. Two lines of evidence suggest that the cerebellum plays a key role not only in improving the accuracy of macrosaccades but also of microsaccades. First, lesions of the fastigial oculomotor regions (FOR) cause horizontal dysmetria of both micro- and macrosaccades. Secondly, our previous work on Purkinje cell simple spikes in the oculomotor vermis (OV) has established qualitatively similar response preferences for these two groups of saccades. In this work, we investigated the control signals for micro- and macrosaccades in the FOR, the target of OV Purkinje cell axons. We found that the same FOR neurons discharged for micro- and macrosaccades. For both groups of saccades, FOR neurons exhibited very similar dependencies of their discharge strength on direction and amplitude and very similar burst onset time differences for ipsi- and contraversive saccades and, in both, response duration reflected saccade duration, at least at the population level. An intriguing characteristic of microsaccade-related responses is that immediate pre-saccadic firing rates decreased with distance to the target center, a pattern that strikingly parallels the eye position dependency of both microsaccade metrics and frequency, which may suggest a potential neural mechanism underlying the role of FOR in fixation. Irrespective of this specific consideration, our study supports the view that microsaccades and macrosaccades share the same cerebellar circuitry and, in general, further strengthens the notion of a microsaccade–macrosaccade continuum.

Introduction

High-resolution vision in primates is limited to the foveal region, which is why saccades are needed to shift the images of peripheral targets requiring further analysis into the fovea. Microsaccades, small saccades having an amplitude of $< 1°$ down to a few minutes of arc, seen during fixation (Martinez-Conde *et al.*, 2004) had at first been interpreted as oculomotor noise (Kowler & Steinman, 1980). However, the current consensus is that microsaccades serve vision. Ditchburn and Ginsborg noted images tended to fade if image shifts due to microsaccades were prevented by technical means (Ditchburn & Ginsborg, 1952). In addition to preventing fading, recent work suggests that microsaccades are well-controlled goal-directed movements (Winterson & Collewijn, 1976; Bridgeman & Palca, 1980; Cui *et al.*, 2009; Ko *et al.*, 2010; McCamy *et al.*, 2013; Thaler *et al.*, 2013), ensuring that the retinal image is moved from the foveal periphery into its center, the rod-free foveola (Gass, 1999; Li *et al.*, 2010). This allows vision to exploit the resolution peak accommodated by this region (Putnam *et al.*, 2005; Poletti *et al.*, 2013).

A mounting number of studies have indicated that micro- and macrosaccades share most, if not all, of their kinematic properties and may actually share a common generator (Zuber *et al.*, 1965; Van Gisbergen & Robinson, 1977; Van Gisbergen *et al.*, 1981; Engbert, 2006; Rolfs *et al.*, 2006; Otero-Millan *et al.*, 2008, 2011a,b).

It is well known that the cerebellum plays a crucial role in securing the precision and reliability of saccadic eye movements. Lesions of the oculomotor vermis (OV), the major saccade-related region of cerebellar cortex (Ritchie, 1976; Optican & Robinson, 1980; Takagi *et al.*, 1998; Barash *et al.*, 1999; Golla *et al.*, 2008; Ignashchenkova *et al.*, 2009), as well as lesions of its major target, the caudal

Correspondence: Peter Thier, as above.
E-mail: thier@uni-tuebingen.de

fastigial nucleus (Vilis & Hore, 1981; Robinson *et al.*, 1993; Straube *et al.*, 1994; Goffart *et al.*, 2004), compromise the precise control of saccades, leading to 'saccadic' dysmetria.

Arguably, the requirements for the precise control of microsaccades are even higher than for macrosaccades, assuming that their metric should be precisely determined to shift an image feature exactly into the foveola. Two findings live up to this expectation: (i) Purkinje cells in the OV are tuned for both macro- and microsaccades (Arnstein *et al.*, 2015). (ii) Unilateral inactivation of the caudal fastigial nucleus, the fastigial oculomotor region (FOR), causes dysmetria not only of macro- but also of microsaccades (Guerrasio *et al.*, 2010). However, there has so far been no attempt to identify microsaccade-related activity in the FOR and to assess its features. Furthermore, the mechanism underlying the fixation offset induced by the dysfunction of FOR (Sato & Noda, 1992; Robinson *et al.*, 1993; Goffart *et al.*, 2004; Guerrasio *et al.*, 2010) is still vague. Here, we report that neurons in the FOR of rhesus monkeys are indeed tuned for both macro- and microsaccades, and we reveal an activity change in FOR that may be related to the precise fixation.

Materials and methods

Animal preparation – behavioral tasks

Three rhesus macaques, purchased from the German Primate Centre, Göttingen, were used in these experiments. Before being trained on the task, the monkeys underwent a surgery, in which a titanium head post was mounted on the skull for head stabilization during the experiments and magnetic scleral search coils were implanted into the eyes to record the eye position. Moreover, a recording chamber, whose position and orientation were carefully planned based on presurgical MRI and confirmed by post-surgical MRI, was placed over the midline of the cerebellum. Surgeries were carried out under combination anesthesia with remifentanil and isoflurane under aseptic conditions (see Arnstein *et al.* (2015) for details). Post-operative analgesia was continued until full recovery. All operations and experiments were approved by the local animal care committee (Regierungspräsidium Baden-Württemberg) and conducted in accordance with German and European law and the guidelines of the National Institutes of Health for Care and Use of Laboratory Animals.

After recovery, each monkey was trained to enter the primate chair voluntarily. During the experiments, they were seated in their primate chairs with their head restrained within the center of the magnetic field driving the eye search coils. To calibrate the search coil signal, a monkey had to fixate a red spot of light (diameter 0.4°) presented on a dark CRT monitor 37 cm in front. On each trial the spot appeared in a new position, randomly chosen from a set of nine positions, forming a 30 × 30° grid with a spacing of 15°. Proper fixation, allowing the alignment of the known position and the search coil output voltages, was rewarded by units of juice, delivered through a mouth tube and manually controlled by the experimenter. The actual experiments required monkeys to perform visually guided saccades to peripheral targets (in most cases, amplitude: 10°) in eight random directions (horizontal, vertical, and the four diagonal directions). The animal was asked to make a saccade to the new target location starting from a central fixation target. This central target had the same features (red dot, diameter 0.2–0.3°) as the peripheral target and was on for an unpredictable period of 500–1500 ms. This was accomplished by choosing a period of 500–1300 ms for a particular recording session and adding randomly a time increment of 0–200 ms in each trial. The disappearance of the central target served as go signal to make a saccade to the peripheral target that appeared at the same time. Fixation of both the central and the peripheral target required that eye gaze stayed inside an eye position window of 2°–4° square centered on the target. A trial was aborted if the monkey broke fixation or the monkey did not initiate a saccade within 400 ms after the target shift and did not stay for a minimum time of 300 ms on the peripheral target. In case the behavior did not meet the requirements the fluid reward which would have been delivered for correct performance was withheld. The motivation to work on the fixation and saccade task was promoted by restricting fluid provisions outside the experiment (see Arnstein *et al.* (2015) for details on the protocol).

Electrophysiological recordings

Post-surgical MRI scans were used to reassess the chamber orientation and select the chamber positions suitable for the electrode approach to the FOR. Neuronal activity recorded from physiological landmarks such as the brainstem oculomotor nuclei helped to double check the orientation of the recording chamber relative to the FOR, allowing us to optimize the approach of the glass-coated tungsten microelectrodes (impedances 1–2 MΩ; Alpha Omega Engineering, Nazareth, Israel) to the FOR. A successful electrode approach to the FOR was characterized by a characteristic sequence of background activity along a tract: first, the appearance of the hallmarks of cerebellar grey matter activity like the dense granule cell background activity and the occurrence of complex spikes; then a longer stretch of a silent background reflecting the passage through white matter separating cerebellar cortex and the fastigial nucleus; and finally, when entering the fastigial nucleus, again relatively dense background activity along with the occurrence of characteristic saccade-related burst firing in its caudal part and the absence of complex spikes.

Data analysis

All analyses were performed offline with self-written MATLAB programs (The MathsWorks Inc., Natick, MA). We sampled the eye movement records at a rate of 1000 Hz. Microsaccades were detected in a similar way as described before (Arnstein *et al.*, 2015): First, the eye trace was smoothed using a Savitzky-Golay filter (second order with 20 ms width) and then eye velocity was derived from the eye position records. We employed a velocity threshold (7°/s) to identify saccades. If eye velocity exceeded this threshold, we searched the velocity record back for the moment, the velocity record first crossed a 4°/s threshold and forward to identify the moment, it fell back below this value, taking the two moments as saccade onset and offset times, respectively.

Saccades that were initiated within the fixation window centered on the straight ahead fixation target and whose amplitudes were smaller than 1° were classified as microsaccades (Martinez-Conde *et al.*, 2004). Correspondingly any saccades larger than that were classified as macrosaccades. The macrosaccade class includes macrosaccades detected during fixation, violating task requirements, as well as the saccades made to the eccentric targets. The median microsaccade amplitude was 0.59°. Neurons were recorded from both sides, but for statistical analysis, FOR neurons recorded from the right FOR were added to the pool of neurons recorded from the left FOR by flipping the horizontal component of the associated eye movement, while leaving the vertical component unaltered. This procedure assumes that the representation of the vertical direction is

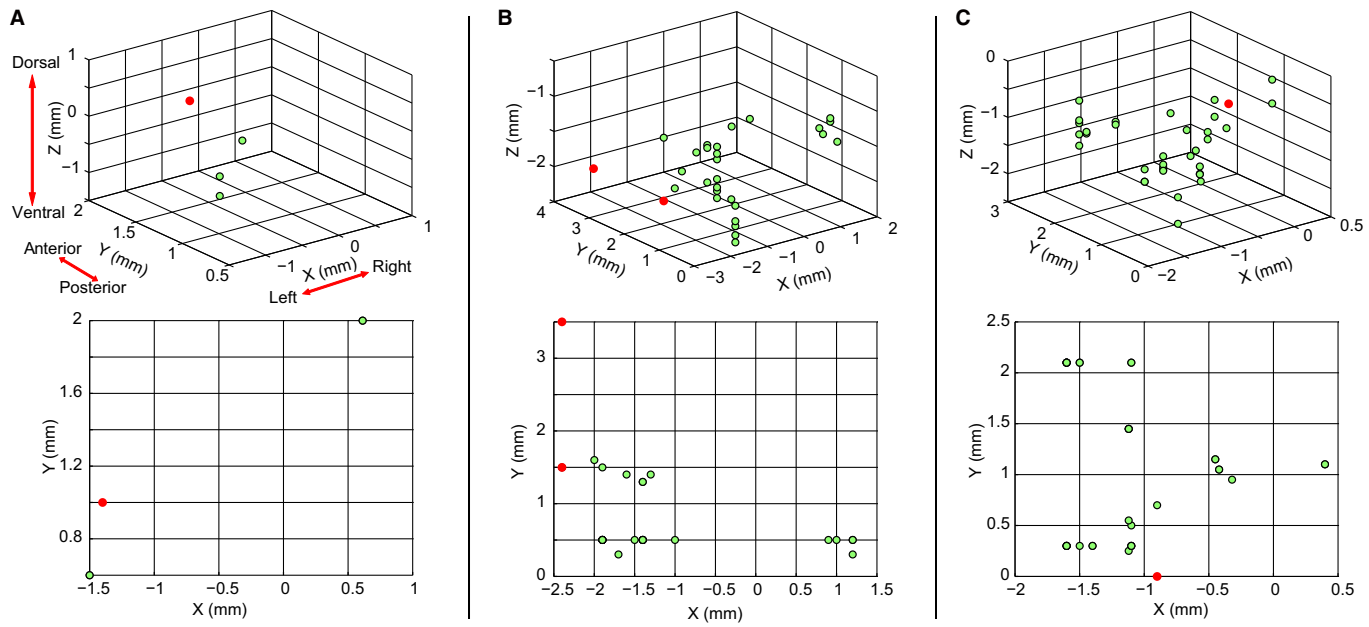

FIG. 1. Reconstruction of recording sites of fastigial oculomotor region neurons. Reconstructed neuron locations (green circles; see Methods for details of the procedure used) are given in a Cartesian coordinate system ($x = 0$: estimated sagittal midline, $y = 0$: estimated caudal end of fastigial nucleus, $z = 0$: estimated topmost layer of fastigial nucleus). (A–C) Show data for the three monkeys used. Note that individual symbols may stand for several neurons, which is why the number of symbols is much smaller than the actual number of recorded neurons. The red circles mark the locations of dye injections that fell inside the volume shown. More were located outside.

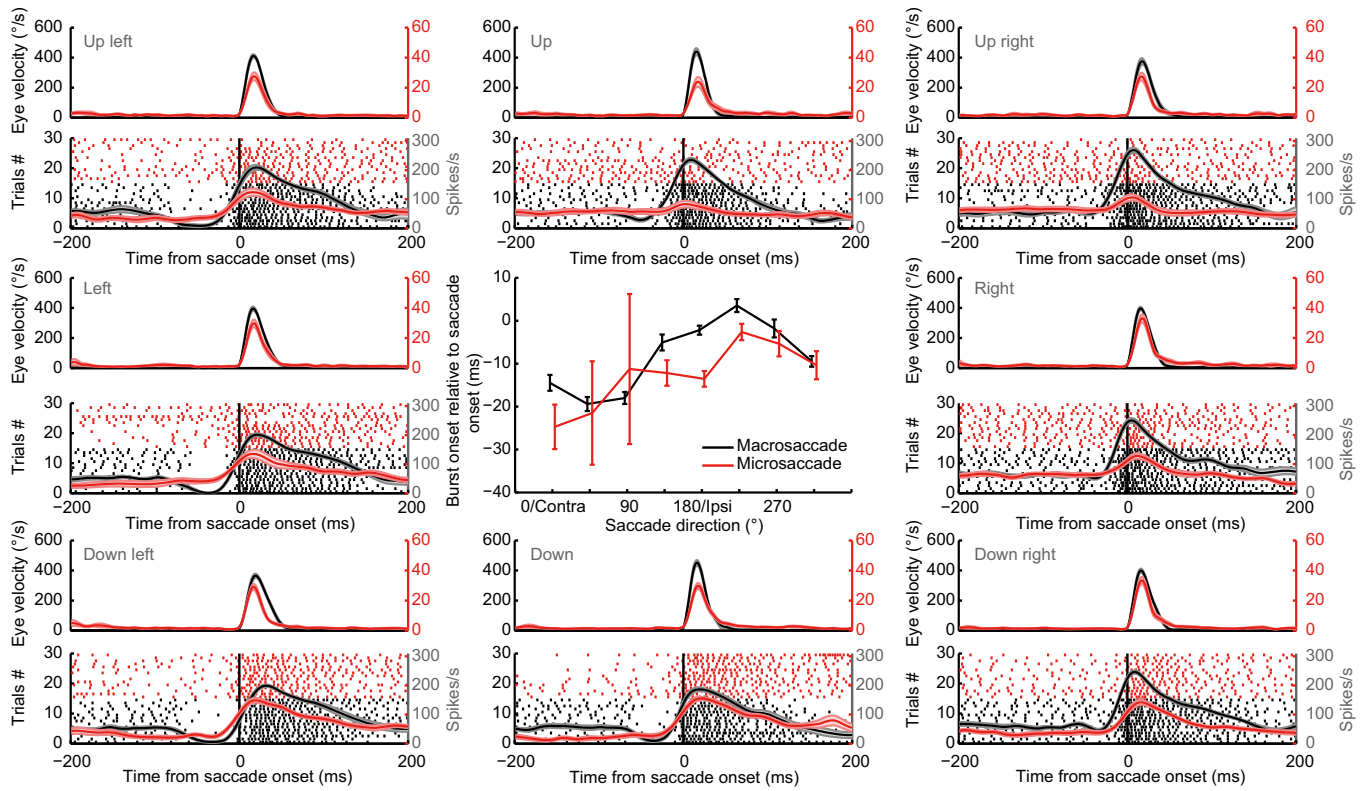

FIG. 2. Perisaccadic neural discharge patterns of exemplary fastigial oculomotor region neuron during microsaccades (red) and macrosaccades (black). Saccades in eight different directions are shown in the frontoparallel plane (outer panels). For each direction, 15 trials for microsaccades and macrosaccades are included. The means and standard errors (± SEM plotted in lighter, semitransparent colors) of eye velocity are shown and neural activity is represented by raster plots aligned relative to saccade onset. In addition, mean spike density functions (± SEM plotted in lighter, semitransparent colors) are shown superimposed on the raster plots. The vertical lines indicate saccade onset. The center panel plots the burst onset time as a function of direction. Error bars indicate ± SEM. The means and standard deviations of the amplitudes of the macrosaccade and microsaccade made were 10.02 ± 0.58° and 0.54 ± 0.23°, respectively.

the same in the left and the right FOR. This assumption is supported by the fact that the most direction-dependent parameter – onset latency – showed the same dependence on the vertical for neurons recorded from the left and the right FOR (see Fig. 3E). Hence, in the pooled data, the direction right corresponds to contralateral relative to the recorded (left) side. Both micro- and macrosaccades were binned into eight direction classes (0°/right, 45°, 90°/upward, 135°, 180°/leftward, 215°, 270°/down, and 315°; bin size 45°). Macro- and microsaccades falling in one of these bins that were centered on the eight directions were associated with the respective direction. Each direction class had to contain at least five saccades, otherwise this direction was not considered. The means and SD of the number of micro- and macrosaccades per neuron were 135 ± 72 (range from 28 to 410) and 378 ± 187 (range from 154 to 1151), respectively. For the calculation of the baseline firing rate, we used an interval from −200 to −100 ms relative to saccade onset. To calculate the baseline firing rate, we considered all saccades independent of direction.

The instantaneous firing rate was estimated by convolving each spike train with a Gaussian kernel having a width of σ = 10 ms. Simple spike times were aligned with respect to saccade onset. FOR neurons were tested for saccade-related activity by comparing the mean firing rate between saccade onset and offset with the mean baseline firing rate during the period from −200 to −100 ms relative to saccade onset (Wilcoxon signed-rank test, $P < 0.05$). A Poisson spike train analysis was applied to detect the onset and the offset of burst activity of FOR neurons in single trials (Hanes *et al.*, 1995). The Poisson spike train analysis determines the probability of the occurrence of a certain number of spikes within a given interval of time based on the assumption of Poisson distributed spikes with the distribution parameters determined from the baseline firing rate. The measurement of the burst onset times was confined to a time window of −60 to 60 ms relative to saccade onset to avoid the detection of spurious saccade-related bursts. By the same token, burst offset latencies were confined to a time window of 0 to 200 ms relative to saccade onset. To investigate

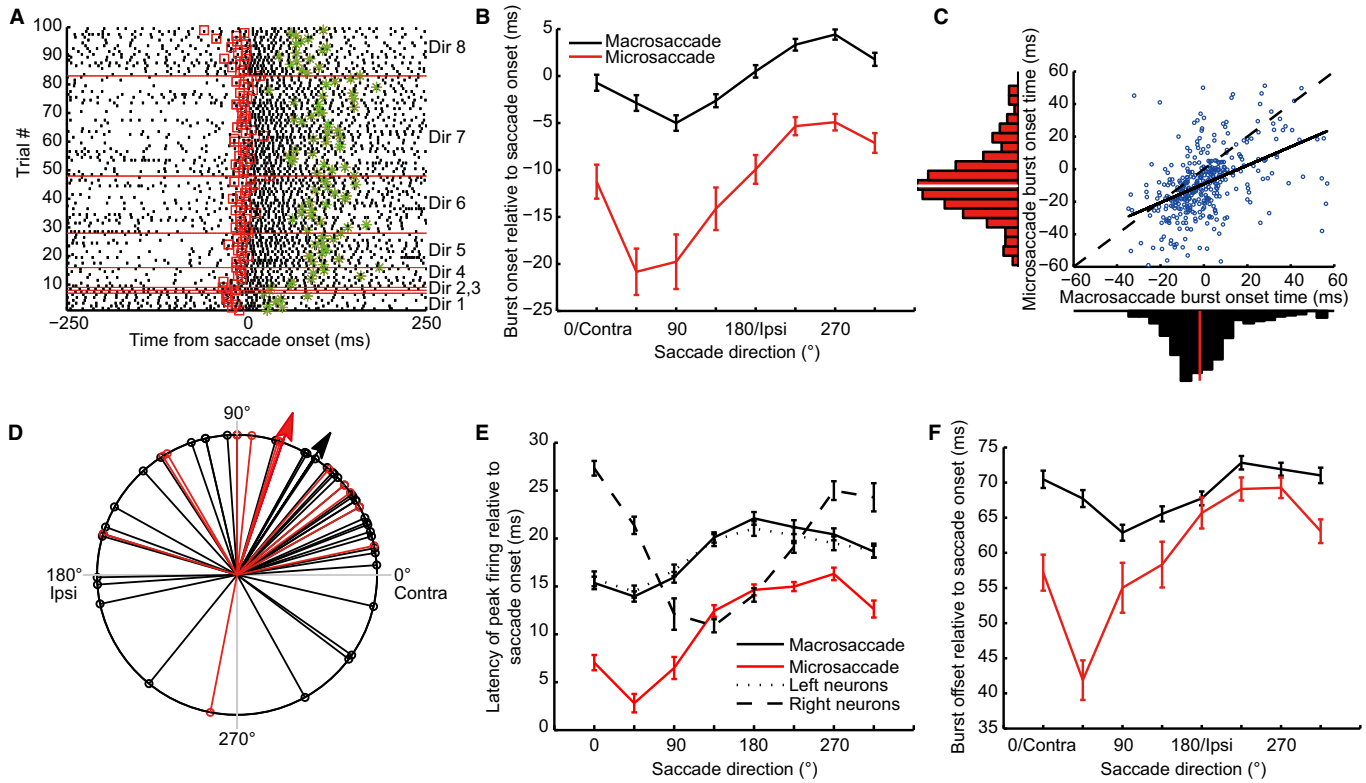

FIG. 3. Analysis of burst timing. (A) Exemplary fastigial oculomotor region (FOR) neuron responding to microsaccades made in different directions in the frontoparallel plane. The individual trials shown are arranged according to direction bins and red horizontal lines separate trials falling into different direction bins, specified on the right side: Dir 1–8 represent 0°, 45°, 90°, 135°, 180°, 225°, 270°, and 315°, respectively. Burst onset and offset time as detected by Poisson spike train in individual trials is indicated by red squares and green asterisks, respectively. Note the substantially larger variability in offset times. (B) Burst onset time relative to saccade onset as function of direction for macrosaccades (black) and microsaccades (red). (C) Linear regression of burst onset time of microsaccades as function of burst onset time of macrosaccades in eight directions. The histograms next to the axes give the individual burst onset time distributions. In these distributions, the medians are indicated by red (microsaccades) and white lines (microsaccades), respectively. The black dashed line indicates the identity line ($y = x$) and the regression line (solid black line) ($y = 0.57*x-9.15$; $R^2 = 0.21$) is displaced and tilted relative to it. (D) Polar diagram showing the distribution of the directions of individual neurons exhibiting the shortest burst onset time for microsaccades (red) and macrosaccades (black). The circular means are indicated by red and black arrows, respectively. (E) Latency of peak firing rates relative to saccade onset as function of direction for macrosaccades (black) and microsaccades (red). The closed lines represent pooled data assuming that all neurons were recorded from the left side (see Methods). In addition, the latency dependencies of macrosaccade-related responses of left and right FOR neurons are shown separately (dotted line: left neurons, dashed line: right neurons). Please note that the plot of latency as function of direction for the subgroup of neurons recorded from the right side ('right neurons') is phase shifted relative to 'left neurons' because the x axis specifies saccade direction in absolute terms with 0° indicating saccades to the right and 90° up. For both 'left' and 'right' neurons the horizontal direction yielding the shorted latency is contralateral to the recorded side. Please recall that the plots for macrosaccades are based on the assumption that neurons were recorded from the left (see Methods). (F) Burst offset time relative to saccade onset as function of direction for macrosaccades (black) and microsaccades (red).

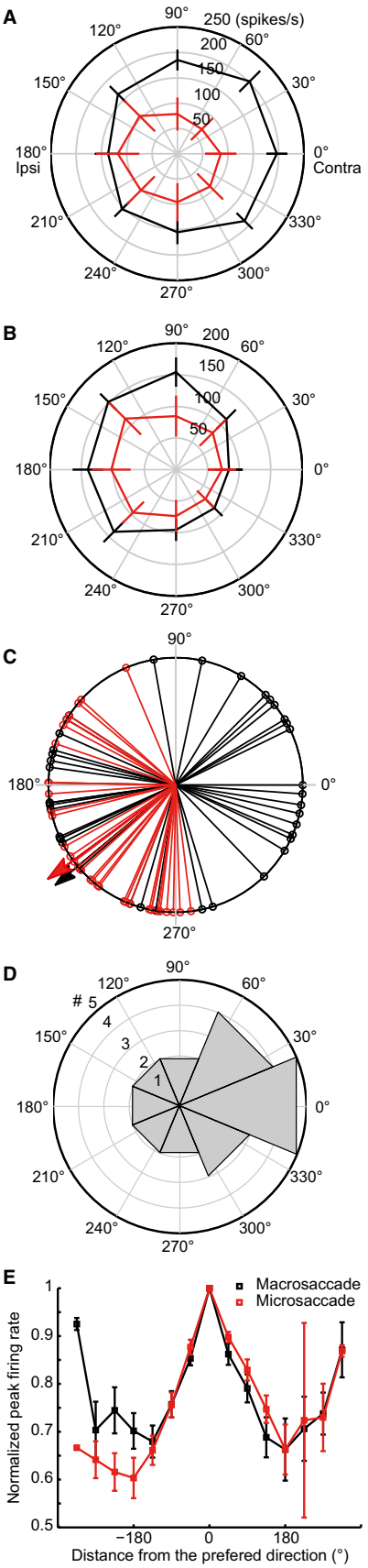

FIG. 4. Direction dependency of mean discharge rate during saccade-related bursts for macrosaccades (black) and microsaccades (red). (A, B) Two exemplary fastigial oculomotor region neurons (mean discharge rate ± SD). (C) Polar diagram showing the distribution of preferred directions of individual neurons for microsaccades (red) and macrosaccades (black). The circular means are indicated by red and black arrows, respectively. (D) Polar plot of the differences between the preferred directions for microsaccades and macrosaccades of individual neurons. # = number of neurons. 0° indicates perfect correspondence between the two preferred directions, 180° indicates opposite selectivity, 45–135° indicate counterclockwise shifts of the preferred direction for microsaccades relative to the preferred direction for macrosaccades, and 225–315° indicate clockwise shifts. (E) Plot of mean normalized discharge rate in saccade-related bursts as function of saccade direction relative to the individual preferred directions pooled across all neurons. For each neuron, the direction giving the strongest response was set to 0 and the firing rate to 1. Positive angles represent a counterclockwise shift relative to the preferred direction; negative angles indicate clockwise shifts. Error bars indicate ± SEM.

direction-dependent differences in the timing of microsaccade-related bursts, we in addition considered the time of peak firing.

Directional preference of timing parameters or mean discharge rates was assumed if a non-parametric Kruskal–Wallis test of the respective parameter as function of saccade direction revealed significant ($P < 0.05$) differences between directions. The preferred direction was estimated by fitting sine functions to the mean firing rate and burst onset latency, respectively, as function of direction. Only neurons that contained adequate data in at least six direction bins and for which the fit led to coefficients of determination bigger than 0.5 were considered. A circular statistical analysis of angular distances was carried out using the circ_stat toolbox for MATLAB (Berens, 2009). To compare the neural activity associated with saccades of different amplitudes, we pooled saccades made in any of the eight directions and divided them into eight bins according to saccade amplitude: 0–0.4°, 0.4–0.7°, 0.7–1°, 1–2°, 2–3°, 3–8°, 8–10°, and 10–15°. The resulting plot of discharge rate as function of amplitude was normalized relative to the bin with the highest discharge rate set to 1. Next, the resulting normalized amplitude tuning curves of individual FOR neurons were aligned relative to the bin that exhibited the highest mean firing rate to calculate a normalized average amplitude tuning curve. Furthermore, we calculated population averages of individual instantaneous firing rates as function of time relative to saccade onset for each amplitude bin. Burst onset and offset in the resulting population average were taken as the points in time at which the firing rate went above and below, respectively, a level corresponding to 30% of the distance between the baseline firing rate and the burst peak. For the baseline firing rate and saccade amplitude analysis as a function of eye starting position, all micro- and macrosaccades made during fixation were included.

Anatomy and histology

At the end of the recording sessions, 0.5–1.5 μL of a concentrated solution of rhodamine-labeled latex beads dissolved in saline was injected into 1–2 locations, each in the vicinity of the recording sites in each of the fastigial nuclei explored, serving as reference points in the later reconstructions of recording sites. Several days or a few weeks after the injections, the monkeys were deeply anesthetized and perfused with 4% paraformaldehyde. The fixed brain was cut into 60-μm serial sagittal sections. Alternative sections were Nissl

stained or mounted unstained for the detection of the rhodamine fluorescence. The reconstruction of the recording sites based on the microdrive readings, the localization of the rhodamine injections, and occasional subtle histological alterations due to electrode penetrations in the sections allowed us to confirm that all neurons reported here were recorded from the FOR (Fig. 1).

Results

We recorded 74 saccade-related FOR neurons from three rhesus monkeys. Their locations were confirmed by a careful reconstruction of individual electrode tracks (see Methods). Of these, six neurons were only macrosaccade but not microsaccade related. Another neuron was excluded because the records did not contain a sufficient number of microsaccades. Hence, for the detailed comparison of macrosaccades and microsaccades, 67 neurons could be considered (M1: 3, M2: 30, M3: 34). Fifty-seven of 67 neurons were recorded from the left and 10 from the right FOR. In accordance with previous reports, most macrosaccade-related discharges were characterized by a conspicuous burst component (Ohtsuka & Noda, 1990, 1991; Robinson *et al.*, 1993; Helmchen *et al.*, 1994; Scudder & McGee, 2003). The same held for responses to microsaccades (see Fig. 2 for a representative example of a neuron located in the left FOR tested for saccades in eight directions).

Timing of saccade-related bursts

Previous studies have shown that the burst for contraversive macrosaccades starts earlier than the one for ipsiversive saccades (Ohtsuka & Noda, 1990, 1991; Robinson *et al.*, 1993). To study the burst onset and offset quantitatively, we relied on a Poisson spike train analysis to detect the two in individual trials. As exemplified in Fig. 3A, this method worked quite well for both onset and offset. This neuron also documents that, in general, offset latency measurements were characterized by a much higher trial-by-trial variability, arguably the consequence of the fact that the decline in the discharge back to baseline levels was in general more gradual than the initial build-up, rendering the latency detection more susceptible to noise. In our sample, 41 of the 67 neurons tested exhibited a significant lead of bursts associated with contraversive macrosaccades (two-sample t test comparison of burst onset latencies in the two bins representing ipsi- and contraversive saccades, respectively, $P < 0.05$). To investigate the influence of saccade direction on burst timing of both macrosaccade- and microsaccade-related bursts in more detail, we ran two-way ANOVAS with the factors 'direction' and 'saccade class'. In general, independent of direction, microsaccade-related bursts started about 9 ms earlier than macrosaccade-related bursts (Fig. 3B,C) (main effect of saccade class, $P = 2 \times 10^{-11}$; main effect of direction, $P = 7 \times 10^{-6}$; no significant interaction between factors, $P = 0.19$). The fact that burst onsets for macrosaccades are in general later than for microsaccades is illustrated in Fig. 3B, which plots mean burst onset latency as a function of direction separately for microsaccades and macrosaccades. The positive correlation between burst onset latencies of macrosaccades and microsaccades (Fig. 3C) indicates that neurons with earlier burst onset for macrosaccades also started to fire earlier for microsaccades and *vice versa*. And independent of saccade class, bursts for the direction with the earliest burst onset started about 8 ms earlier than those for direction with the latest burst onset (t test comparing the earliest with the latest onset latencies, data collapsed across macro- and microsaccades, $P = 5 \times 10^{-5}$; same test for macrosaccades only, $P = 5 \times 10^{-7}$; microsaccades only, $P = 0.4878$). As can be

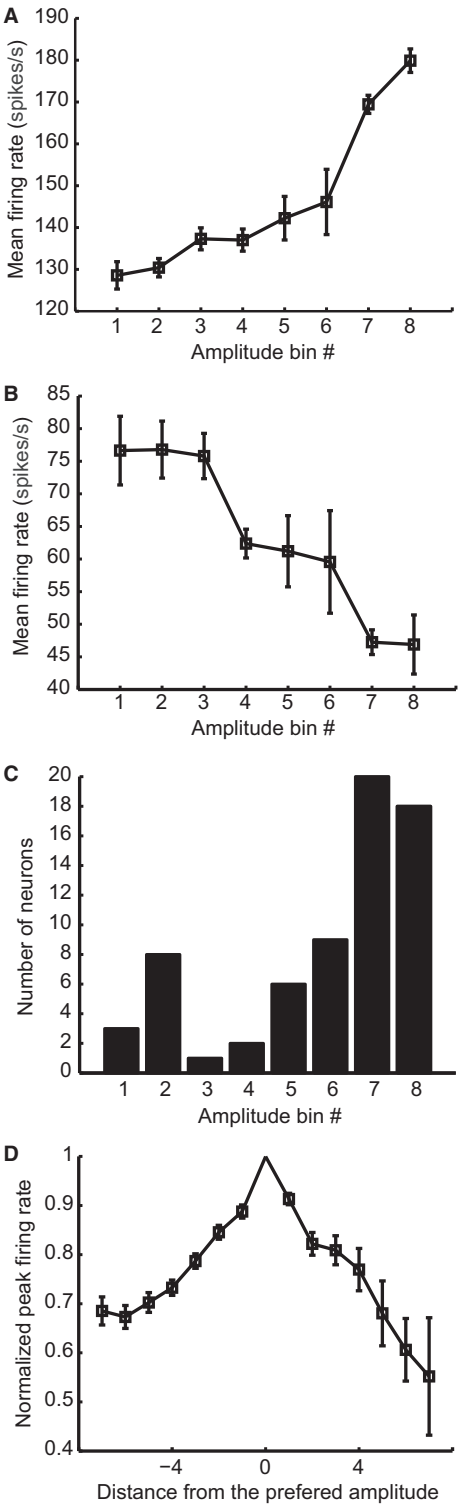

FIG. 5. Amplitude dependency of mean discharge rate in saccade-related bursts. (A, B) Exemplary fastigial oculomotor region (FOR) neurons. Mean firing rate (± SEM) is plotted as function of saccade amplitude class (see Methods). (C) Histogram plotting the number of FOR neurons preferring particular saccade amplitude bins. (D) Population amplitude tuning curve. Normalized mean firing rate is plotted against distance from preferred amplitude bin. For each neuron, the amplitude bin giving the strongest response was set to 0 and the firing rate to 1. Positive amplitude distances correspond to saccades larger than the preferred amplitude; negative distances indicate saccades smaller than the preferred amplitude. Error bars indicate ± SEM.

seen in Fig. 3B, the direction giving the shortest burst latencies deviated from the contraversive horizontal in an upward direction for both micro- and macrosaccades. To characterize this deviation quantitatively, we determined the direction giving the shortest latency response by fitting sine functions to individual plots of burst onset latency as a function of direction for neurons with a significant direction dependency of macrosaccade-related burst onset (Kruskall–Wallis test, $P < 0.05$), separately for micro- and for macrosaccades and pinpointed the direction giving the minimal functional value. The resulting circular distribution is centered at about 60–70° (Fig. 3D), with no significant difference between the two saccade classes (two-sample t test, $P = 0.62$). The conclusion that the directions giving the shortest latency responses are the same for micro- and macrosaccades is also supported by an analysis of the angular distance between the directions with minimal latency for micro- and macrosaccades for individual neurons. The resulting distribution is significantly different from a uniform circular distribution (Rayleigh test, $P = 5 \times 10^{-4}$) and centered on 0°. Finally, the analysis of the dependence of latencies of peak firing on saccade direction was able to reveal similar effects of saccade direction on the time of peak firing as the one for burst onset (two-way ANOVA of the effects of saccade class and direction, significant effects of saccade class and direction, $P = 3 \times 10^{-11}$ and 3×10^{-8}) (Fig. 3E). We finally asked how the offset of the burst would change for different directions. Burst offset times for microsaccades and macrosaccades, respectively, were plotted as a function of direction (Fig. 3F). We found a pattern that was very similar to that of the burst onset: microsaccade-related bursts not only started earlier than macrosccade-related bursts but also generally ended earlier (two-way ANOVA with the factors saccade class and direction, significant effect of direction, $P = 0.0005$) and the directions yielding the shortest burst offset latencies were shifted upward by 50–70° counterclockwise relative to the horizontal axis, with no significant difference between the two (two-sample t test, $P = 0.63$).

Direction tuning of response strength

Saccade direction also influenced the number of action potentials from burst onset to offset. Figure 4A presents the polar plots of the mean firing rate of the burst as a function of direction for an exemplary neuron, separately for micro- and macrosaccades. This neuron had been recorded from the left FOR. For macrosaccades, it exhibited a broad, albeit clear directional tuning with stronger responses to contraversive saccades. However, the microsaccade-related responses showed directional preference for ipsiversive saccades. Figure 4B depicts another neuron that, unlike the preceding one, demonstrated very similar preferences for macro- and microsaccades made to the ipsiversive side. Whereas 93% (62 of 67) of the units exhibited a significant direction dependence of their discharge for macrosaccades (Kruskal–Wallis test, $P < 0.05$), this percentage amounted to only 66% (44 out of 67) for microsaccades.

For those neurons for which the Kruskall–Wallis test had established a significant direction dependence at least for one of the two saccade classes, we estimated the preferred direction by fitting a sine function to the mean firing rate as a function of direction (see Methods) for each saccade class. Figure 4C depicts the circular distribution of the preferred directions obtained for both classes of saccades. It clearly shows that independent of saccade class, more neurons preferred ipsiversive directions (macrosaccades: 21 of 40, microsaccade: 33 of 35). Although as mentioned before, individual neurons could exhibit clear differences between their direction preferences for micro- and macrosaccades, in most cases these differences were very small. This is indicated by the distribution of differences between preferred directions for micro- and macrosaccades (Fig. 4D) which peaks at 0°.

Microsaccade- and macrosaccade-related responses were also very similar in terms of the modulation depth and width of their direction tuning functions. This becomes apparent when plotting the mean direction tuning curves relative to their respective preferred direction (Fig. 4E). The conspicuous congruency is documented by the high similarity between the two tuning curves. In short, direction tuning curves were very similar for micro- and macrosaccades, although individual preferred directions could occasionally show very little correspondence.

Amplitude tuning

To investigate the influence of saccade amplitude on the discharge we grouped saccades, independent of direction, into eight amplitude bins (0–0.4°, 0.4–0.7°, 0.7–1°, 1–2°, 2–3°, 3–8°, 8–10°, and 10–15°). Figure 5A,B depicts the resulting amplitude tuning curves for two exemplary neurons, exhibiting clear dependencies of their respective firing rates on amplitude. Whereas the neuron shown in Fig. 5A was characterized by a monotonic increase in firing rate with amplitude, the one shown in Fig. 5B displayed the highest firing rate for the microsaccade bins 1–3, from where the response declined monotonically with increasing amplitude. Other neurons (not shown) had their strongest response in particular amplitude bins other than the extreme ones. For most neurons, the amplitude bin yielding the largest response was one of the three largest ones. In

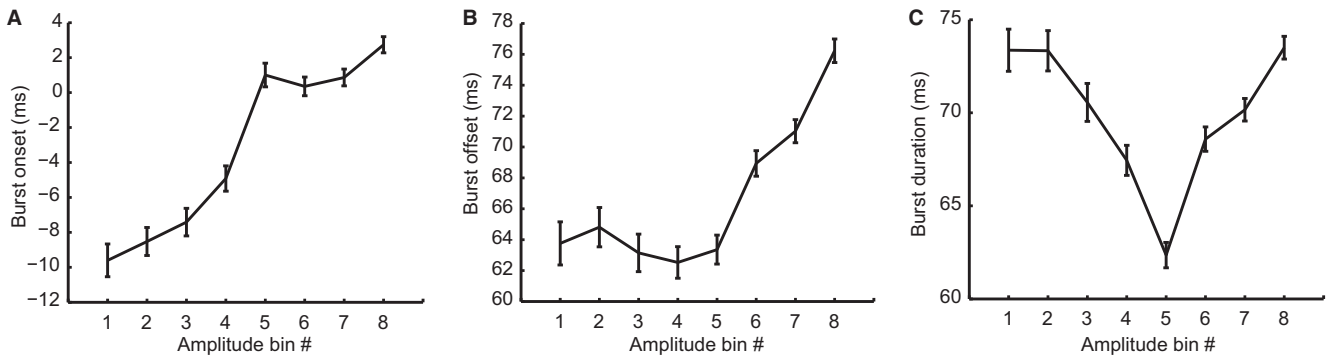

FIG. 6. Plots of burst onset, offset and duration as a function of amplitude bins. (A) Burst onset time as function of amplitude. (B, C) Burst offset time and duration, respectively, as a function of amplitude bins. Error bars indicate ± SEM.

other words, the distribution of amplitude preferences was profoundly skewed toward larger amplitudes (Fig. 5C). After aligning each individual tuning curve to the preferred amplitude, an almost symmetric average tuning curve was obtained. In other words, the firing rate decreased in a similar way to either side of the preferred amplitude bin, independent of the location of that bin (Fig. 5D). To study the influence of saccade amplitude on the timing of saccade-related bursts, we determined the latencies of burst onset and offset of individual neurons for each amplitude bin and plotted them as well as burst duration as a function of the amplitude bin (Fig. 6). As can be seen there, the latency of burst onset increased with saccade amplitude in a linear fashion (Fig. 6A). A dependency of the offset latency on amplitude was limited to larger amplitude saccades but not exhibited by smaller amplitude saccades whose offset latencies fluctuated around a latency of 64 ms independent of amplitude bin, arguably a reflection of a statistical plateau effect without biological relevance (Fig. 6B). This view is supported by the analysis of the population response, following below, which did not yield a plateau. Finally, burst duration reached a minimum in amplitude bin 5 (Fig. 6C), the necessary resultant of the amplitude dependencies of burst onset and offset.

The influence of saccade amplitude on the discharge rate can also be seen in the plot obtained by averaging the collective instantaneous discharge rates of all 67 neurons in our sample as a function of time relative to saccade onset for the same distinct saccade amplitude bins also underlying Figs 5 and 6. We either lumped all eight directions tested (Fig. 7A) or pooled ipsi- and contraversive saccades separately (Fig. 7B,C). Instantaneous discharge rate was approximated by calculating the mean collective discharge rate in time bins of 10 ms, aligned with saccade onset. The analysis of the plots clearly demonstrated that the duration of the population burst increased smoothly with saccade size from the first bin to the last one (correlation between duration of the population burst and saccade duration: $r = 0.95$, $P = 0.0003$). Surprisingly, the population burst onset did not exhibit differences in onset times for ipsi- versus contraversive saccades (t test, $P = 0.17$) (Fig. 7B,C), a finding that contrasts with the direction dependency of saccade-related bursts of individual neurons discussed earlier. Furthermore, the population firing rate for ipsiversive microsaccades was higher than the one for contraversive microsaccade, in accordance with the aforementioned preponderance of neurons preferring ipsiversive microsaccades (t test, $P = 4 \times 10^{-5}$). Finally, the population activity for ipsiversive saccades exhibited a weak pause preceding the saccade-related bursts before ipsiversive large amplitude (> 8°) saccades only (see inset in Fig. 7B). This pre-burst pause was largely confined to ipsiversive saccades, an observation which is consistent with previous findings (Ohtsuka & Noda, 1990; Robinson *et al.*, 1993).

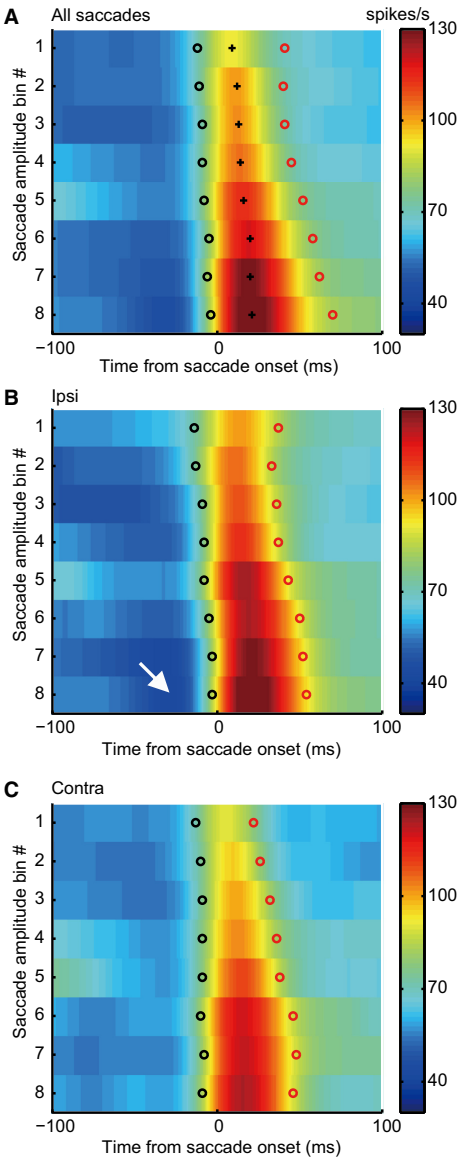

FIG. 7. Instantaneous population discharge aligned relative to saccade onset. (A) Instantaneous population activity plotted as a function of saccade time (x axis) and amplitude class (y axis), pooling across all saccades, independent of direction. See Methods for further technical details. Microsaccades are shown in the top three bins. Black circles, stars, and red circles indicate burst onset, timing of peak firing, and burst offset, respectively. (B) Population activity for ipsiversive saccades only. The white arrow indicates the discharge pause before saccade onset preceding the later burst. (C) Population activity for contraversive saccades only.

Baseline firing rate

The microsaccades used in this study were collected during the time in which the monkey was supposed to stay within the fixation window, waiting for the go signal to make a saccade to the new target. Hence, microsaccades and other small amplitude saccades not breaking the fixation window could be started from any position within the fixation window. Plots of the vectors of all saccades made during fixation of the target as a function of the starting position (see Fig. 8A for an exemplary session and Fig. 8B for a plot based on all sessions) clearly indicate that saccades tried to drive the eyes to the center of the fixation window, arguably corresponding to the highest acuity region of the fovea: saccades were not only directed toward the center but also their amplitudes got smaller the closer the starting point was relative to the center (Cornsweet, 1956; Engbert & Kliegl, 2004; Guerrasio *et al.*, 2010; Arnstein *et al.*, 2015). Actually, a two-dimensional locally weighted scatterplot smoothing (LOWESS) model of saccade amplitude as a function of the starting position based on the data shown in Fig. 8C predicts the smallest amplitude saccades to be generated for starting positions very close to the center of the fixation window (coordinates: $x = -0.06°$, $y = -0.15°$; $R^2 = 0.81$), arguably coinciding with the foveola. If the goal of the oculomotor system was to stabilize the target image on the foveola, one might expect that the model would have predicted zero-degree saccade amplitudes at this point. However, the predicted amplitude for this position was actually 0.58° and not zero. We

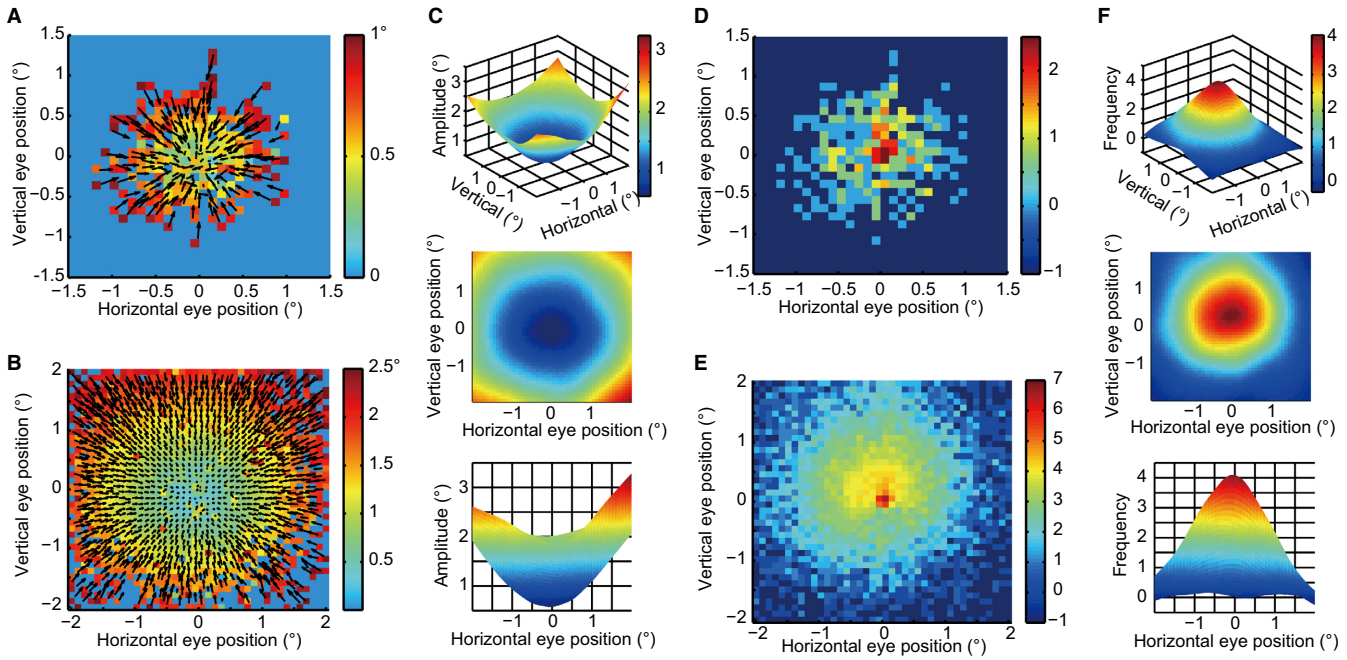

FIG. 8. Relationship between the starting position of the eyes and saccade metrics. Mean saccade direction and amplitude are represented by arrows originating from a particular binned starting position relative to the target position and ending at the new position acquired. Means were based on averaging all saccades originating from a spatial bin of 0.1° × 0.1°. (A) Example session (n = 410 saccades) and (B) all sessions (n = 14 443 saccades). For the sake of clarity, the mean amplitude of saccades starting from particular bins is also color coded. (C) Different views of a fit of the data shown in (B) based on a locally weighted scatterplot smoothing (LOWESS) model with a span of 0.1 (R^2 = 0.81). (D, E) Dependency of saccade frequency on initial eye position. Exemplary session (D) and all sessions (E). For the sake of visual clarity, the natural logarithm of frequency was used. (F) Different views of a fit of the data shown in (E) based on a LOWESS model with a span of 0.1 (R^2 = 0.84).

think that this may be a consequence of the fixation point having a finite diameter (0.2–0.3°) and therefore offering varying anchor points for the foveola. Surprisingly, also the frequency of saccades depended on the starting position (Fig. 8D–F). This is clearly exhibited by the plots shown in Fig. 8D–F that show that the frequency of saccades gets the higher, the closer the eyes get to the target.

We wondered if the subtle changes in eye position during fixation of the target, as discussed before relevant for the metrics of microsaccades, also had an effect on the fixation-related discharge. To address this question we plotted the mean discharge rate within a 100-ms period before the onset of the next saccade ('presaccadic' discharge rate) as a function of eye position in the fixation plane. The resulting plot (see Fig. 9A) is characterized by a decrease in the pre-saccadic firing rate toward the center, giving it an appearance that is strikingly similar to the plot of saccade amplitude as a function of eye starting position shown in Fig. 8B. The mean saccade-related discharge rate was relatively independent of the starting position (Fig. 9B), whereas the discharge contrast, the difference between the mean saccade-related discharge rate and the pre-saccadic discharge rate, exhibited an increase around the center (Fig. 9C). As the number of microsaccades associated with the short fixation of the peripheral target was very small, we were unable to address the interesting question if the patterns discussed before are independent of the eccentricity of the fixation target relative to straight ahead.

Discussion

This study shows that individual FOR neurons respond to micro- as well as to macrosaccades. In agreement with previous observations on macrosaccades (Ohtsuka & Noda, 1990, 1991; Robinson *et al.*, 1993; Helmchen *et al.*, 1994; Scudder & McGee, 2003), we found that FOR neurons exhibited saccade-related bursts earlier for contraversive saccades than for ipsiversive saccades, yet for both macro- and microsaccades. In general, the burst for macrosaccades started later compared to the one for microsaccades. These qualitative similarities suggest in principle similar contributions to the control of saccades of very different amplitudes.

Previous studies of macrosaccades have suggested that the early burst associated with contraversive saccades might help to initiate contraversive saccades. On the other hand, the late burst for ipsiversive saccades is thought to contribute to terminating them (Ohtsuka & Noda, 1991; Robinson *et al.*, 1993). This control concept (referred to here as the 'timing concept') that emphasizes a role of the FOR in saccade timing was based on experiments in which only horizontal (macro) saccades were considered, which is why it ignores the requirements of saccades made in other directions. In this study, we extended the analysis of the dependence of burst onset latencies on direction to other directions in the frontoparallel plane. Burst onset latencies exhibited a gradual dependence on direction. Moreover, we did not observe the shortest and longest burst onset latencies, respectively, for saccades made along the horizontal axis but for saccades made along an axis rotated by 60° counterclockwise relative to the horizontal with gradual deviation of burst onset for directions deviating from this axis. This pattern was the same for microsaccades and for macrosaccades. Although we cannot offer an explanation of the rotation of the non-preferred axis relative to the horizontal axis, we may conclude that this deviation and, in general, the gradual burst onset tuning clearly indicate that FOR neurons are hardly committed to horizontal saccades as tacitly assumed by the original timing concept.

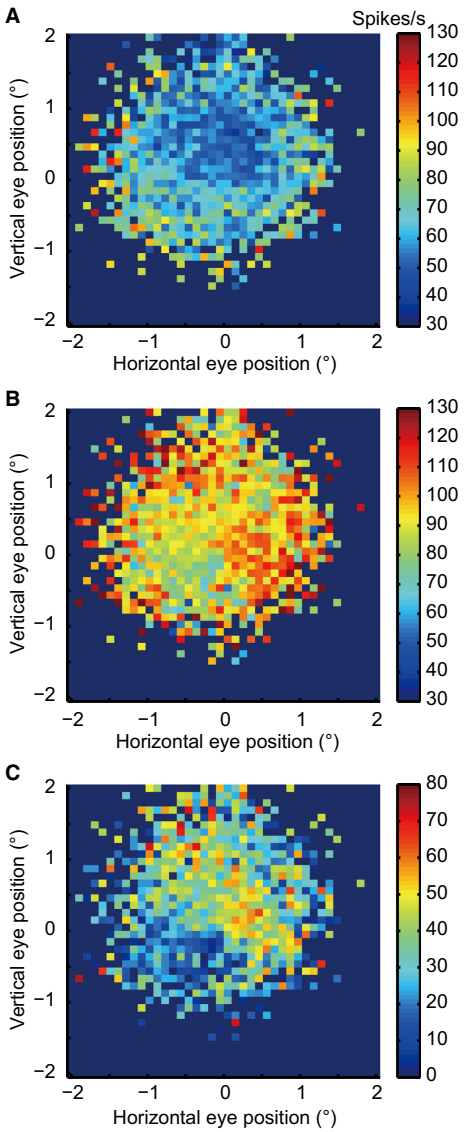

FIG. 9. Analysis of dependency of pre-saccadic discharge on the starting position of the eyes for periods in which the eyes stayed within the confines of the fixation window. (A) Mean pre-saccadic discharge (color coded) pooled across all fastigial oculomotor region (FOR) neurons as function of binned horizontal and vertical eye positions relative to the target (bin size 0.1° × 0.1°). Each spatial bin had to contain at least five baseline samples preceding insipient saccades. (B) Mean saccade-related discharge rate during saccade (color coded) pooled across all FOR neurons as function of binned horizontal and vertical eye positions relative to the target (bin size 0.1° × 0.1°). Minimum of five samples per bin. (C) Contrast map obtained by subtracting the mean baseline map depicted in (A) from the mean firing map shown in (B).

Actually, the similarities between micro- and macrosaccade timing are not confined to the influence of direction but involve the influence of saccade amplitude on saccade duration. Previous work on macrosaccades had shown that burst duration is correlated with the duration of macrosaccades (Ohtsuka & Noda, 1991; Robinson *et al.*, 1993; Helmchen *et al.*, 1994). Our study clearly shows that this correlation extends to microsaccades, at least when considering the population responses, once again arguing for a control principle conveyed by the FOR which is shared by the two saccade classes.

Fastigial oculomotor region neurons also exhibited a clear direction tuning of the number of spikes in a burst for both macro- and microsaccades. Like the directional dependence of burst timing, it turned out to be gradual for both groups of saccades. Surprisingly, the direction preferences for micro- and macrosaccades could differ in individual cases. However, in general, neurons preferring macro- as well as microsaccades into the ipsiversive hemifield dominated our sample. This contrasts with the only study we are aware of, a study by Helmchen *et al.* (1994) which mentioned that 55% of neurons exhibited stronger saccade-related bursts for contra- than for ipsiversive (macro) saccades. In any case, the laterality bias was not strong neither in our sample nor in the one of Helmchen *et al.* The timing concept posits a directional dependence of burst timing but not of burst strength. This is why it does not offer a functional explanation of the observation of the latter and in particular no explanation of the difference between micro- and macrosaccade preferred directions in some of the neurons. One possible explanation of the occasionally deviating directional preferences of microsaccade-related responses may be the confounding influence of eye position relative to the fixation spot. Microsaccades made into a particular direction started from different positions relative to target. Further below we will come back to the profound impact of eye starting position on the discharge.

Inactivation studies of the FOR have demonstrated the occurrence of eye position-dependent saccadic dysmetria (Vilis & Hore, 1981; Robinson *et al.*, 1993), suggesting that saccade-related activity in the FOR might depend on eye position. However, previous work is inconclusive as to the influence of eye position on the discharge of individual FOR neurons. Whereas Ohtsuka & Noda (1991) did not report changes in saccade-related bursts of FOR neurons or tonic firing rates during stationary fixation by eye positions, Kleine *et al.* (2003) seemed to suggest such an influence. They compared centripetal and centrifugal saccades of the same amplitude and direction. Some neurons tested exhibited higher peak discharge rates for centripetal saccades than for centrifugal saccades, a difference that might have been due to the difference in starting positions, associated with opposite directions of elastic forces impinging on the eyeballs. As the macrosaccades made in our study always started from straight ahead, we cannot contribute to the discussion of the question if larger deviations in eye position from straight ahead modulate the baseline firing rate of FOR neurons before a macrosaccade or the size of a macrosaccade-related burst. However, the variability in fixation positions within the small fixation window allowed us to address the question if the baseline firing rate before microsaccades made to new fixation positions within the straight ahead fixation window would be influenced by eye position. This turned out to be the case. Baseline firing rate was the smaller the closer the pre-microsaccadic eye position was to the center of the fixation window. Interestingly, it exhibited full radial symmetry relative to the target; in other words, it did not matter to which side the eyes deviated before a microsaccade. In accordance with previous reports (Cornsweet, 1956; Guerrasio *et al.*, 2010), we found that microsaccade direction – and the ones of slightly larger saccades with amplitudes not satisfying the arbitrary 1° criterion – is always such as to move the eyes to the target, arguably aligning the target image with the foveola. Moreover, the closer the eyes are relative to the target, the smaller microsaccades get. Actually, the dependence predicts a virtual absence of measurable microsaccades, once the foveola is aligned with the target. This is a pattern that is in full accordance with the notion that microsaccades are precisely controlled eye movements ensuring that the high-resolution center of the fovea is used for the visual scrutiny of tiny objects. We found that the dependence of the pre-saccadic firing rate on eye position paralleled the

dependence of microsaccade metrics on the starting position of the eyes. This intriguing similarity suggests a causal relationship between the baseline firing rate and microsaccade metrics. For instance, one might speculate that microsaccade-related bursts may be constrained to directions that promise the steepest decline in fixation-related tonic activity.

Our demonstration of microsaccade-related control signals in the FOR may be considered not surprising in view of the fact that FOR lesions affect not only macrosaccades but also microsaccades (Goffart *et al.*, 2004). Hence, the interesting aspect is not so much their existence but the fact that they are continuous with those for macrosaccades at the level of single neurons. FOR neurons offer control signals for saccades which have qualitatively very similar features, independent of saccade size. This similarity is in line with comparable properties of saccade-related OV Purkinje cell simple spikes (Arnstein *et al.*, 2015), a major, although not sole source of input to the FOR (Yamada & Noda, 1987; Noda *et al.*, 1990). At first glance, it seems to support the general notion that there is no principle difference between the cerebellar control of microsaccades and macrosaccades. However, this conclusion is only warranted if we restrict our view to the properties of saccade-related bursts. A unique feature of FOR neurons is the aforementioned conspicuous radially symmetric dependence of their baseline firing rate on eye position relative to the target as soon as the target image is positioned within the confines of the fovea and the intriguing correlation of this baseline firing rate with the metrics of the next microsaccade. As the microsaccades issued tend to move the target image closer to the foveola, the possibility of a specific contribution to the optimization of fixation arises. Indeed previous studies have demonstrated that lesions of the FOR result not only in saccadic dysmetria but also fixation offsets (Sato & Noda, 1992; Robinson *et al.*, 1993; Goffart *et al.*, 2004; Guerrasio *et al.*, 2010). Arguably, also the fact that the FOR projection to the representation of the visual field center in the SC (May *et al.*, 1990) may fit into the picture of a prominent role of the FOR – and the cerebellum at large – in the optimization of visual fixation.

Acknowledgments

The work was supported by a Marie Curie Initial Training Network (PITN-GA-2009-238214; to P.T.), the German Ministry of Education, Science, Research, and Technology through the Bernstein Center for Computational Neuroscience (FKZ 01GQ1002), and a grant from the Deutsche Forschungsgemeinschaft (FOR 1847-A3 TH425/13-1; to P.T).

Abbreviations

FOR, fastigial oculomotor regions; OV, oculomotor vermis; LOWESS, locally weighted scatterplot smoothing.

Conflict of interest

The authors declare no competing financial interests.

Author contributions statement

Z.S. and P.T. conceived and designed the experiments. Z.S. and P.W.D. performed the experiments. Z.S. and M.J. analyzed the data. Z.S. and P.T. wrote this article. All authors reviewed the manuscript.

References

Arnstein, D., Junker, M., Smilgin, A., Dicke, P.W. & Thier, P. (2015) Microsaccade control signals in the cerebellum. *J. Neurosci.*, **35**, 3403–3411.

Barash, S., Melikyan, A., Sivakov, A., Zhang, M., Glickstein, M. & Thier, P. (1999) Saccadic dysmetria and adaptation after lesions of the cerebellar cortex. *J. Neurosci.*, **19**, 10931–10939.

Berens, P. (2009) CircStats: a MATLAB toolbox for circular statistics. *J. Stat. Softw.*, **31**, 1–21.

Bridgeman, B. & Palca, J. (1980) The role of microsaccades in high acuity observational tasks. *Vision. Res.*, **20**, 813–817.

Cornsweet, T.N. (1956) Determination of the stimuli for involuntary drifts and saccadic eye movements. *J. Opt. Soc. Am.*, **46**, 987–993.

Cui, J., Wilke, M., Logothetis, N.K., Leopold, D.A. & Liang, H. (2009) Visibility states modulate microsaccade rate and direction. *Vision. Res.*, **49**, 228–236.

Ditchburn, R.W. & Ginsborg, B.L. (1952) Vision with a stabilized retinal image. *Nature*, **170**, 36–37.

Engbert, R. (2006) Microsaccades: a microcosm for research on oculomotor control, attention, and visual perception. *Prog. Brain Res.*, **154**, 177–192.

Engbert, R. & Kliegl, R. (2004) Microsaccades keep the eyes' balance during fixation. *Psychol. Sci.*, **15**, 431–436.

Gass, J.D. (1999) Muller cell cone, an overlooked part of the anatomy of the fovea centralis: hypotheses concerning its role in the pathogenesis of macular hole and foveomacualr retinoschisis. *Arch. Ophthalmol.*, **117**, 821–823.

Goffart, L., Chen, L.L. & Sparks, D.L. (2004) Deficits in saccades and fixation during muscimol inactivation of the caudal fastigial nucleus in the rhesus monkey. *J. Neurophysiol.*, **92**, 3351–3367.

Golla, H., Tziridis, K., Haarmeier, T., Catz, N., Barash, S. & Thier, P. (2008) Reduced saccadic resilience and impaired saccadic adaptation due to cerebellar disease. *Eur. J. Neurosci.*, **27**, 132–144.

Guerrasio, L., Quinet, J., Buttner, U. & Goffart, L. (2010) Fastigial oculomotor region and the control of foveation during fixation. *J. Neurophysiol.*, **103**, 1988–2001.

Hanes, D.P., Thompson, K.G. & Schall, J.D. (1995) Relationship of presaccadic activity in frontal eye field and supplementary eye field to saccade initiation in macaque: poisson spike train analysis. *Exp. Brain Res.*, **103**, 85–96.

Helmchen, C., Straube, A. & Buttner, U. (1994) Saccade-related activity in the fastigial oculomotor region of the macaque monkey during spontaneous eye movements in light and darkness. *Exp. Brain Res.*, **98**, 474–482.

Ignashchenkova, A., Dash, S., Dicke, P.W., Haarmeier, T., Glickstein, M. & Thier, P. (2009) Normal spatial attention but impaired saccades and visual motion perception after lesions of the monkey cerebellum. *J. Neurophysiol.*, **102**, 3156–3168.

Kleine, J.F., Guan, Y. & Büttner, U. (2003) Saccade-related neurons in the primate fastigial nucleus: what do they encode? *J. Neurophysiol.*, **90**, 3137–3154.

Ko, H.K., Poletti, M. & Rucci, M. (2010) Microsaccades precisely relocate gaze in a high visual acuity task. *Nat. Neurosci.*, **13**, 1549–1553.

Kowler, E. & Steinman, R.M. (1980) Small saccades serve no useful purpose: reply to a letter by R. W. Ditchburn. *Vision. Res.*, **20**, 273–276.

Li, K.Y., Tiruveedhula, P. & Roorda, A. (2010) Intersubject variability of foveal cone photoreceptor density in relation to eye length. *Invest. Ophthalmol. Vis. Sci.*, **51**, 6858–6867.

Martinez-Conde, S., Macknik, S.L. & Hubel, D.H. (2004) The role of fixational eye movements in visual perception. *Nat. Rev. Neurosci.*, **5**, 229–240.

May, P.J., Hartwich-Young, R., Nelson, J., Sparks, D.L. & Porter, J.D. (1990) Cerebellotectal pathways in the macaque: implications for collicular generation of saccades. *Neuroscience*, **36**, 305–324.

McCamy, M.B., Najafian Jazi, A., Otero-Millan, J., Macknik, S.L. & Martinez-Conde, S. (2013) The effects of fixation target size and luminance on microsaccades and square-wave jerks. *PeerJ*, **1**, e9.

Noda, H., Sugita, S. & Ikeda, Y. (1990) Afferent and efferent connections of the oculomotor region of the fastigial nucleus in the macaque monkey. *J. Comp. Neurol.*, **302**, 330–348.

Ohtsuka, K. & Noda, H. (1990) Direction-selective saccadic-burst neurons in the fastigial oculomotor region of the macaque. *Exp. Brain Res.*, **81**, 659–662.

Ohtsuka, K. & Noda, H. (1991) Saccadic burst neurons in the oculomotor region of the fastigial nucleus of macaque monkeys. *J. Neurophysiol.*, **65**, 1422–1434.

Optican, L.M. & Robinson, D.A. (1980) Cerebellar-dependent adaptive control of primate saccadic system. *J. Neurophysiol.*, **44**, 1058–1076.

Otero-Millan, J., Troncoso, X.G., Macknik, S.L., Serrano-Pedraza, I. & Martinez-Conde, S. (2008) Saccades and microsaccades during visual fixation, exploration, and search: foundations for a common saccadic generator. *J. Vis.*, **8**, 21.1–18.

Otero-Millan, J., Macknik, S.L., Serra, A., Leigh, R.J. & Martinez-Conde, S. (2011a) Triggering mechanisms in microsaccade and saccade generation: a novel proposal. *Ann. NY Acad. Sci.*, **1233**, 107–116.

Otero-Millan, J., Serra, A., Leigh, R.J., Troncoso, X.G., Macknik, S.L. & Martinez-Conde, S. (2011b) Distinctive features of saccadic intrusions and microsaccades in progressive supranuclear palsy. *J. Neurosci.*, **31**, 4379–4387.

Poletti, M., Listorti, C. & Rucci, M. (2013) Microscopic eye movements compensate for nonhomogeneous vision within the fovea. *Curr. Biol.*, **23**, 1691–1695.

Putnam, N.M., Hofer, H.J., Doble, N., Chen, L., Carroll, J. & Williams, D.R. (2005) The locus of fixation and the foveal cone mosaic. *J. Vis.*, **5**, 632–639.

Ritchie, L. (1976) Effects of cerebellar lesions on saccadic eye movements. *J. Neurophysiol.*, **39**, 1246–1256.

Robinson, F.R., Straube, A. & Fuchs, A.F. (1993) Role of the caudal fastigial nucleus in saccade generation. II. Effects of muscimol inactivation. *J. Neurophysiol.*, **70**, 1741–1758.

Rolfs, M., Laubrock, J. & Kliegl, R. (2006) Shortening and prolongation of saccade latencies following microsaccades. *Exp. Brain Res.*, **169**, 369–376.

Sato, H. & Noda, H. (1992) Saccadic dysmetria induced by transient functional decortication of the cerebellar vermis [corrected]. *Exp. Brain Res.*, **88**, 455–458.

Scudder, C.A. & McGee, D.M. (2003) Adaptive modification of saccade size produces correlated changes in the discharges of fastigial nucleus neurons. *J. Neurophysiol.*, **90**, 1011–1026.

Straube, A., Helmchen, C., Robinson, F., Fuchs, A. & Buttner, U. (1994) Saccadic dysmetria is similar in patients with a lateral medullary lesion and in monkeys with a lesion of the deep cerebellar nucleus. *J. Vestibul. Res.*, **4**, 327–333.

Takagi, M., Zee, D.S. & Tamargo, R.J. (1998) Effects of lesions of the oculomotor vermis on eye movements in primate: saccades. *J. Neurophysiol.*, **80**, 1911–1931.

Thaler, L., Schutz, A.C., Goodale, M.A. & Gegenfurtner, K.R. (2013) What is the best fixation target? The effect of target shape on stability of fixational eye movements. *Vision. Res.*, **76**, 31–42.

Van Gisbergen, J.A.M. & Robinson, D.A. (1977) Generation of micro and macrosaccades by burst neurons in the monkey. In Baker, R. & Berthoz, A. (Eds), *Control of Gaze by Brain Stem Neurons*. Elsevier/North-Holland, Amsterdam, pp. 301–308.

Van Gisbergen, J.A., Robinson, D.A. & Gielen, S. (1981) A quantitative analysis of generation of saccadic eye movements by burst neurons. *J. Neurophysiol.*, **45**, 417–442.

Vilis, T. & Hore, J. (1981) Characteristics of saccadic dysmetria in monkeys during reversible lesions of medial cerebellar nuclei. *J. Neurophysiol.*, **46**, 828–838.

Winterson, B.J. & Collewijn, H. (1976) Microsaccades during finely guided visuomotor tasks. *Vision. Res.*, **16**, 1387–1390.

Yamada, J. & Noda, H. (1987) Afferent and efferent connections of the oculomotor cerebellar vermis in the macaque monkey. *J. Comp. Neurol.*, **265**, 224–241.

Zuber, B.L., Stark, L. & Cook, G. (1965) Microsaccades and the velocity-amplitude relationship for saccadic eye movements. *Science*, **150**, 1459–1460.